ELSEVIER

Prog. Polym. Sci. 26 (2001) 443–533

PROGRESS IN
POLYMER SCIENCE

Microstructure of polypropylene

Vincenzo Busico*, Roberta Cipullo

Dipartimento di Chimica, Università di Napoli Federico II, Complesso Universitario di Monte S. Angelo, Via Cintia, I-80126 Naples, Italy

Dedicated to Anna Laura Segre, 'Alma Mater' of the High-Field ^{13}C NMR Microstructural Approach

Received 16 July 2000; accepted 6 December 2000

Abstract

For over thirty years after the discovery of stereoselective olefin polymerization in 1954, the word 'polypropylene' has meant, both scientifically and commercially, little else than the predominantly isotactic polymer achievable with the classical heterogeneous Ziegler–Natta catalysts. The picture, however, has changed dramatically in the last 15 years, due to the development of a variety of new transition metal catalysts with tunable structures and selectivities. Nowadays, 'polypropylene' means a whole world of innovative polymers with novel and well-controlled microstructures, and — as a result — tailored properties and applications. With the powerful aid of high-field ^{13}C NMR data, this review aims at introducing the reader to this fascinating and challenging frontier of macromolecular stereochemistry. © 2001 Elsevier Science Ltd. All rights reserved.

Keywords: Polypropylene; Microstructure; Stereoselectivity; Regioselectivity; ^{13}C NMR; Polymerization mechanisms; Polymerization catalysts; Ziegler–Natta catalysts; Metallocene catalysts

Contents

* Corresponding author. Fax: +39-081-67-4355.
E-mail address: busico@chemna.dichi.unina.it (V. Busico).

0079-6700/01/$ - see front matter © 2001 Elsevier Science Ltd. All rights reserved.
PII: S0079-6700(00)00046-0

1. Introduction

1.1. Polypropylene: a short biography

Polypropylene was born in Milan, Italy on March 11, 1954 [1].[1] In the first months, the infant gave sign of a polyhedric character, with a charming combination of isotactic, syndiotactic and stereoblock traits [2]. However, by will of his father, Giulio Natta, a renowned chemical engineer who held the chair of industrial chemistry at the Polytechnic of Milan, it was subjected to a rigorous education, and already at one year the rigid and inflexible characteristics of the isotactic complexion were largely predominant [3]. The following years saw a continuous strengthening of these features, and the adolescent polymer apparently lost any other inclination. As a matter of fact, by the end of the 1970s it had turned into a practically perfect professional, able to compete successfully with older colleagues in the field of thermoplastic materials [4], but also devoid of fascination due to its same monochordic perfection.

However, against all appearances, the Latin character was still alive. Indeed, in the mid 1980s, once the father's influence had faded out, new experiences in the United States [5] and in Germany [6] catalyzed an unexpected, spectacular re-birth. Polypropylene proved able to be not only highly isotactic, but also highly syndiotactic, perfectly atactic, and even — as a divertissement — hemiisotactic [7,8]. Moreover, it developed the capability to mix all these features almost at will, with unprecedented results [7,8].

Today, in its splendid maturity, polypropylene is a new polymer, and no achievements look too

[1] This opening is an attempt of capturing readers' attention, and should not be considered as a historically accurate reconstruction. In particular, the first paragraph does not intend to assume a position in the long patent querelle on isotactic polypropylene; this has been settled in court, as the interested readers can learn, e.g. from Ref. [1].

ambitious for it [1]. Its performance is constantly under the spotlight, and the number of fans worldwide is steadily increasing. Therefore, it is an appropriate time for this review.

1.2. About this review

In a synthetic polymer like polypropylene, no two macromolecules are equal. Therefore, the only way to describe the chemical structure is to make use of statistics. Convenient averages, for instance, can be adopted in order to define a molecular mass. Similarly, chain constitution and configuration can be expressed in terms of average mole fractions of monomeric units in the various possible arrangements.

A much more informative description, however, makes use of *sequence distributions of monomeric units*. As far as the molecular mass is concerned, it is possible to determine the complete distribution from oligomers to ultra-high molecular weights. The tools for chemical structure analysis, instead, are by far less satisfactory, because their resolution is limited to comparatively short chain segments (a few monomeric units long); it is this *local* structural information that we name *microstructure* [9].

For most vinyl polymers, ^{13}C NMR is the elective technique of microstructural analysis [10–12], and the progress in this spectroscopy parallels that in our stereochemical understanding of such materials. In recent years, in particular, the use of high-field ^{13}C NMR has led to substantial advances in the determination of polypropylene configuration [13–15], which is the main subject of this review.

Evaluating in depth the microstructure of a polypropylene sample is important for two main reasons, the first and most obvious being that it is a way to understand its physical properties, and in particular the melting and crystallization behavior. The other reason is that polymerization kinetics and polymer microstructure are intimately related. Each macromolecule is like a tape, where the story of the catalytic process that led to its generation is faithfully and sequentially recorded: in order to know that story, one must be able to read the tape.

In Sections 4 and 5, both aspects are addressed in detail for the various classes of propene polymers that can be identified in terms of the peculiar microstructural *fingerprints* of the catalysts used to produce them. The number of such classes has considerably increased in the last two decades, due to the discovery of a variety of new types of *single-site catalysts* with well-defined structures [7,8,16–18], which have flanked the 'classical' heterogeneous *Ziegler–Natta systems* [1,3,4] that still dominate the industrial scenario. We actually open Section 4 with these new polypropylenes of comparatively simple microstructure, which can be described in terms of rigorous statistical models, and use them as a reference for facing the intriguing and highly complicated stereochemical problem represented by Ziegler–Natta polypropylenes.

Prior to that, however, we illustrate the progress in the experimental techniques of microstructural analysis (Section 2), with special attention to the recent applications of high-field ^{13}C NMR, and briefly introduce the stochastic methods for the quantitative description of polypropylene configuration (Section 3).

1.3. Definitions and nomenclature

Nowadays, the fundamentals of polymer science are part of the theoretical background of all chemists. However, some aspects and definitions of macromolecular stereochemistry can be tricky even for specialists; therefore, it may be worthwhile to provide the reader with a short compendium of 'technical' terms and concepts that will be used throughout this review.

$$\underset{1}{CH_2}=\underset{2}{CH}-\underset{3}{CH_3}$$

Chart 1.

(A) $-CH_2-CH(CH_3)-$ (B) $-CH(CH_3)-CH_2-$

Chart 2.

According to IUPAC rules for organic chemistry, the three C atoms in the molecule of propene should be numbered as shown in Chart 1.

However, when referring to propene as a monomer, it is also common to say that it has a *head* (the $=CH(CH_3)$ moiety) and a *tail* (the $CH_2=$ moiety).

Propene polymerization is promoted by *coordination catalysts [1,3,4,7,8,16–18]*, and the active site is a σ-bond connecting a transition metal center to the last C atom of the growing chain. The reaction proceeds by sequential monomer *insertions* into the said bond, via *cis* openings of the olefinic double bond [20].

Each insertion is denoted as 1,2 or 2,1 depending on whether the incoming monomer binds to the active metal with C-1 or C-2, respectively (Scheme 1; P = polymeryl).

The alternative notations *primary* and *secondary* are also used, particularly in the less recent literature. Although, according to IUPAC recommendations [19], such two terms should be abandoned, they are still tolerated, and — in particular — continue to be the basis for the definition of the specific monomer insertion rates. These are usually labelled as k_{ij}, the subscripts i and j being 'p' or 's' to indicate a 1,2 (primary) or a 2,1 (secondary) insertion, respectively. By convention, it must be intended that insertion j followed insertion i; for instance, k_{sp} is the specific rate of a 1,2 (primary) insertion following a previous 2,1 (secondary) one.

In general, the enchainment of the monomeric units in polypropylene is not random, one of the two insertion modes (usually, the 1,2 mode) being (largely) preferred for electronic and/or steric reasons. In the extreme (and ideal) case that the other mode is totally forbidden, the polymer is said to be *regioregular*, and its structure can be described in terms of a single *constitutional base unit* (Chart 2).

Less rigorously, it can also be said that such a polymer has a perfect *head-to-tail enchainment*.

From the mechanistic viewpoint, it is fundamental to know whether a polymerization proceeds (predominantly) via 1,2 or 2,1 insertion. On the other hand, for the microstructural description of the resulting polymer it is immaterial to discriminate between (A) and (B) in Chart 2, unless the nature of the chain ends is considered.

In real polypropylene chains, a certain amount of *regiodefects* are invariably present. In most cases,

$$Mt\text{-}P + CH_2=CH(CH_3) = Mt\text{-}CH_2\text{-}CH(CH_3)\text{-}P \qquad \textbf{\textit{1,2 (primary) insertion}}$$

$$Mt\text{-}P + CH(CH_3)=CH_2 = Mt\text{-}CH(CH_3)\text{-}CH_2\text{-}P \qquad \textbf{\textit{2,1 (secondary) insertion}}$$

Scheme 1.

-[CH_2-CH(CH_3)]$_x$-**CH_2-CH(CH_3)-CH(CH_3)-CH_2**-[CH_2-CH(CH_3)]$_y$-

Chart 3.

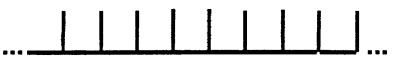

Chart 4.

Chart 5.

these are isolated monomeric units with an enchainment which is opposite to the predominant one (*head-to-head/tail-to-tail* arrangement, Chart 3).

However, when the regioregularity is at least decent (>95 mol% regioregular units, indicatively), it is common practice to ignore the regiodefects for the discussion of polymer *configuration*; in such a case, the concept of microstructure actually reduces to that of *microtacticity*.

Propene is a prochiral monomer, and gives rise to monomeric units containing a center of stereoisomerism at the backbone tertiary C atom. One may say that the latter is a truly asymmetric C, in the sense that it bears four different substituents, as long as the two sides of a polymer chain of finite length can be considered to be non-identical. However, it is easy to realize that the priority of these two substituents is virtually the same, the more so the higher is chain length. Moreover, even if one was able to assign an absolute chirality (*R* or *S*) to each tertiary C atom in the chain, the result would be of no real use or — even — misleading.

As an example, let us make the case of the regioregular chain shown in Chart 4. The representation is an adapted Fischer projection, which assumes a hypothetical zig-zag conformation of the chain backbone, whose plane is perpendicular to that of the figure (for the sake of clarity, only C–C bonds are traced).

A slightly different version, which better explicates the individual monomeric units, is shown in Chart 5 (the symbol ⌋ obviously standing for —CH_2—CH(CH_3)—).

In the charts, all substituents of the same type (CH_3 or H) lie on the same side of the zig-zag plane, which makes it clear that all tertiary C atoms have the same *relative* configuration. On the other hand, upon moving from one side of the chain to the other, it is obvious that at a given point the priority of the two chain segments attached to each tertiary C atom will invert, and so will their absolute configuration. This result looks so incongruous that absolute configurations are never used in the stereochemical description of polypropylene (with the notable exception of propene *oligomers*).

The way-out is to make reference to the relative configurations of the tertiary C atoms, and in particular to those in consecutive couples of monomeric units, each of which is said to constitute a (*steric*) *diad*. The two diads of Chart 6, corresponding to *equal* or *opposite* relative configurations of the stereogenic centers, can be labelled as *meso* (abbreviation, *m*) or *racemo* (abbreviation, *r*), respectively.

In the current language, the prefix *racemo* is almost invariably corrupted to *racemic*, which is

Chart 6.

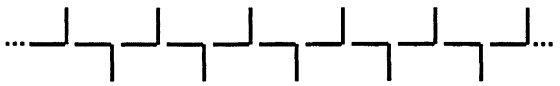

Chart 7.

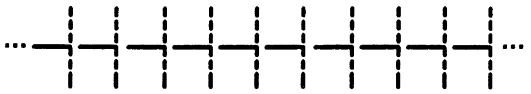

Chart 8.

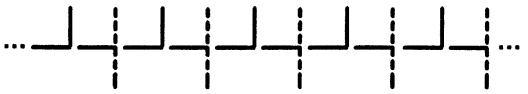

Chart 9.

unfortunate due to the different meaning of the term *racemic* in organic chemistry. However, the contexts are different enough to avoid confusion.

A number of ideal stereostructures can be simply described in terms of sequences of steric diads. As an example, the arrangement shown in Charts 4 and 5, corresponding to a conceptually infinite succession of *meso* diads, is known as *isotactic*. Similarly, a conceptually infinite sequence of *racemo* diads is said to be *syndiotactic* (Chart 7).

Two more ideal cases with fully or partly disordered configurations can also be defined. A conceptually infinite succession of equally numbered and randomly distributed *meso* and *racemo* diads gives rise to an *atactic* chain. A more exotic chain in which all even monomeric units have the same relative configuration, whereas all odd ones have a perfectly random configuration, is called *hemiisotactic*.

The graphic representation of these disordered structures is somewhat more complicated. In the following, we shall use the symbol ⊣⋮ to indicate a monomeric unit of random configuration; on this basis, atactic and hemiisotactic polypropylene segments can be represented as shown in Charts 8 and 9, respectively.

The ideal definitions just illustrated can only be used as limiting references when referred to real polymers, due to the presence in the latter of *stereodefects*. On this delicate point, it is instructive to read the paragraph which follows, taken from an official document on stereochemical definitions and notations relating to polymers, elaborated by the Commission on Macromolecular Nomenclature of the IUPAC Macromolecular Division [19]: "Deviations from ideality arise with polymers at both molecular and bulk levels in ways that have no parallel with the ordinary small molecules of organic or inorganic

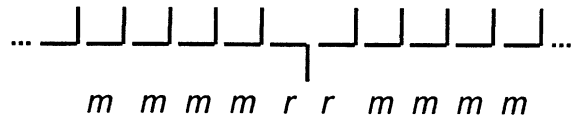

Chart 10.

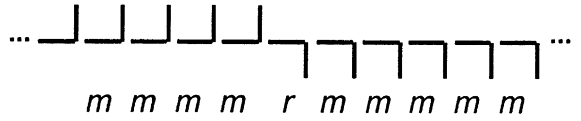

Chart 11.

chemistry. Although such deviations are not explicitly taken into account in the (proposed) definitions […], the nomenclature recommended can usefully be applied to the *predominant* structural features of real polymer molecules, if necessary with self-explanatory, if imprecise, qualifications such as *almost completely isotactic* or *highly syndiotactic*. Although such expressions lack the rigour beloved of the purist, every experienced polymer scientist knows that communication in this discipline is impossible without them".

We gratefully acknowledge the Commission for this license, of which we shall try to make good use. However, there are a few cases in which, in spite of good will and common sense, it is almost impossible to avoid ambiguity. One of special importance to this review is illustrated below.

Charts 10 and 11 show two predominantly isotactic polypropylene chain segments. In Chart 10, it is obvious that one monomeric unit has a 'wrong' configuration and represents a stereodefect (isolated *rr* triad).

The case of Chart 11 is less trivial. The structure unquestionably contains two contiguous isotactic blocks with opposite relative configurations; therefore, it can be described as a *stereoblock polypropylene* segment. On the other hand, it can also be stated that, similarly to the case of Chart 10, the whole structure is isotactic with just one stereodefect (in the form of an isolated *r* diad, rather than of an *rr* triad. As a matter of fact, in Section 2 we shall see that these two types of stereodefects are typical of isotactic chain propagation under the chiral control of the growing chain end or of the active transition metal center, respectively).

Both standpoints are formally correct. However, throughout this review we will adopt the latter, and define as stereoblock polypropylenes only materials in which the tacticity of the blocks is different in nature (e.g. isotactic/syndiotactic, isotactic/atactic) or at least in degree (e.g. highly isotactic/poorly isotactic).

2. Experimental determination of polypropylene microstructure

2.1. Before NMR

Isotactic polypropylene was the first highly stereoregular synthetic polymer ever made

[21],[2] and the chemical community was largely unprepared to face the formidable problems of the new discipline that was born along with it and is known today as macromolecular stereochemistry. As a matter of fact, even terms such as *isotactic* were invented for the occasion.

The existence of some regularity in the chemical structure of the new polymer was obvious already on inspection, in the sense that part of the material was recognized to be crystalline, and it was clear already at that time that only a regular vinyl polymer would have been able to develop crystallinity. For a lucky circumstance, already in 1942 it had been predicted by Bunn, one of the pioneers of X-ray crystallography, that if a polymer like isotactic polypropylene was ever made, it would crystallize in helical form, because the steric hindrance between contiguous methyl substituents would prevent the planar zig-zag conformation typical of straight-chain paraffins and linear polyethylene [22]. This prediction was nicely confirmed by Corradini, who recognized in the X-ray diffraction patterns of the first isotactic polypropylene samples produced in the Natta group the features of the now famous 3,1 helix (Fig. 1) [23].

If X-ray diffraction provided a means for identifying the type of tacticity of the new polymer, the quantification of its stereoregularity remained an arduous problem for several years to come. Polypropylene samples prepared with the first heterogeneous Ziegler–Natta catalysts were mixtures of macromolecules embracing an extremely wide range of stereoregularities (from highly isotactic to almost atactic), and one of the fundamental contributions of the Natta group was to develop an effective method for separating fractions with different degrees of crystallinity, based on sequential exhaustive extractions with solvents of increasingly high boiling point (Fig. 2) [24].

The first attempts to evaluate a degree of isotacticity in molecular terms on such fractions were made in the late 1950s by means of IR spectroscopy. It was observed indeed that the IR spectra of semicrystalline samples show distinctive absorptions that are absent in those of amorphous samples (either non-crystallizable or examined above their melting temperature). The intensity of these so-called 'helix' bands, assigned to normal modes of vibration of comparatively long chain segments in helical conformation due to a regular isotactic arrangement, was found to increase with increasing crystallinity. Later on, similar observations were made also on the first propene polymers with predominantly syndiotactic structure. For quantitative estimates of stereoregularity, a variety of calibration methods, based on either internal or external standards, were proposed. Their description, which would be of purely historical concern, is out of the scope of this review; interested readers can consult, e.g. Ref. [4, p. 240–246; 25].

2.2. ^{1}H NMR

Absolute determinations of stereoregularity on vinyl polymers became possible only in the 1960s, with the spreading of ^{1}H NMR [10]. For polypropylene, in particular, it is fairly obvious that the methyl, methylene and methine protons have different chemical shifts; this, however, would be of no use for tacticity measurements, if it was not for the fact that the methylene protons are sensitive to the steric environment (Fig. 3 and Chart 12) [10,26].

[2] "Nature synthesizes many stereoregular polymers, for example cellulose and rubber. This ability has so far been thought to be a monopoly of Nature operating with biocatalysts known as enzymes. But now Professor Natta has broken this monopoly." Citation from the presentation speech by Professor A. Fredga, Member of the Nobel Committee for Chemistry of the Royal Academy of Sciences, on the occasion of the official ceremony for the 1963 Nobel Prize in Chemistry awarded to Profs. Giulio Natta and Karl Ziegler. The complete transcription of the speech can be found at the official Web site of the Nobel Foundation (http://www.nobel.se/).

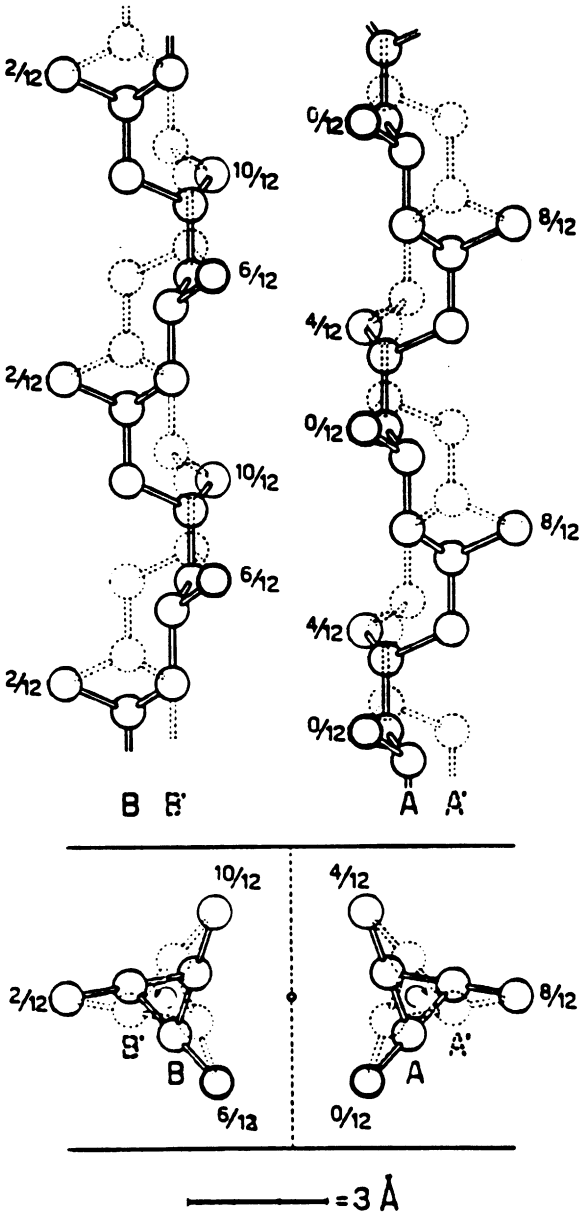

Fig. 1. The 3,1 helix of isotactic polypropylene. Reprinted with permission from J Polym Sci 1959; 39:29. © 1959 John Wiley and Sons, Inc. [23].

On inspection of Chart 12, it can be realized that the two protons of a $-CH_2-$ group in between two tertiary C atoms with opposite configurations are magnetically equivalent; in particular, each of them is *syn* to one CH_3 group (i.e. on the same side of the chain backbone in the hypothetical zig-zag conformation), and *anti* (i.e. on the opposite side) to the other. In the ^1H NMR spectrum of syndiotactic

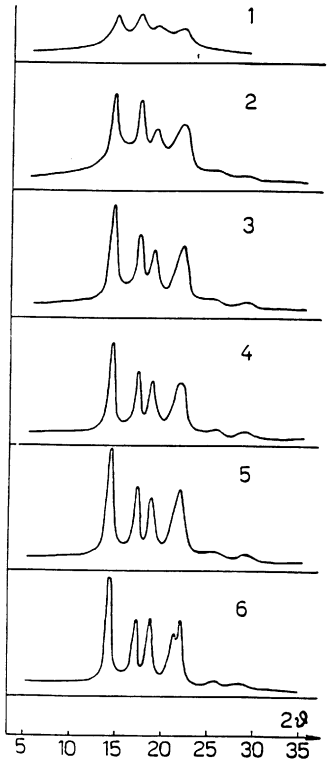

Fig. 2. Powder X-ray diffraction spectra (Cu K_α radiation) of different fractions of a polypropylene sample prepared with a $TiCl_3$-based catalyst. (1) Soluble in boiling pentane: X-ray crystallinity (X_c) = 27%, melting temperature (T_m) = 115°C; (2) Insoluble in boiling pentane, soluble in boiling hexane: X_c = 36%, T_m = 130°C; (3) Insoluble in boiling hexane, soluble in boiling heptane: X_c = 52%, T_m = 160°C; (4) Insoluble in boiling heptane, soluble in boiling 2-ethylhexane: X_c = 62%, T_m = 170°C; (5) Insoluble in boiling 2-ethylhexane, soluble in boiling octane: X_c = 64%, T_m = 174°C; (6) Insoluble in boiling octane: X_c = 66%, T_m = 175°C. (Reproduced with permission from Ref. [24]).

Chart 12.

polypropylene (Fig. 3b), they actually give rise to a single resonance (at around $\delta = 1.05$ ppm downfield of tetramethylsilane, TMS), which appears as a multiplet only due to the coupling with neighboring protons.

On the other hand, the same two protons in an isotactic arrangement are magnetically unequivalent; indeed, one is *syn* and the other is *anti* to both CH_3 groups, which means that they undergo a different shielding. As a result, in the ^1H NMR spectrum of isotactic polypropylene (Fig. 3a), the methylene resonance is split in two multiplets, at around $\delta = 1.25$ ppm (*anti* proton)

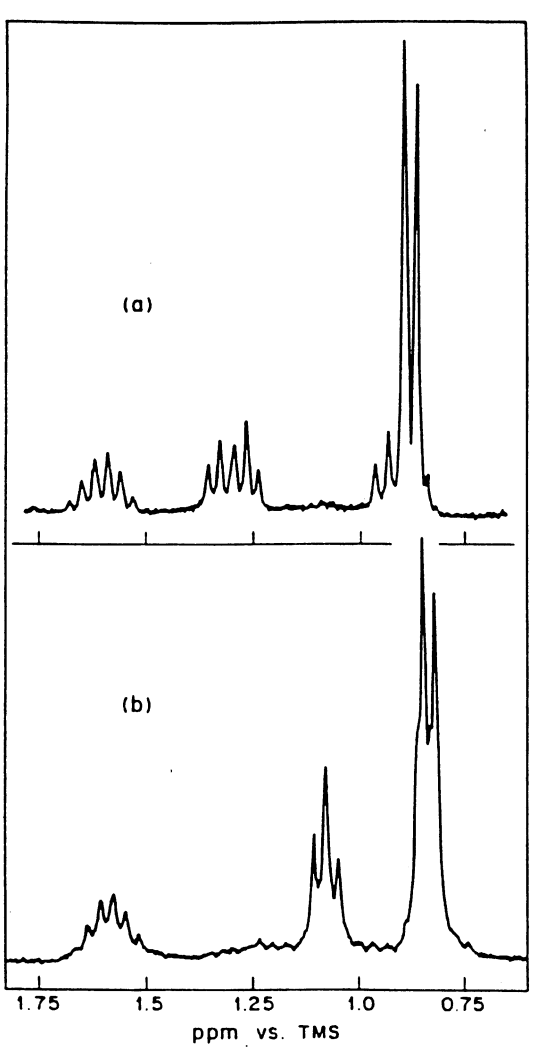

Fig. 3. 220 MHz ^{1}H NMR spectra of isotactic (a) and syndiotactic (b) polypropylene (in 1,2-dichlorobenzene at 165°C). Reprinted with permission from Chain Structure and Conformation of Macromolecules. © 1982 Academic Press, NY [10, Fig. 3.20].

and $\delta = 0.90$ ppm (*syn* proton), the latter largely overlapping the resonance of the methyl protons ($\delta = 0.87$ ppm).

Unfortunately, at variance with other vinyl polymers containing heteroatoms (such as poly(vinyl ether)s, poly(acrylate)s or poly(vinyl chloride)), for polypropylene the resolution of ^{1}H NMR is limited by the modest chemical shift spreading (less than 1 ppm), due to the fact that all protons are chemically similar [10]. This means that if it is possible to recognize the predominant tacticity of a sample, and even — from the integration of the methylene resonance — to evaluate the fractions of *meso* and *racemo* diads, a configurational analysis at the level of longer stereosequences is precluded. This limitation is

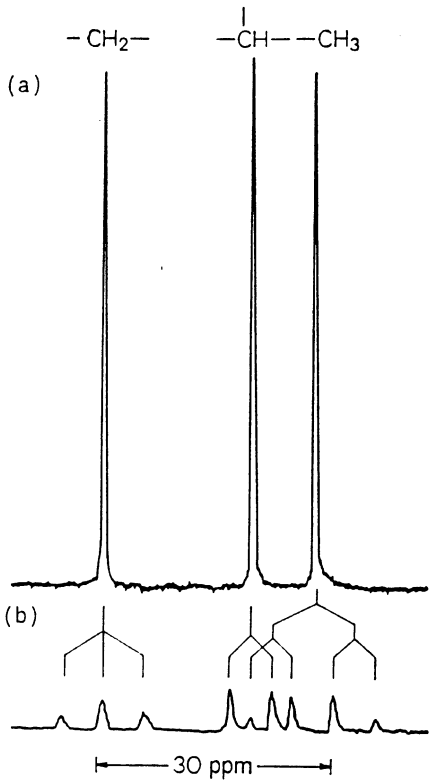

Fig. 4. 25 MHz ^{13}C NMR spectra of isotactic polypropylene (in 1,2-dichlorobenzene at 140°C). Top: proton-decoupled spectrum. Bottom: spectrum obtained without proton decoupling. Reprinted with permission from Makromol Chem 1973; 168:163. © 1973 Wiley–VCH [29].

particularly severe, because it rules out the possibility of recognizing the nature of the stereodefects, which can be diagnostic for the origin of the stereocontrol.

The problem was solved — to some extent — with the synthesis and ^{1}H NMR characterization of selectively deuterated polypropylenes, an elegant and sophisticated exercise of logics applied to stereochemistry, which resulted into a partial assignment of the methylene resonance at *tetrad* level [27,28]. However, this complicated route was abandoned as soon as Fourier transform ^{13}C NMR became available.

2.3. ^{13}C NMR

2.3.1. Polymer configuration

Fig. 4 shows one of the first published $^{13}C\{^{1}H\}$ NMR spectra of isotactic polypropylene [29]. It is fairly obvious that the three sharp peaks, of equal intensity within the experimental error, correspond to the three different C atoms in the constitutional base unit (methyl, methine and methylene). The assignment reported in the same figure was made on the basis of the semiempirical methods (developed in the 1960s) for the prediction of the chemical shifts of saturated hydrocarbons in terms of additive effects

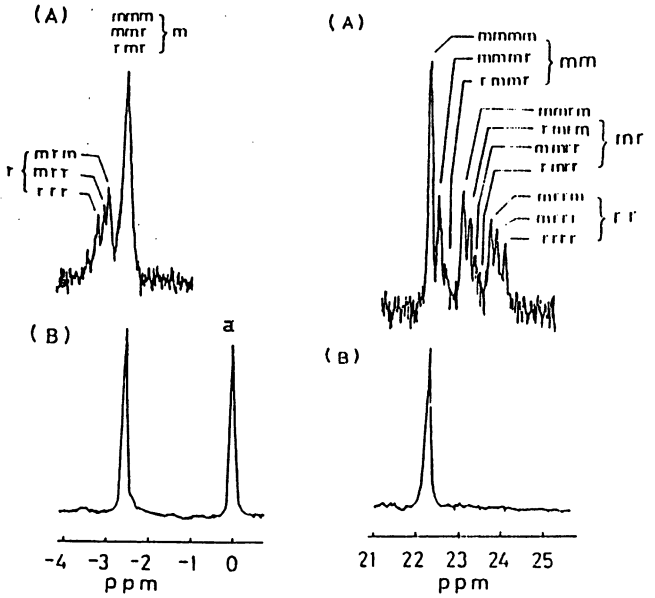

Fig. 5. Methylene (A, left) and methyl (A, right) regions of the 25 MHz ^{13}C NMR spectrum (in *trans*-decalin at 150°C; methyl region chemical shift scale in ppm downfield of TMS) of a polypropylene sample of low stereoregularity obtained with a $TiCl_3$-based catalyst, compared with the corresponding regions of the spectrum of highly isotactic polypropylene (B; peak (a) due to *trans*-decalin). Tentative attributions at tetrad (methylene) and pentad (methyl) level are also shown. Reprinted with permission from Makromol Chem 1972; 152:15. © 1972 Wiley–VCH [32].

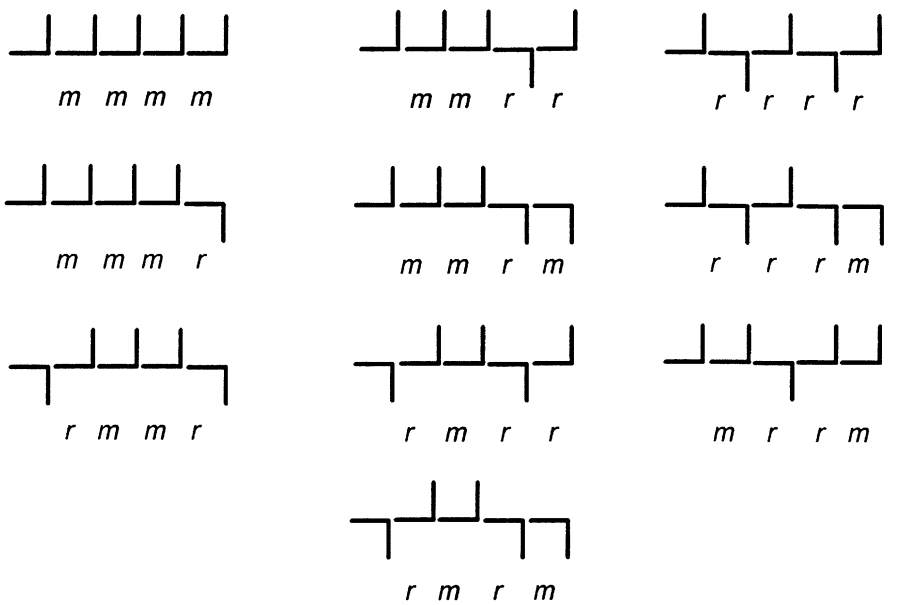

Chart 13.

Table 1
Experimental ^{13}C NMR chemical shift values (in 1,2,4-trichlorobenzene at 137°C; ppm downfield of TMS) for the methyl pentads of regioregular polypropylene [33], compared with calculated ones at the same temperature, according to the method proposed by Tonelli [11]

Pentad	δ (exp.)	$\Delta\delta$ (calc.)	δ (calc.)
mmmm	21.78	0	21.780
mmmr	21.55	−0.276	21.504
rmmr	21.33	−0.550	21.230
mmrr	21.01	−0.728	21.052
mmrm	20.85	−0.913	20.867
rmrr	20.85	−1.009	20.771
rmrm	20.71	−1.201	20.579
rrrr	20.31	−1.499	20.281
rrrm	20.17	−1.712	20.068
mrrm	20.04	−1.940	19.840

[30,31]. It is important to note that the chemical shift spreading of the spectrum is almost 30 ppm, that is over 30 times that of the proton spectrum.

Fig. 5 shows instead an early $^{13}C\{^{1}H\}$ NMR spectrum of a polypropylene fraction of low stereoregularity [32]; in this case, the same three resonances appear as complicated multiplets. It is natural to associate the fine structure with the disordered microstructure, and to infer a sensitivity of the chemical shifts to the configuration. The methyl resonance, in particular, is split in nine major peaks, and it was soon realized that these correspond to the ten non-equivalent steric *pentads* (Chart 13) [10–12]. This represented a real break-through in the evaluation of polypropylene tacticity.

In the absence of predictive methods, the attributions of Fig. 5 [32] were only tentative (with the obvious exception of the *mmmm* peak), and as a matter of fact they turned out to be partly incorrect. Reaching a definitive assignment required years of laborious investigations and the intelligent use of low-molecular-mass model compounds. In particular, the ^{13}C NMR characterization of diastereoisomeric mixtures of 3,5,7,[9-^{13}C],11,13,15-heptamethyl-heptadecanes enabled Zambelli et al. [33] to assign all steric pentads centred on the ^{13}C-labelled methyl, whose chemical shift values are practically coincident with those of the methyl pentads in polypropylene. These assignments are summarized in Table 1.

Predictive methods for the configurational dependence of the ^{13}C NMR chemical shifts of regioregular vinyl polymers were developed only in the early 1980s, when it was recognized that such a dependence has a conformational origin [11]. Previous studies on low-molecular-weight hydrocarbons had proved that in aliphatic chains, each magnetic C (**C**) is shielded by its γ substituents (when present) to an extent which is strongly affected by rotations around the C(α)–C(β) bonds; in particular, for each γ substituent, the resonance of **C** shifts upfield by approximately 5 ppm when the **C**–C(α)–C(β)–C(γ) internal rotation angle is *gauche*, relative to the case in which it is *trans*.

Fig. 6. Methyl region of the 90.5 MHz ^{13}C NMR spectra of a polypropylene sample of low stereoregularity obtained with a $TiCl_3$-based catalyst, recorded in: (a) heptane at 67°C; (b) 1,2,4-trichlorobenzene/*p*-dioxane-d_8 at 82°C; (c) 1,2,4-trichlorobenzene/*p*-dioxane-d_8 at 20°C. A line spectrum calculated to the heptad level at the temperature of observation appears below each spectrum. Reprinted with permission from Macromolecules 1980; 13:270. ©1980 American Chemical Society [38].

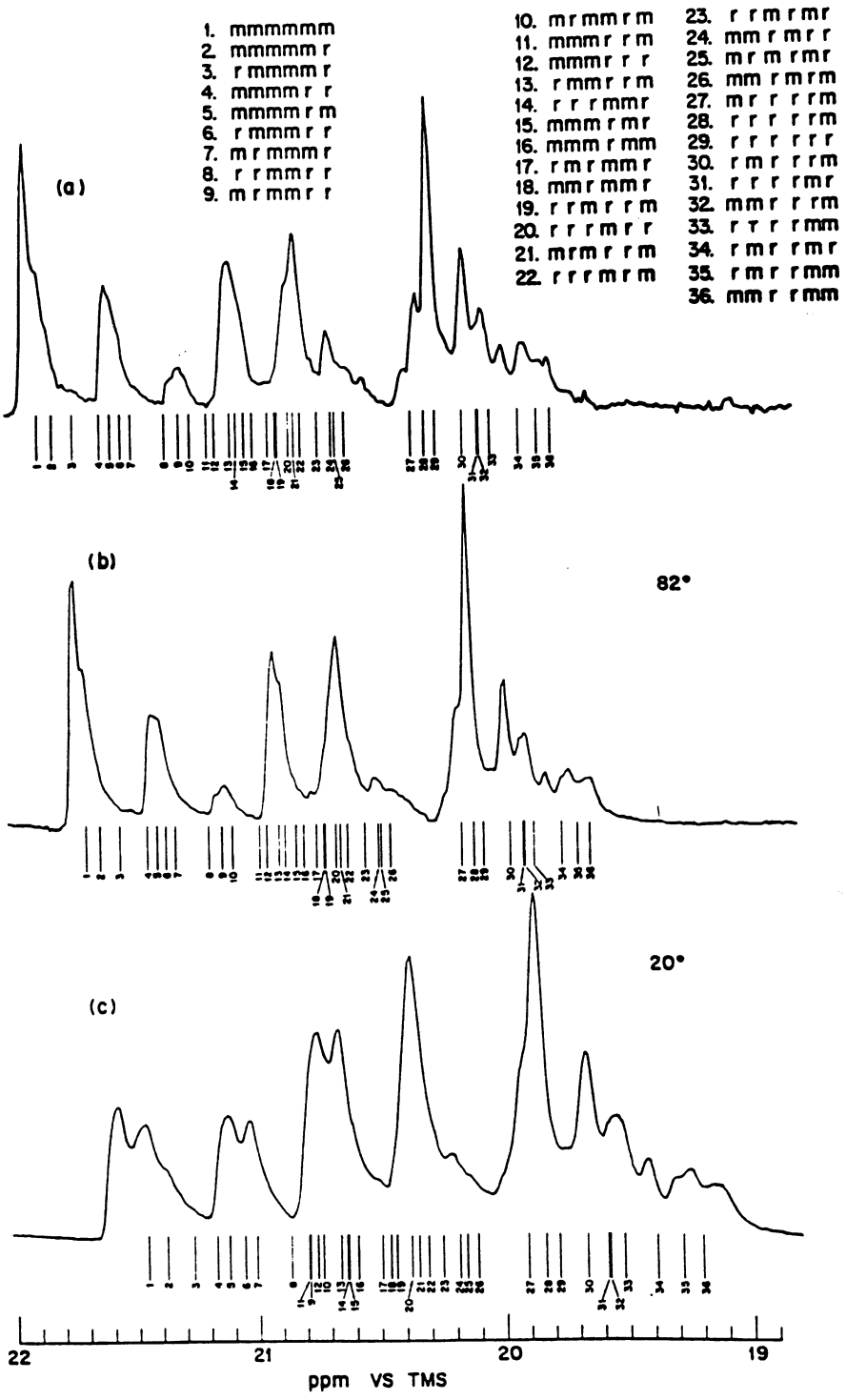
1. mmmmmm
2. mmmmm r
3. r mmmm r
4. mmmm r r
5. mmmm r m
6. r mmm r r
7. m r mmm r
8. r r mm r r
9. m r mm r r
10. m r mm r m
11. mmm r r m
12. mmm r r r
13. r mm r r m
14. r r r mm r
15. mmm r mr
16. mmm r mm
17. r m r mm r
18. mm r mm r
19. r r m r r m
20. r r r m r r
21. m r m r r m
22. r r r m r m
23. r r m r mr
24. mm r m r r
25. m r m r mr
26. mm r m r m
27. m r r r r m
28. r r r r r m
29. r r r r r r
30. r m r r r m
31. r r r r mr
32. mm r r r m
33. r r r r mm
34. r m r r m r
35. r m r r mm
36. mm r r mm
(a)
(b)
82°
(c)
20°
22
21
20
19
ppm VS TMS

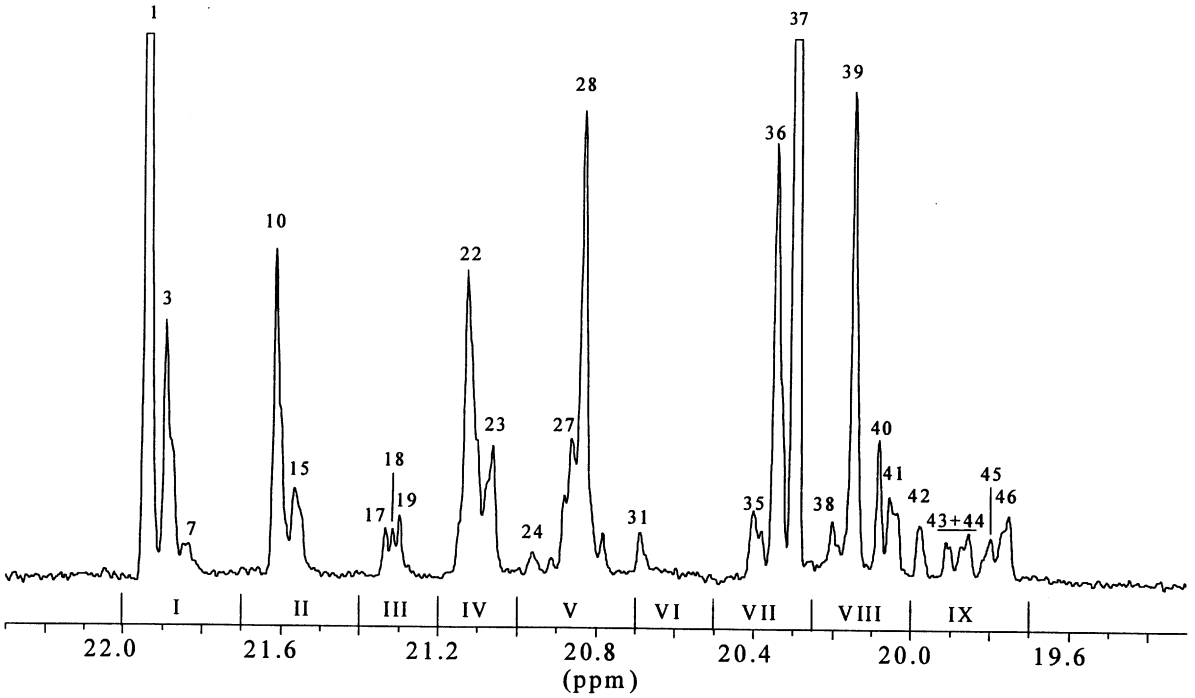

Fig. 7. Methyl region of the 150 MHz ^{13}C NMR spectrum of a polypropylene sample of low stereoregularity obtained with a $MgCl_2/TiCl_4$-based catalyst (recorded in tetrachloroethane-1,2-d_2 at 70°C; chemical shift scale in ppm downfield of TMS). Peak numbering refers to the full assignment reported in Refs. [14,15]; for attributions, see Table 2 (adapted from Ref. [39]).

Of course, aliphatic chains are flexible, and in solution they undergo continuous conformational rearrangements. These are fast on the time scale of NMR, which means that their effects on the chemical shifts are mediated and can be expressed in terms of *average conformations*, which in turn depend on the configuration.

The previous arguments, along with the assumption of additivity of the γ effects, lead to the following equation [11]:

$$\delta = \delta_0 + \sum_i \gamma_i p_i \tag{2.1}$$

where δ is the relative chemical shift of **C**, δ_0 is the conformation-independent component of δ, and $p_i = p_i^{\mathrm{l}} + p_i^{\mathrm{r}}, p_i^{\mathrm{l}}(p_i^{\mathrm{r}})$ being the Boltzmann probability that the 'left' ('right') C(α)–C(β) bond is in the *i*th rotational state characterized by a screen parameter γ_i.

For practical use, Eq. (2.1) requires a model to describe the conformational statistics, and a weighting scheme for the conformational screen parameters. As far as the latter point is concerned, the most common approximation is that $\gamma_i \neq 0$ only when **C** undergoes at least one γ–*gauche* interaction (γ-*gauche effect*).

The first applications to regioregular polypropylene are due to Provasoli and Ferro [34], who made use of the three-state rotational isomeric state (RIS) model of Boyd and Breitling [35], and to Tonelli [36], who adopted instead the more advanced five-state RIS model of Suter and Flory [37]. The calculated

Table 2
Assignment and chemical shift values of the methyl resonances in the 150 MHz ^{13}C NMR spectrum of Fig. 7 [14,15,39]

Peak no.	Assignment	δ (exp.) (ppm)	δ (calc.)[a] (ppm)
1	*mmmmmm*	21.94	21.900 (52)
3	*mmmmmr*	21.89	21.805 (44)
7	*rmmmmr*	21.83	21.710 (36)
10	*mmmmrr*	21.61	21.634 (40)
15	*rmmmrr*	21.56	21.538 (32)
17	*mrrmmrrm*	21.33	21.385 (10)
18	*mrrmmrrr*	21.31	21.371 (10)
19	*rrrmmrrr*	21.30	21.351 (10)
22	*mmmrrm* +	21.13	21.183 (39)
	mmmrrr		21.137 (37)
23	*rmmrrm* +	21.06	21.082 (31)
	rmmrrr		20.035 (29)
24	*mmmrmr*	20.96	21.030 (39)
27	*rrmrrm*	20.86	20.896 (28)
28	*rrmrrr*	20.83	20.846 (26)
31	*rrmrmr*	20.68	20.730 (28)
35	*mrrrrm*	20.40	20.358 (30)
36	*mrrrrr*	20.34	20.298 (28)
37	*rrrrrr*	20.29	20.236 (25)
38	*mrrrmr*	20.20	20.156 (31)
39	*rrrrmr*	20.14	20.090 (28)
40	*mrrrrmmr*	20.08	20.021 (10)
41	*rrrrrmmm* +	20.05	20.013 (11)
	mrrrrmmm		19.994 (12)
42	*rmrrmr*	19.98	19.934 (31)
43	*mmrrmr*	19.91–19.85	19.854 (37)
44	*rmmrrmmr*	19.85	19.795 (15)
45	*mmmrrmmr*	19.80	19.773 (14)
46	*mmmrrmmm*	19.76–19.75	19.743 (16)

[a] According to Ref. [14].

values of chemical shifts (at 137°C) for the methyl pentads according to Tonelli are compared with the experimental values in Table 1; the agreement is fairly good.

Later on, Schilling and Tonelli [38] reported calculations of chemical shifts for the methyl, methylene and methine resonances at heptad, hexad and pentad level, respectively. However, the resolution of the ^{13}C NMR spectra available at that time did not allow a reliable match with experimental values (Fig. 6).

This has been made possible only in recent years by the use of modern high-field spectrometers. In particular, Busico, Segre and coworkers have published the full assignment of the 150 MHz ^{13}C NMR spectra of regioregular polypropylene at heptad/undecad level for the methyl resonance, hexad/decad level for the methylene resonance, pentad/heptad level for the methine resonance [13–15]. As an example, Fig. 7 shows the methyl region of the 150 MHz ^{13}C NMR spectrum of a polypropylene fraction of poor stereoregularity, similar to that characterized by Schilling and Tonelli at 90 MHz (Fig. 6); peak attributions are given in Table 2.

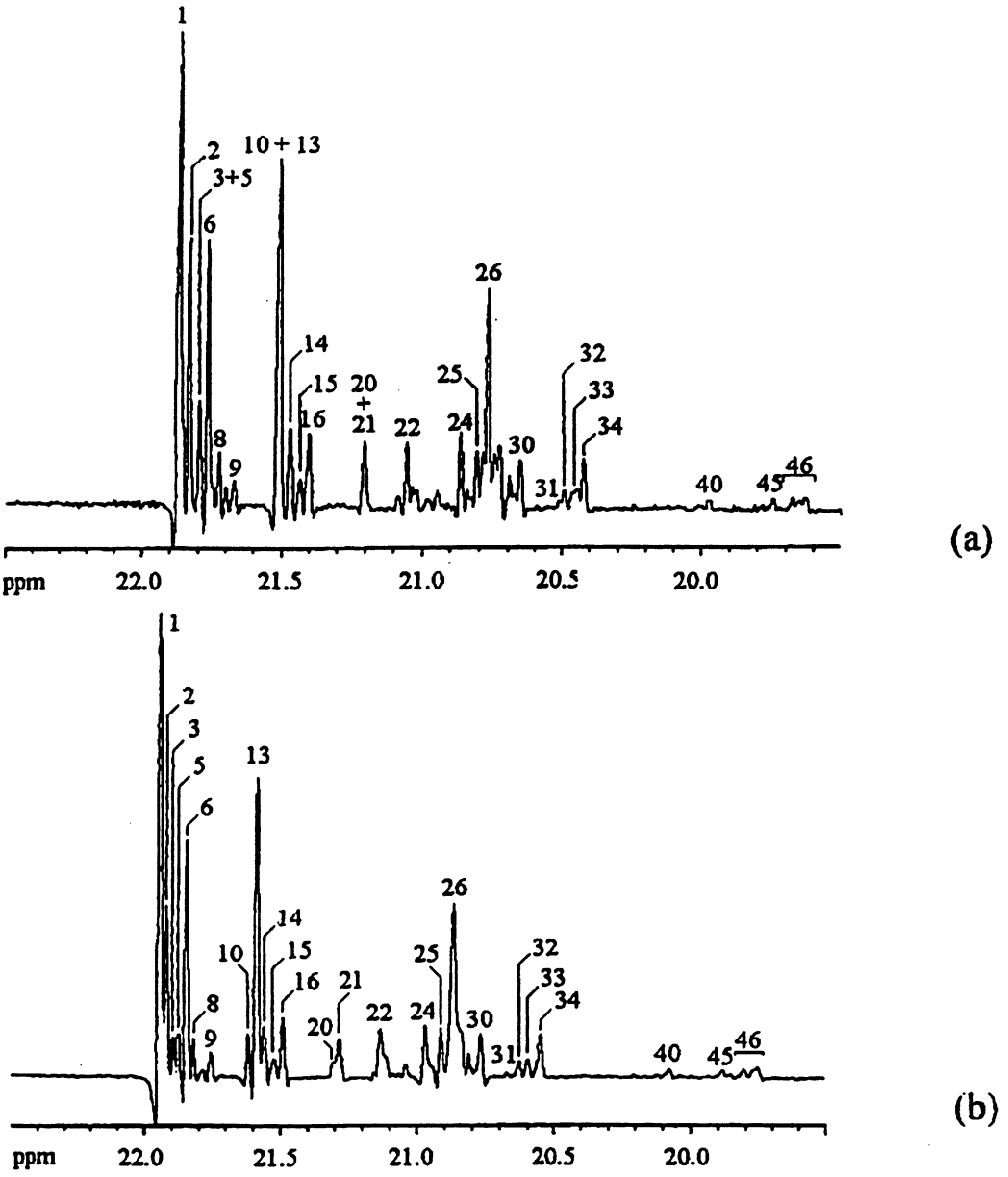

Fig. 8. Methyl region of the 150 MHz ^{13}C NMR spectra of a predominantly isotactic polypropylene sample (obtained with the catalyst system Cp_2TiCl_2/MAO at −30°C), recorded at 70°C in cyclohexane-d_{12} (a) and in tetrachloroethane-1,2-d_2 (b). The chemical shift scale is in ppm downfield of TMS. Peak numbering refers to the full assignment reported in Refs. [14,15]; for attributions and comparison of chemical shift values, see Table 3. Reprinted with permission from Macromolecules 1997; 30:6251. ©1997 American Chemical Society [14].

Table 3
Assignment and relative chemical shift values of the methyl resonances in the 150 MHz ^{13}C NMR spectra of Fig. 8 [14]

Peak no.	Assignment	$\Delta\delta$ (exp.)[a] (ppm)	
		Cyclohexane-d_{12}	Tetrachloroethane-1,2-d_2
1	*mmmmmmmm*	0.00	0.00
2	*mmmmmmmmmrm*	−0.04	−0.02
3	*mmmmmmmrr*	−0.08	−0.05
5	*mmmmmmmrmr*	−0.08	−0.07
6	*mmmmmmmrmm* + *rmmmmmmrmm*	−0.11	−0.10
8	*rmmmmmrm*	−0.15	−0.12
9	*mrmmmmrm*	−0.20	−0.19
10	*mmmmmrrm*	−0.36	−0.33
13	*mmmmmrm* + *mmmmmrmm*	−0.36	−0.36
14	*rmmmmrmm*	−0.40	−0.38
15	*rmmmrr* + *rrmmmrmm* + *mrmmmrmr*	−0.44	−0.42
16	*mrmmmrmm*	−0.47	−0.45
20	*mrmmrr*	−0.67	−0.64
21	*mrmmrm*	−0.67	−0.66
22	*mmmrrm*	−0.82	−0.81
24	*mmmrmr*	−1.00	−0.97
25	*mmmmrmmr*	−1.06	−1.03
26	*rmmmrmmm* + *mmmmrmmm*	−1.08 −1.10	−1.08
30	*mrmmrmmm*	−1.21	−1.17
31	*rrmrmr*	−1.35	−1.27
32	*rrmrmm*	−1.37	−1.31
33	*mrmrmr*	−1.43	−1.34
34	*mrmrmm*	−1.45	−1.39
40	*mrrrmm*	−1.90	−1.87
45	*mmmrrmmr*	−2.13	−2.14
46	*mmmrrmmm*	−2.22	−2.19

[a] The δ scale is referred to the *mmmmmmmm* noned, set at $\delta = 0$ ppm.

From the comparison between experimental and calculated chemical shifts, it is immediately apparent that the predictive methods based on Eq. (2.1) and the γ-*gauche* approximation are inadequate to such a level of detail. This is by no means surprising; indeed, it can be seen from Fig. 7 that at 150 MHz the fine structure is revealed with a separation between neighboring peaks often below 0.05 ppm, whereas Fig. 8 and Table 3 prove that a different choice of the solvent used for the measurements results in variations of relative chemical shift values up to 0.1 ppm. Considering that, in all semiempirical calculations of chemical shifts, solvent effects on conformer populations are neglected [11], it is not difficult to realize why resonance assignment in high-field ^{13}C NMR spectra of polypropylene cannot rely entirely on such methods, which can be taken only as a first approximation.

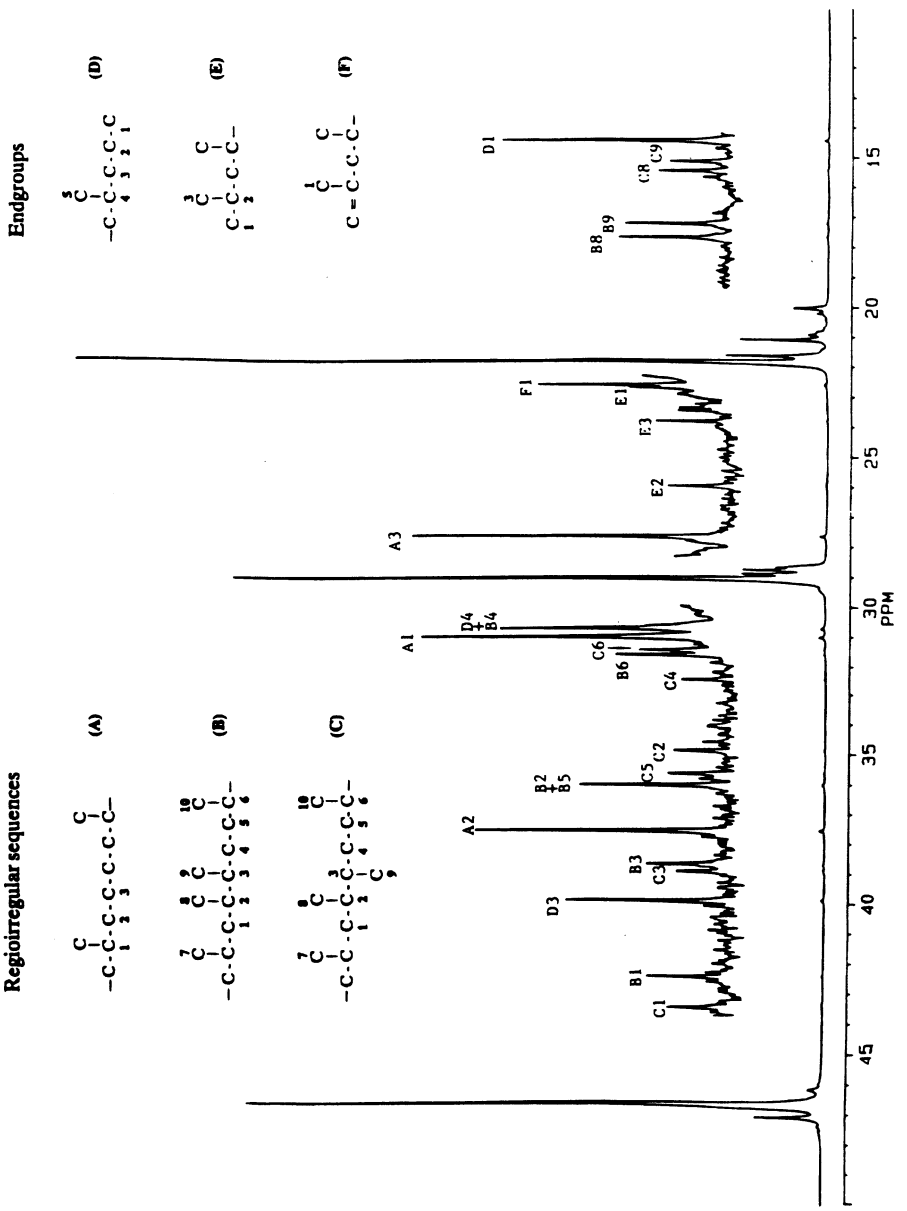

Fig. 9. 125 MHz ^{13}C NMR spectrum (in 1,2,4-trichlorobenzene at 130°C; chemical shift scale in ppm downfield of TMS) of a typical isotactic polypropylene sample prepared with a C_2-symmetric *ansa*-zirconocene catalyst. The minor peaks arising from the main regioirregular sequences and chain end-groups are explicitly assigned (reproduced with permission from Ref. [40]).

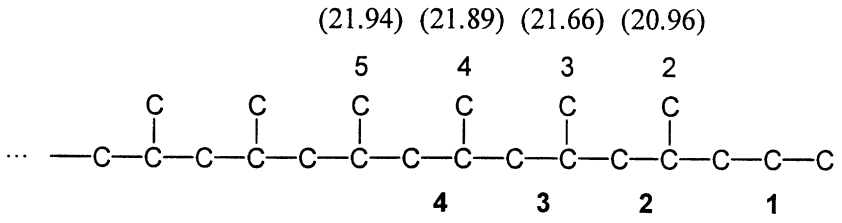

Chart 14.

In this respect, the assignment of spectra like that of Fig. 7 represented a problem similar to that faced at the time of the early low-field spectra before the *γ-gauche* approach. The solution came once again from the characterization of model compounds [13–15], this time in the convenient form of polypropylenes of known and controlled configuration prepared with suitable homogeneous catalysts (fortunately become available since the late 1980s) [7,8,16].

As we shall see, high-field ^{13}C NMR has opened new perspectives in the configurational analysis of propene polymers, and in this review 150 MHz ^{13}C NMR microstructural data will always be used when available. It is worth noting, however, that the fine structure of such spectra is strongly dependent on the experimental conditions (and in particular on acquisition temperature, nature of the solvent, sample concentration); this means that anyone working at this level of detail must be aware that the acritical use of literature attributions may lead to misguesses. A general protocol for the interpretation of high-field ^{13}C NMR polypropylene spectra has been proposed in Ref. [14].

2.3.2. Polymer constitution

Regioirregular monomeric units in predominantly head-to-tail polypropylene have distinctive ^{13}C NMR chemical shifts and can be easily identified, provided that their concentration is high enough for detectability (for samples at natural ^{13}C abundance, the threshold is somewhere in between 0.1 and 1 mol%, depending on the experimental setup and on polymer configuration). The same applies to chain end-groups.

The additive rules for the prediction of ^{13}C NMR chemical shifts of aliphatic hydrocarbons [30,31] can be used advantageously for polypropylene, although the latter case is complicated by tacticity effects. On the other hand, rather complete assignments can be found in the literature for the most common regioirregularities and end-groups (both saturated and unsaturated) occurring in polypropylene chains (see, for instance, Fig. 9 [40] and Refs. [8,40–47]).

An important point to keep in mind is that sequences of monomeric units close to regioerrors or to end-groups have 'anomalous' values of chemical shifts, and that this can affect the measurement of polymer stereoregularity to a substantial extent. As an example, Chart 14 shows an isotactic polypropylene segment ending with a propyl group (the most common saturated chain end).

The experimental values of the chemical shifts (in dichloroethane-1,2-d_2 at 70°C, in ppm downfield of TMS) for all methyl Cs in the sequence are also given in the chart. It can be noted that, moving from the propyl end towards the chain interior, three monomeric units (labelled as **2**, **3** and **4** in the chart) are needed before the δ value of the methyl groups converges to that typical of isotactic polypropylene. Unfortunately, the $\delta(CH_3)$ values for such three *stereoregular* units are very close to those of monomeric units far from the chain ends and centred in (*mmrm* + *rmrr*), *mmmr* and *mmmmmr* sequences (20.96, 21.61 and 21.89 ppm, respectively [14]). If this is not taken into account when evaluating the

stereosequence distribution from the methyl resonance, polymer tacticity is underestimated, the more so the higher is the fraction of chain ends.

The main types of regioirregularities and of end-groups specific to the various microstructural classes of polypropylene will be discussed in detail in Section 4. Before concluding this section, however, we give a brief account of the techniques of selective ^{13}C enrichment implemented in order to overcome the problems arising from the low sensitivity of natural abundance ^{13}C NMR, which often fails — as already noted — to detect such structural features.

Propene polymerizations promoted by transition metal catalysts in combination with a *^{13}C-labelled alkylating agent* (typically, an Al-Alkyl or Zn-Alkyl) can be carried out in order to investigate the regio- and stereoselectivity of the first monomer insertion(s). The mechanistic relevance of this approach can hardly be overestimated; indeed, it allowed to determine the preferred monomer insertion mode (1,2 or 2,1) in most regioselective propene polymerizations [48]. As an example, when using $Al(^{13}CH_3)_3$ as the co-catalyst, the ^{13}C NMR observation of $-CH_2-CH(CH_3)-^{13}CH_3$ end-groups is a strong indication that the predominant insertion mode is 1,2.

Additional, unexpected features can also be discovered. In particular, already in the 1970s Zambelli and coworkers found out [48–50] that in isotactic propene polymerization promoted by heterogeneous Ziegler–Natta catalysts, the enantioselectivity of 1,2 monomer insertion into initial Mt–(^{13}C-enriched-Alkyl) bonds is different from that of the subsequent ones: they observed no enantioselectivity for insertion into a $Mt-^{13}CH_3$ bond and only partial enantioselectivity for that into a $Mt-^{13}CH_2-CH_3$ bond, even when the following propagation steps were almost completely enantioselective. These findings highlighted the steric requirements for the asymmetric induction, and proved — in particular — that for the onset of the stereocontrol it is necessary that the alkyl group bound to the active metal has at least two C atoms. An explanation was provided by molecular mechanics studies on models of Ziegler–Natta active sites carried out by Corradini and coworkers [20,51], indicating that the chiral ligand environment of the transition metal constrains the first C–C bond of the growing polymer chain (when present) to a chiral orientation, which in turn forces the incoming monomer to insert with the CH_3 substituent *anti* to the said C–C bond (*growing chain orientation* mechanism). A similar behavior was documented [48,52] and explained [51] by the same research groups for the newly developed homogeneous C_2-symmetric metallocene catalysts [7,8] (and seems to have been recently re-discovered in Ref. [53]).

The use of *^{13}C-enriched ethene*, on the other hand, can help quantify polymer regioregularity. In many cases, indeed (e.g. polypropylenes produced with heterogeneous Ziegler–Natta catalysts), the concentration of regiodefects is too low for natural abundance ^{13}C NMR. In other cases, like that of isotactic polypropylene prepared with C_2-symmetric *ansa*-metallocene catalysts, the regioirregular sequences may well occur in comparatively high cumulative amounts (typically, 0.5–1 mol%), but also in different forms: the misinserted units with 2,1 enchainment can be followed, e.g. by 1,2 units with opposite configurations (Charts 15 and 16) and/or rearrange to 3,1 units (Chart 17; on this point, see Section 4.2.2.3). This results in an increased number of resonances with correspondingly lower individual intensities.

A possible (though prohibitively expensive) way-out would be to homopolymerize ^{13}C-enriched propenes (e.g. propene-[3-^{13}C]).

In the case of predominant 1,2 insertion mode, however, a convenient alternative is provided by the polymerization kinetics. Indeed, it is well-proved that as a rule, occasional 2,1 misinsertions strongly slow-down 1,2 propagation: the ratio of specific rates k_{pp}/k_{sp} (for definitions, see Section 1.3) is typically

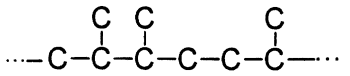

Chart 15.

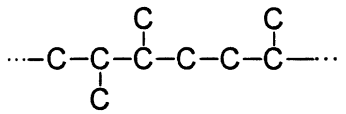

Chart 16.

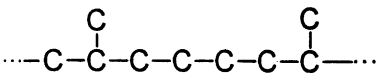

Chart 17.

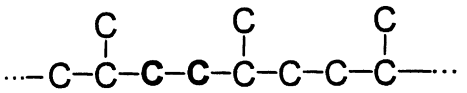

Chart 18.

in the range 10^2–10^3, which means that a growing polypropylene chain with a sterically hindered 2,1 last-inserted unit can be viewed as a *dormant* site [40,54–56].

A few molecules of small size, however, can easily react with the 'dormant' sites. One of these is ethene; as a matter of fact, it has long been known that, in a copolymerization, ethene inserts in a growing chain ending with a 2,1 propene unit (much) faster than propene [57], to the point that in the copolymers, already at very low ethene incorporations, nearly all 2,1 propene units are followed by an ethene one (Chart 18) [58].

In the ^{13}C NMR spectra of such copolymers, the resonances of isolated ethene units flanked by propene units with opposite enchainments, well assigned [43,59] and not overlapped with other peaks, can be taken as markers of the regioirregularities [58]. The important point is that by using ethene-[1-^{13}C] in the place of ethene at natural ^{13}C abundance, the threshold for the spectroscopic detectability is lowered by a factor 50 (i.e. from 0.1 to 0.002 mol%, indicatively).

This approach has been recently adopted for metallocene catalysts [58,60]. As an illustration, Fig. 10 shows, for a series of propene/ethene-[1-^{13}C] copolymers prepared in the presence of the catalyst system *rac*-$Me_2Si(1\text{-}Ind)_2ZrCl_2$/MAO (Me = methyl; Ind = indenyl; MAO = methyl-aluminoxane), a plot of the fraction (Q_{sE}) of ethene-[1-^{13}C] units following a regioirregular 2,1 propene unit vs. total ethene incorporation (Q_E). It can be seen that, for $Q_E > 2.5$ mol% (indicatively), the curve reaches a plateau, which corresponds to the 'saturation' of the dormant sites by ethene, at a value of Q_{sE} ($= 0.40 \pm 0.01$ mol%) which can be taken as the fraction of 2,1 misinsertions in propene homopolymerization. Applications of this method to several coordination catalysts will be reported in Section 4.

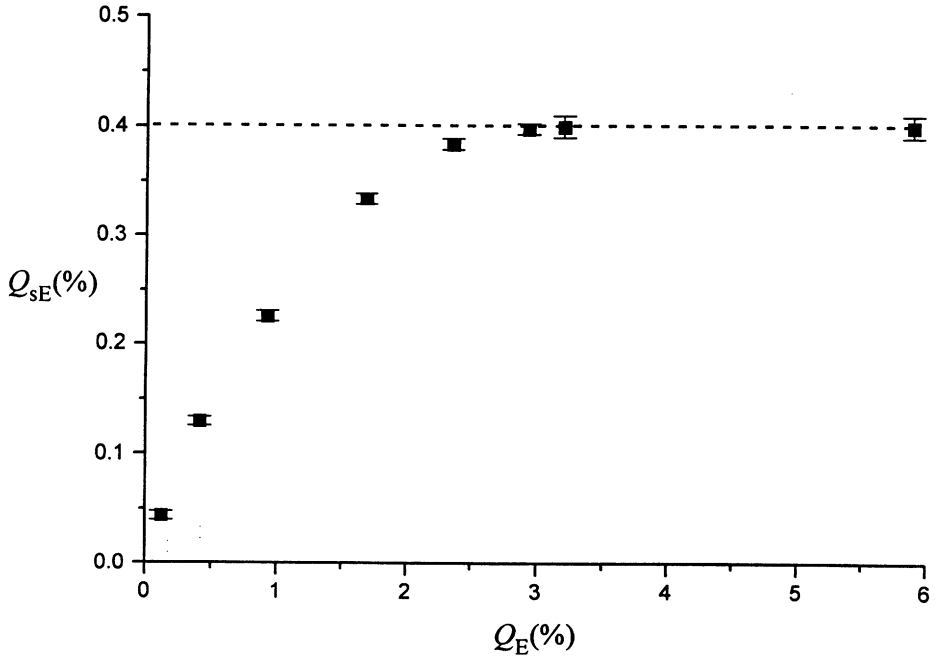

Fig. 10. Fraction of ethene-[1-^{13}C] units adjacent to a regioirregular 2,1 propene unit (Q_{sE}) vs. total ethene-[1-^{13}C] content (Q_E) for a series of propene/ethene-[1-^{13}C] copolymers prepared with the catalyst system *rac*-$Me_2Si(1\text{-}Ind)_2ZrCl_2$/MAO at 10°C. The plateau value of $Q_{sE} = 0.40\%$ can be assumed as the fraction of 2,1 misinsertions in propene homopolymerization at the same temperature (reproduced with permission from Ref. [58]).

3. Stochastic methods for the description of polypropylene configuration

In the present section, we introduce the mathematical formalism for the configurational description of regioregular polypropylene. Without loss of generality, the simple limiting cases of chain propagation under the steric control of chiral transition metal centres or of the growing chain end [20] will be used as convenient exemplifications. The occurrence of chain termination events will be neglected.

Charts 19 and 20 show the two main types of stereoerrors in predominantly isotactic polypropylene chains (see also Section 1.3, Charts 10 and 11).

The above two stereostructures have long been recognized [20] as the 'signature' of an enantioselective polymerization in which the stereocontrol is exerted by the intrinsic chirality of the catalytic species (*rr*-type stereodefects, Chart 19) or by the configuration of the last-inserted monomeric unit (*r*-type stereodefects, Chart 20). Indeed, it is easy to understand that in the former case an occasional monomer insertion with the 'wrong' enantioface, which has no effect on the chirality of the active metal, tends to remain isolated, whereas in the latter case the same occasional misinsertion inverts the chirality of the chain end and — consequently — the preferred monomer enantioface.

The two situations can be described in terms of simple Markovian models of chain propagation. We consider site control first; typically, catalysts that propagate with this mechanism are racemic mixtures of active species of opposite chirality, and in the most simple formulation the corresponding model (*enantiomorphic-site* model [61]) assumes that: (i) opposite enantiofaces of the prochiral monomer are

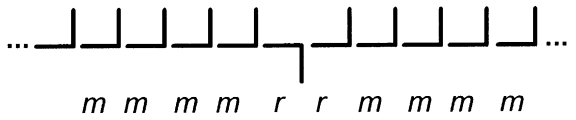

Chart 19.

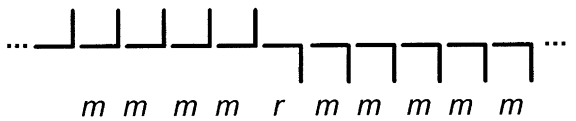

Chart 20.

preferred at catalytic sites of opposite chirality; (ii) the chirality of each catalytic site is invariant; (iii) the configuration of the last-inserted monomeric unit has no influence on the enantioselectivity.

If σ and (1-σ) are the conditional probabilities that the two opposite monomer enantiofaces are selected at an active site of given chirality, thus generating monomeric units with opposite configurations, chain propagation tends to ideal isotacticity for $\sigma \rightarrow 1$ or $\sigma \rightarrow 0$, and to ideal atacticity for $\sigma \rightarrow 0.5$. In all cases, the resulting distribution of *configurations* is Bernoullian (zero-order Markovian), and the normalized fractions of *meso* and *racemo* diads in the polymer are given by:

$$[m] = \sigma^2 + (1 - \sigma)^2 \tag{3.1}$$

$$[r] = 2\sigma(1 - \sigma) \tag{3.2}$$

The most common model for *chain-end-controlled propagation*, instead, assumes a first-order Markovian distribution of *configurations*, with conditional probabilities $P_{XY} = P_{YX}$ ($X = R$ or S, $Y = S$ or R), which results in a Bernoullian (zero-order Markovian) distribution of *steric diads [62]*:

$$[m] = P_m \tag{3.3}$$

$$[r] = 1 - P_m = P_r \tag{3.4}$$

Of course, the propagation is predominantly isotactic for $P_m > 0.5$; predominantly syndiotactic for $P_m < 0.5$ (with the generation of *m*-type stereodefects, Chart 21); perfectly atactic for $P_m = 0.5$.

Extending Eqs. (3.1)–(3.4) to longer stereosequences is trivial (Table 4). This analytical approach, however, becomes unfeasible in more complex cases.

Let us assume, for instance, that chain propagation can switch from site control to chain end control, and vice versa. As we shall see in Section 4, this is actually what happens for most polypropylenes produced with heterogeneous Ziegler–Natta catalysts, which contain site-controlled isotactic and (pseudo?) chain-end-controlled syndiotactic sequences, partly in the form of stereoblock macromolecules [39,63].

In this or similar cases, developing a set of equations analogous to those in Table 4 would be very complicated, and it is advisable instead to make use of an alternative formalism based on matrix multiplication techniques [13]. This requires, in the first place, to write down the stochastic matrix

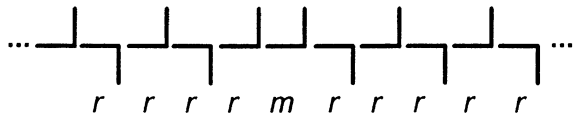

Chart 21.

(**M**) of the conditional probabilities in chain propagation. Both for the (enantiomorphic-)site (ES) model and the chain end (CE) model chosen as exemplifications, **M** is a simple 2×2 matrix, as shown below:

$\mathbf{M}_{ES} =$

	R or S	S or R
R or S	σ	1-σ
S or R	σ	1-σ

$\mathbf{M}_{CE} =$

	R	S
R	P_m	$1 - P_m$
S	$1 - P_m$	P_m

In each matrix, the rows are indexed to the configuration (S or R) of the last-inserted monomeric unit, the columns to that of the monomeric unit to be generated.

In order to evaluate the stereosequence distribution in the framework of each statistical model, let us define now matrices $\mathbf{M}_m$ and $\mathbf{M}_r$ as the matrices $[P_{ij}] = \mathbf{A}$ in which all elements P_{ij} with $(i + j)$ odd or with $(i + j)$ even, respectively, are set equal to zero. The fractional abundance of a given stereosequence

Table 4
Probability of occurrence of the steric triads and pentads according to the enantiomorphic-site (ES) [61] and to the chain end (CE) [62] model

Stereosequence	Normalized fraction	
	ES model	CE model
mm	$\sigma^3 + (1 - \sigma)^3$	P_m^2
mr	$2[\sigma^2(1 - \sigma) + (1 - \sigma)^2\sigma]$	$2P_m(1 - P_m)$
rr	$\sigma^2(1 - \sigma) + (1 - \sigma)^2\sigma$	$(1 - P_m)^2$
mmmm	$\sigma^5 + (1 - \sigma)^5$	P_m^4
mmmr	$2[\sigma^4(1 - \sigma) + (1 - \sigma)^4\sigma]$	$2P_m^3(1 - P_m)$
rmmr	$\sigma^3(1 - \sigma)^2 + (1 - \sigma)^3\sigma^2$	$P_m^2(1 - P_m)^2$
mmrr	$2[\sigma^4(1 - \sigma) + (1 - \sigma)^4\sigma]$	$2P_m^2(1 - P_m)^2$
mmrm	$2[\sigma^3(1 - \sigma)^2 + (1 - \sigma)^3\sigma^2]$	$2P_m^3(1 - P_m)$
rrmr	$2[\sigma^3(1 - \sigma)^2 + (1 - \sigma)^3\sigma^2]$	$2P_m(1 - P_m)^3$
rmrm	$2[\sigma^3(1 - \sigma)^2 + (1 - \sigma)^3\sigma^2]$	$2P_m^2(1 - P_m)^2$
rrrr	$\sigma^3(1 - \sigma)^2 + (1 - \sigma)^3\sigma^2$	$(1 - P_m)^4$
rrrm	$2[\sigma^3(1 - \sigma)^2 + (1 - \sigma)^3\sigma^2]$	$2P_m(1 - P_m)^3$
mrrm	$\sigma^4(1 - \sigma) + (1 - \sigma)^4\sigma$	$P_m^2(1 - P_m)^2$

$d_1d_2\ldots d_n$, with $d_i = m$ for *meso* diads and $d_i = r$ for *racemo* diads, is given by:

$$\mathbf{f}(d_1d_2\ldots d_n) = \mathbf{f}_0^{\mathrm{T}}\mathbf{A}_1\mathbf{A}_2\ldots\mathbf{A}_n\mathbf{J} \tag{3.5}$$

where $\mathbf{A}_i = \mathbf{A}_m$ when $d_i = m$ and $\mathbf{A}_i = \mathbf{A}_r$ when $d_i = r$; $\mathbf{J} = |1\ 1\ 1\ldots|^{\mathrm{T}}$; $\mathbf{f}_0^{\mathrm{T}}$ is the vector of the stationary probabilities of the accessible states, evaluated by numerically solving the system of equations:

$$\mathbf{f}_0^{\mathrm{T}}A = \mathbf{f}_0^{\mathrm{T}} \tag{3.6}$$

For handling the case in which chain propagation can switch reversibly from site control to chain end control, all we need is to write the corresponding stochastic matrix ($\mathbf{M}_{\mathrm{ES/CE}}$), by appropriately combining matrices $\mathbf{M}_{\mathrm{ES}}$ and $\mathbf{M}_{\mathrm{CE}}$. One possibility is the following 4×4 matrix:

$$\mathbf{M}_{\mathrm{ES/CE}} = \begin{array}{c|cccc} & R & S & R & S \\ \hline R & \multicolumn{2}{c}{\mathbf{M}_{\mathrm{ES}}(1\text{-}P_{\mathrm{ES/CE}})} & \multicolumn{2}{c}{\mathbf{M}_{\mathrm{CE}}\,P_{\mathrm{ES/CE}}} \\ S & & & & \\ R & \multicolumn{2}{c}{\mathbf{M}_{\mathrm{ES}}P_{\mathrm{CE/ES}}} & \multicolumn{2}{c}{\mathbf{M}_{\mathrm{CE}}(1\text{-}P_{\mathrm{CE/ES}})} \\ S & & & & \end{array}$$

where $P_{\mathrm{ES/CE}}$ is the probability of switching from site-controlled to chain-end-controlled propagation, and $P_{\mathrm{CE/ES}}$ that of the reverse switch. In writing the matrix, it was assumed that such two probabilities are independent of the configuration of the last-inserted monomeric unit, and that the preferred chirality of monomer insertion under site control is invariant; more complex hypotheses, however, can easily be handled by suitably modifying the matrix.

The stereosequence distribution can be calculated by applying Eqs. (3.5) and (3.6), as illustrated before. The overall probability w_{ES} that monomer insertion takes place under site control (i.e. the weight fraction of site-controlled stereosequences), coincident with the sum of the first two elements of $\mathbf{f}_0^{\mathrm{T}}$, is given by:

$$w_{\mathrm{ES}} = P_{\mathrm{CE/ES}}/(P_{\mathrm{ES/CE}} + P_{\mathrm{CE/ES}}) \tag{3.7}$$

A special case is when $P_{\mathrm{ES/CE}} = P_{\mathrm{CE/ES}} = 0$ (i.e. when the steric control exerted by each catalytic species is not allowed to change during chain growth). In such a case, which can be used to treat a mixture of independent catalytic sites [63] (and correspondingly, a physical blend of polymerization products), w_{ES} is an independent parameter. Of course, $w_{\mathrm{ES}} = 1$ and $w_{\mathrm{ES}} = 0$ correspond to the limiting cases of pure site control and of pure chain end control, respectively.

In Section 4, the configurational description of the various classes of propene polymers considered will be based on this general formalism. For each specific case, the stochastic matrix of the conditional probabilities used in the calculations will be reported and motivated.

4. Microstructural types in polypropylene

4.1. Basis for the classification

The term ‘polypropylene’ does not identify a single polymer, but a variety of polymers having in common little more than the monomer used to make them. For their microstructural description, simple

stereochemical attributions like 'isotactic' or 'syndiotactic' are reductive, because they can apply to samples with totally different features (e.g. type and distribution of regio- and/or stereodefects, chain end-groups, etc.).

A better classification makes reference to the *fingerprint* left by the catalyst in the polymer. The list below may not include all known catalysts for polypropylene, but is reasonably complete in terms of microstructural types.

Homogeneous column 4 metallocene catalysts
- Metallocenes with C_{2v}-symmetry
- Bridged metallocenes with *rac*-C_2-symmetry
- Bridged metallocenes with *meso*-C_s-symmetry
- Bridged metallocenes with C_s-symmetry
- Bridged metallocenes with C_1-symmetry
- Metallocenes with 'oscillating' structure
- Bridged half-metallocenes

Homogeneous late transition metal catalysts

Ziegler–Natta catalysts
- $TiCl_3$ and $MgCl_2/TiCl_4$-based systems
- In situ $TiCl_4/AlR_3$ mixtures and other Ti-based systems
- V-based systems

Although we are firmly convinced that this taxonomic principle is sound, we admit that its application may lead to results that are not immediately obvious. As a matter of fact, most of the above cathegories embrace polymers with largely variable stereoregularity and, on the other hand, polymers with the same predominant tacticity may well turn out to be 'genetically' unrelated.

In the following, for each microstructural type in the list we discuss: (i) the main features of the catalyst and of the polymerization mechanism; (ii) chain configuration, in terms of (high-field) ^{13}C NMR stereosequence distribution, and of corresponding stochastic model of chain propagation; (iii) chain constitution and structure of the end-groups. It is important to note that, although the catalyst is the key element for the classification, the emphasis of this review is on the polymer; therefore, the description of the catalyst systems will be kept to the minimum level of detail needed for a rational understanding of polymer microstructure. On the other hand, many excellent reviews dealing primarily with catalyst synthesis and performance have recently been published [1,7,8,16–18,64], and we will make reference to them at the beginning of each (sub-)section, as well as to the original literature when that is the case.

4.2. Polypropylenes from homogeneous column 4 metallocene catalysts

4.2.1. Metallocenes with C_{2v}-symmetry

4.2.1.1. Catalysts and polymerization mechanism. Already in the 1950s, Natta et al. [65] and Breslow et al. [66] found that Cp_2TiCl_2 ($Cp = h^5$-Cyclopentadienyl), in combination with $AlEt_3$ or $AlEt_2Cl$ (Et = Ethyl), is a moderately active catalyst for the homopolymerization of ethene. Twenty

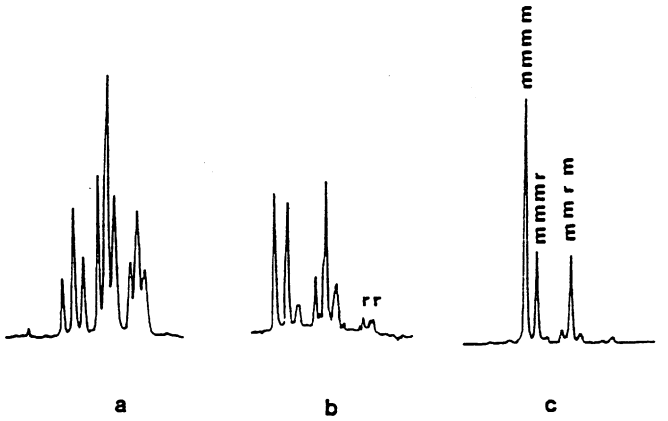

Fig. 11. Methyl region of the ^{13}C NMR spectra of polypropylene samples prepared with the catalyst system Cp_2TiPh_2/MAO at 25°C (a), 0°C (b), −45°C (c). Reprinted with permission from J Am Chem Soc 1984; 106:6355. © 1984 American Chemical Society [5].

years later, a remarkable increase in productivity was achieved by Kaminsky, using homologous Cp_2ZrX_2 complexes (X = halogen or alkyl) and methyl-aluminoxane (MAO) as the cocatalyst [67]. Cp_2ZrX_2/MAO systems promote propene homopolymerization as well, though with low activity, to atactic low-molecular-mass products [68].

Quite unexpectedly, in 1984 Ewen reported [5] the synthesis of predominantly *isotactic* polypropylene in the presence of Cp_2TiPh_2/MAO (Ph = Phenyl) below room temperature. Fig. 11 shows the methyl region of the ^{13}C NMR spectra of polymers obtained with the quoted catalyst at different reaction temperatures: it can be seen that the pattern changes gradually, from that typical of atactic polypropylene ($[m] \approx 0.5$; $[mm]$:$[mr]$:$[rr] \approx 1$:2:1) at $T = 25$°C, to that of a moderately isotactic one ($[m] \approx 0.85$) at −45°C. In the latter case, the distribution of 'defective' pentads ($[mmmr]$:$[mmrm] = 1$:1, $[mmrr] \approx 0$; Chart 22) is indicative of chain end control (1,3-*like* asymmetric induction; Section 3). In Section 1, we already commented on the opportunity of avoiding the definition *stereoblock polypropylene*, even though formally correct, in favor of *chain-end-controlled isotactic*.

Cp_2ZrX_2/MAO systems have a qualitatively similar behavior, though with slightly lower limiting stereoselectivity.

Bridged C_{2v}-symmetric metallocenes, instead, owe their interest to the fact that some of them, such as $Me_2Si(9\text{-}Flu)_2ZrCl_2$ [69] (Flu = Fluorenyl), provide a convenient access to high-molecular-mass atactic polypropylene. This is a remarkable material, which — at variance with low-molecular-weight samples, which are sticky or even oily — performs like a moderate elastomer (although the glass transition temperature (−5 to −10°C) is comparatively high) [69].

4.2.1.2. Chain configuration. The 150 MHz ^{13}C NMR spectrum of a sample of predominantly isotactic

Chart 22.

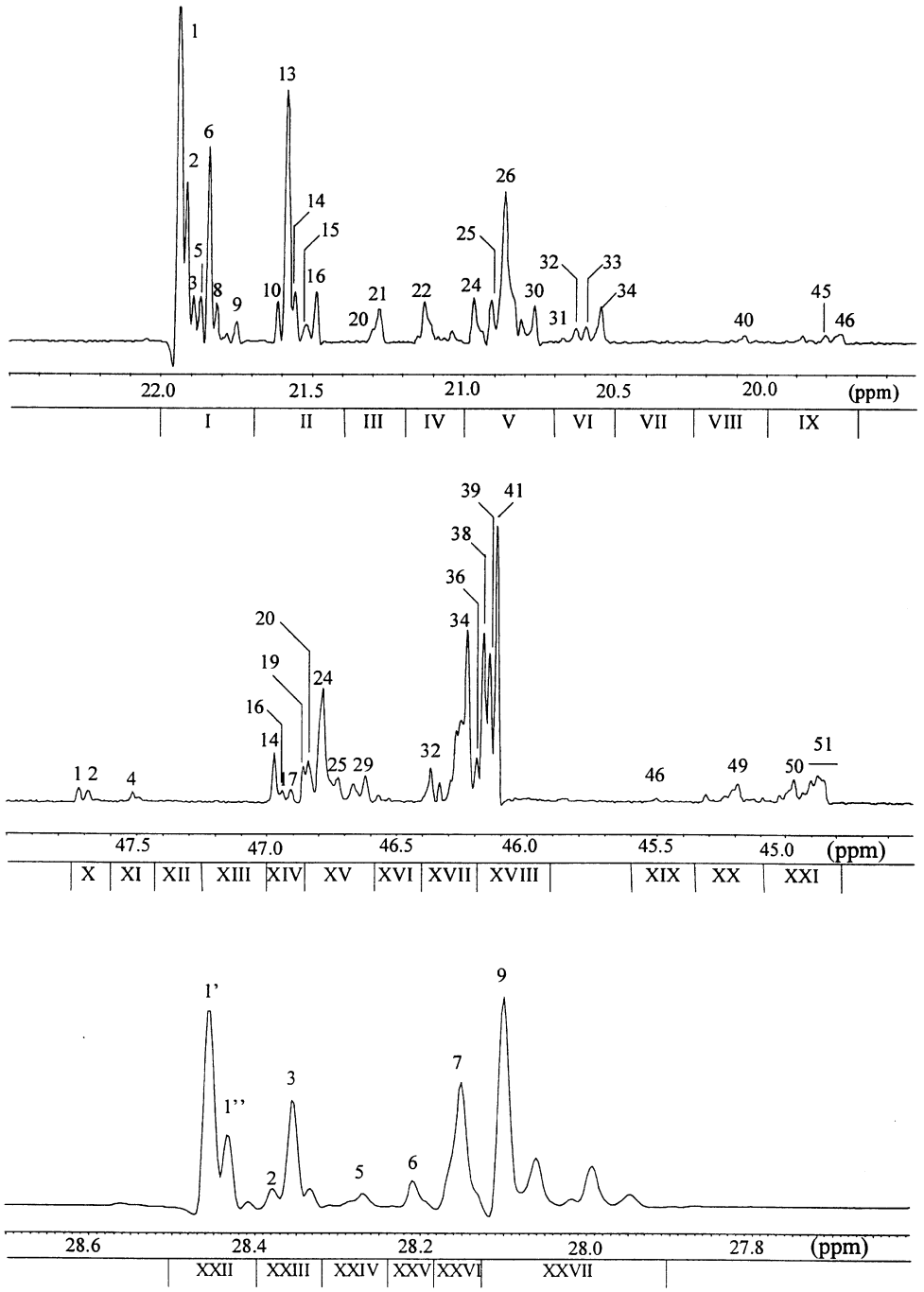

Fig. 12. Methyl (top), methylene (centre) and methine (bottom) regions of the 150 MHz ^{13}C NMR spectrum (recorded in tetrachloroethane-1,2-d_2 at 70°C; chemical shift scale in ppm downfield of TMS) of a predominantly isotactic polypropylene sample prepared with the catalyst system Cp_2TiCl_2/MAO at −30°C. Peak numbering refers to the full assignment reported in Refs. [14,15]; for attributions, see Table 5 (adapted from Refs. [14,15]).

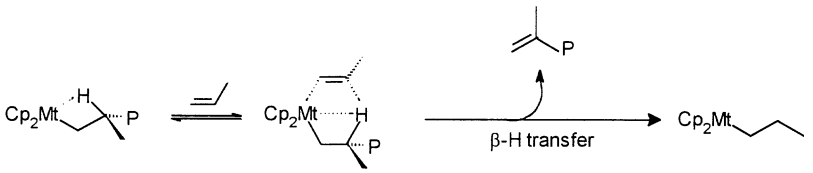

Scheme 2.

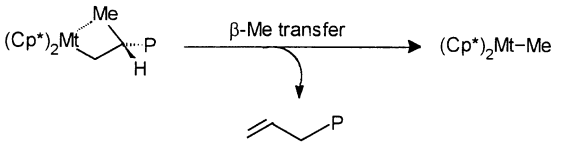

Scheme 3.

polypropylene prepared with Cp_2TiCl_2/MAO at −30°C is shown in Fig. 12; the full assignment of the spectrum is reported in Table 5 [14,15]. Due to the high regioregularity (vide infra) and to a negligible concentration of chain ends, the sample is an almost ideal model for chain-end-controlled propagation [62]; as a matter of fact, the stereosequence distribution calculated in terms of Eqs. (3.5)–(3.6) with matrix $\mathbf{M} = \mathbf{M}_{CE}$ (see Section 3) is in excellent agreement with the experimental one (as can be seen from the same Table 5) for a best-fit value of the conditional probability $P_m = 0.80$.

4.2.1.3. Chain constitution and structure of the end-groups. Although their stereoselectivity is, at most, moderate, Cp_2MtX_2 catalysts may have a remarkably high regioselectivity. ^{13}C NMR characterizations of polymers at natural isotopic abundance usually give no evidence for regioirregular units, either in the chain interior or at the chain ends [7,8,70]. However, it must be noted that in atactic or poorly tactic samples the concentration limit for ^{13}C NMR detectability is higher than in highly stereoregular ones, due to considerable peak broadening. The recent application, in the authors' laboratory, of the propene/ethene-[1-^{13}C] copolymerization method (see Section 2) has revealed, for the two systems Cp_2TiCl_2/MAO and Cp_2ZrCl_2/MAO at −10°C, a fraction of regioirregular propene enchainments of 0.03 mol% and 0.31 mol%, respectively [71].

Mainly propyl and 2-methyl-prop-1-enyl (vinylidene) end-groups are detected in the polymers by means of ^{13}C and ^{1}H NMR, which indicates that the predominant monomer insertion mode is 1,2 and that β-H elimination from a last-inserted 1,2 unit is the major chain transfer pathway. Ref. [70] gives indirect but convincing evidence that the latter process is monomer-assisted (Scheme 2). In polypropylenes prepared with related catalyst systems $(Cp^*)_2ZrX_2$/MAO ($Cp^* = h^5$-pentamethylcyclopentadienyl), on the other hand, it was found [72] that the end-groups are mainly *iso*-butyl and prop-1-enyl (vinyl), which suggests that chain transfer consists predominantly in β-methyl elimination (Scheme 3).

4.2.2. Bridged metallocenes with rac-C_2-symmetry

4.2.2.1. Catalysts and polymerization mechanism. The modification of Cp_2MtX_2 complexes aimed at the development of highly enantioselective polymerization catalysts has been carried out in several

Table 5
Assignment of the 150 MHz ^{13}C NMR spectrum in Fig. 12 [14,15]. In the last two colums, the experimental stereosequence distribution is compared with the best-fit calculated one, according to the chain end model (see text)

Range/Peak no.	δ (ppm)[a]	Assignment	Fraction (exp.) (%)	Fraction (calc.)[b] (%)
I	22.0–21.7	*mmmm*	40.0	40.8
1	21.94	*mmmmmmmm*		16.6
2	21.92	*mmmmmmmmrm*		5.3
3	21.89	*mmmmmmrr*		2.1
5	21.87	*mmmmmmmrmr*		1.3
6	21.84	*mmmmmmmrmm* +		5.3
		rmmmmmmrmm		1.3
8	21.82	*rmmmmmrm*		2.1
9	21.75	*mrmmmmrm*	1.0	1.0
II	21.7–21.4	*mmmr*	20.9	20.5
10	21.61	*mmmmmrrm*	1.8	2.1
13	21.58	*mmmmmrmr* +		2.1
		mmmmmrmm		8.4
14	21.56	*rmmmmrmm*		2.1
15	21.52	*rmmmrr* +	1.8	0.8
		rrmmmrmm +		0.5
		mrmmmrmr		0.5
16	21.49	*mrmmmrmm*	2.4	2.1
III	21.4–21.2	*rmmr*	2.5	2.6
20	21.30	*mrmmrr*		0.8
21	21.28	*mrmmrm*		1.7
IV	21.2–21.0	*mmrr*	4.7	5.2
22	21.13	*mmmrrm*	3.3	3.3
V	21.0–20.7	*mmrm* + *rmrr*	22.8	21.8
24	20.97	*mmmrmr*	3.2	3.3
25	20.91	*mmmmrmmr*	2.0	2.1
26	20.86	*mmmmrmmm* +		8.4
		rmmmrmmm		2.1
30	20.77	*mrmmrmmm*	2.1	2.1
VI	20.7–20.5	*rmrm*	4.8	5.2
31	20.67	*rrmrmr*	0.3	0.2
32	20.63	*rrmrmm*	1.0	0.8
33	20.60	*mrmrmr*	1.0	0.8
34	20.55	*mrmrmm*	2.5	3.3
VII + VIII	20.5–20.0	*rrrm* + *rrrr*	1.7	1.5
40	20.07	*mrrrmm*	0.6	0.8
IX	20.0–19.7	*mrrm*	2.5	2.6
45	19.80	*mmmrrmmr*	0.5	0.5
46	19.75	*mmmrrmmm*	1.1	1.0
X	47.75–47.60	*mrmrm*	1.7	2.1
1	47.72	*mmmrmrmmm*		0.8
2	47.69	*mmrmrmr* +		0.7
		mmmrmrmmr		0.4
XI	47.60–47.42	*mrmrr*	1.1	1.0
4	47.51	*mmrmrrm*		0.7
XII	47.42–47.28	*rrmrr* + *mrrrm*	0.4	0.6
XIII	47.28–47.02	*mrrrr*	n.d.[c]	0.3
XIV	47.02–46.85	*rmmrm* + *rrrrr*	4.2	4.1
14	46.97	*mrmmrmm*		2.6
16	46.94	*mrmmrmr or rrmmrmm*		0.7

Table 5 (*continued*)

Range/Peak no.	δ (ppm)[a]	Assignment	Fraction (exp.) (%)	Fraction (calc.)[b] (%)
17	46.92	*rrmmrmm or mrmmrmr*		0.7
XV	46.85–46.58	*rmmrr* + *mmmrm* + *mmmrr*	20.8	21.5
19	46.86	*mrmmrrm*		0.7
20	46.84	*rmmmrmm*		2.6
24	46.78	*mmmmrmm*		10.5
25	46.73	*mmmmrmr*		2.6
29	46.62	*mmmmrrm*		2.6
XVI	46.58–46.40	*rmrrm*	0.7	1.0
XVII + XVIII	46.40–45.90	*rmmmr* + *mmmmr* + *mmrrm* + *rmrrr* + *mmmmm* + *mmrrr*	57.8	56.4
32	46.37	*mrmmmrm*		1.3
34	46.23	*mmmmmrm*		10.5
36	46.19	*rmmmmmr*		1.3
38	46.17	*mmmmmmr*		10.5
39	46.14	*mmmmmmmmmr*		6.7
41	46.12	*mmmmmmmmm*		13.3
XIX	45.60–45.35	*rmrmr*	0.4	0.5
46	45.50	*mrmrmrm*		0.3
XX	45.35–45.10	*mmrmr*	4.2	4.1
49	45.19	*mmmrmrm*		2.6
XXI	45.10–44.80	*mmrmm*	8.7	8.2
50	44.97	*mmmrmmr*		2.6
51	44.87	*mmmrmmm*		5.2
XXII	28.5–28.4	*mmmmmm*	27.0	26.0
$1'$	28.45	*mmmmmmmm*		16.6
$1''$	28.43	*mmmmmmmr*		8.4
XXIII	28.4–28.32	*mmmmr*	15.2	13.1
2	28.37	*mmmmmmrr*		2.1
3	28.36	*mmmmmmrm*		8.4
XXIV	28.32–28.24	*rmmmmr*	2.0	1.6
5	28.26	*mrmmmmrm*		1.1
XXV	28.24–28.19	*mmmmrr*	2.8	3.3
6	28.20	*mmmmmrrm*		2.1
XXVI	28.19–28.13	*mmmmrm* + *rmmrr* *mmmrrm* + *mmmrrr* *mmmrmr*	18.6	21.3
7	28.15	*mmmmmrmm*		8.4
XXVII	28.13–27.90	*rmmmrm* + *rmmrrm* *rmmrr* + *mmmrmm* *rmmrmr* + *rmmrmm* *rmmr* + *rrmr* *rmrm* + *rr*	34.4	34.6
9		*mmmmrmmm*		8.4
				$P_m = 0.79_9$

[a] Downfield of TMS.
[b] According to the chain end statistical model.
[c] n.d. = not detected.

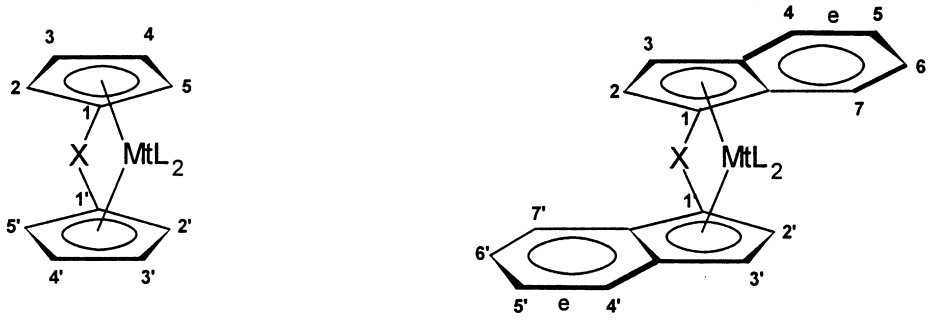

(I) (II)

Chart 23.

ways. The most obvious and — to now — also the most successful strategy towards isotactic-selective catalysts is a substitution of the Cp rings resulting in a chiral, C_2-symmetric coordination environment of the transition metal. Typical precursors can be described in terms of the two structural types (**I**) and (**II**) in Chart 23, with suitable substituents on the aromatic ligands (and usually with Mt=Zr).

The bridge connecting the two Cp rings prevents their rotation and locks them in a chiral configuration. In most cases, –X– is $–Me_2Si–$, $–Me_2C–$ or $–CH_2–CH_2–$, although a number of other examples have been reported [7,8,16]. For type (**I**), highly enantioselective catalysts can be obtained when (preferably bulky) substituents are present at positions 3,3′ or 4,4′. In type (**II**), the role of such substituents is played by the benzene rings of the 1-indenyl moieties, although additional substitution, particularly at positions 4,4′, is highly beneficial. In all cases, ancillary substituents at positions 2,2′ result in a higher average molecular mass of the polymers produced.

The stereoselectivity of catalysts derived from such complexes is well understood, and detailed molecular mechanics calculations have been reported [8,73] for models of the active species, like the one shown in Fig. 13 for a simple representative of type (**II**), i.e. *rac*-$Me_2C(1\text{-Ind})_2ZrCl_2$. The catalytic complex is pseudo-tetrahedral and cationic, with an *iso*-butyl group simulating the growing polymer chain and a propene molecule at the remaining coordination site. The aromatic ligand is in the (*R*,*R*) configuration; other possibilities (not shown) are the mirror (*S*,*S*) configuration, and the non-chiral, C_s-symmetric (*R*,*S*) configuration (see Section 4.2.3). Real catalyst precursors are usually racemic mixtures of (*R*,*R*) and (*S*,*S*) species (*rac*-complex), and should be free of the (*R*,*S*) species (*meso*-complex) which is non-enantioselective.

As is apparent from the model, the growing polymer chain must adopt a conformation that minimizes the steric interaction with one of the two C_6 rings of the bis-indenyl moiety. The first C–C bond, in particular, is bent to one side, and this in turn strongly favors the 1,2 insertion of propene with the enantioface that brings the methyl substituent *anti* to the said C–C bond (*re*-face for the (*R*,*R*)-catalytic complex, *si*-face for the enantiomorphous (*S*,*S*)-complex). 2,1 insertion, on the other hand, is always difficult due to direct steric interactions of the CH_3 group with the aromatic rings.

At the completion of each insertion step, the principle of the least-nuclear-motions suggests that the growing chain will reside at the coordination site previously occupied by the monomer (*chain-migratory* insertion mechanism [7,8]). If that is actually the case or not is immaterial for the stereoselectivity of this specific catalyst class, because the C_2 symmetry ensures the equivalence of the two active sites, which

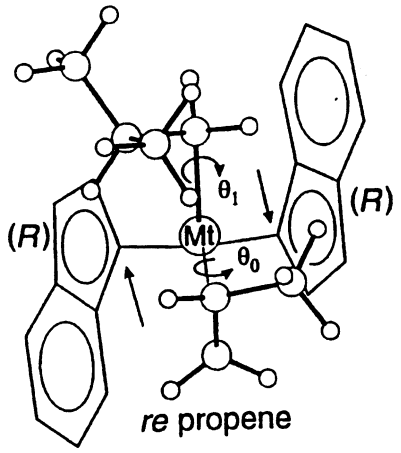

Fig. 13. Model of a (*R*,*R*)-$Me_2C(1\text{-}Ind)_2Mt(iso\text{-}Butyl)]^+$ cation (Mt = Zr), with a *re* h^2-coordinated propene molecule. The mutual arrangement of the first C–C bond of the *iso*-butyl group (simulating a growing polypropylene chain) and of the monomer is the one which minimizes the non-bonded interactions at the 1,2 insertion step (reproduced with permission from Ref. [73]).

are *homotopic* (i.e. prefer the same monomer enantioface). As a result, chain propagation is expected to be isotactic and site-controlled, with occasional …*mmmmrrmmmm*… stereodefects.

4.2.2.2. Polymer configuration. The 100 MHz ^{13}C NMR spectrum of an isotactic polypropylene sample prepared with the catalyst system *rac*-$Me_2Si(1\text{-}Ind)_2ZrCl_2$/MAO at $T = 80°C$, $[C_3H_6] = 5.7$ mol/l is shown in Fig. 14. The methyl resonance is simple, with a strong peak corresponding to the *mmmm* pentad, and much weaker ones arising from the *mmmr*, *mmrr* and *mrrm* pentads in roughly 2:2:1 integral ratio, in agreement with the hypothesis of isotactic propagation under enantiomorphic-site control. Additional small peaks are due to regioirregular sequences (see following sub-section). The pentad distribution (Table 6) can be reproduced in terms of the enantiomorphic-site model [61] (Section 3), and the conditional probability σ in the stochastic matrix $\mathbf{M}_{ES}$ has a best-fit value of 0.97.

The 150 MHz ^{13}C NMR spectrum of a second polypropylene sample, obtained with the same catalyst system and at the same temperature (80°C) but at a much lower monomer concentration ($[C_3H_6] = 0.08$ mol/l), is shown in Fig. 15. It is easy to realize that the polymer is much less stereoregular than that of Fig. 14; as a matter of fact, the experimental stereosequence distribution is still in reasonable agreement with the enantiomorphic-site model (see again Table 6), but the best-fit value of the σ parameter is as low as 0.845.

This puzzling dependence of the stereoregularity on monomer concentration is unexpected on the basis of the chain propagation mechanism discussed in Section 4.2.2.1. The existence of a general trend of decreasing stereoselectivity with decreasing $[C_3H_6]$ for the C_2-symmetric metallocene catalysts was noted by Busico and Cipullo [74], who proposed that it results from an intramolecular reaction of epimerization of the growing polymer chain, which competes with the polymerization. This explanation was validated by Leclerc and Brintzinger, who found [75] that a significant fraction of the stereoirregular units in samples of poly(propene-1-*d*) made with a number of C_2-symmetric zirconocenes contain D in

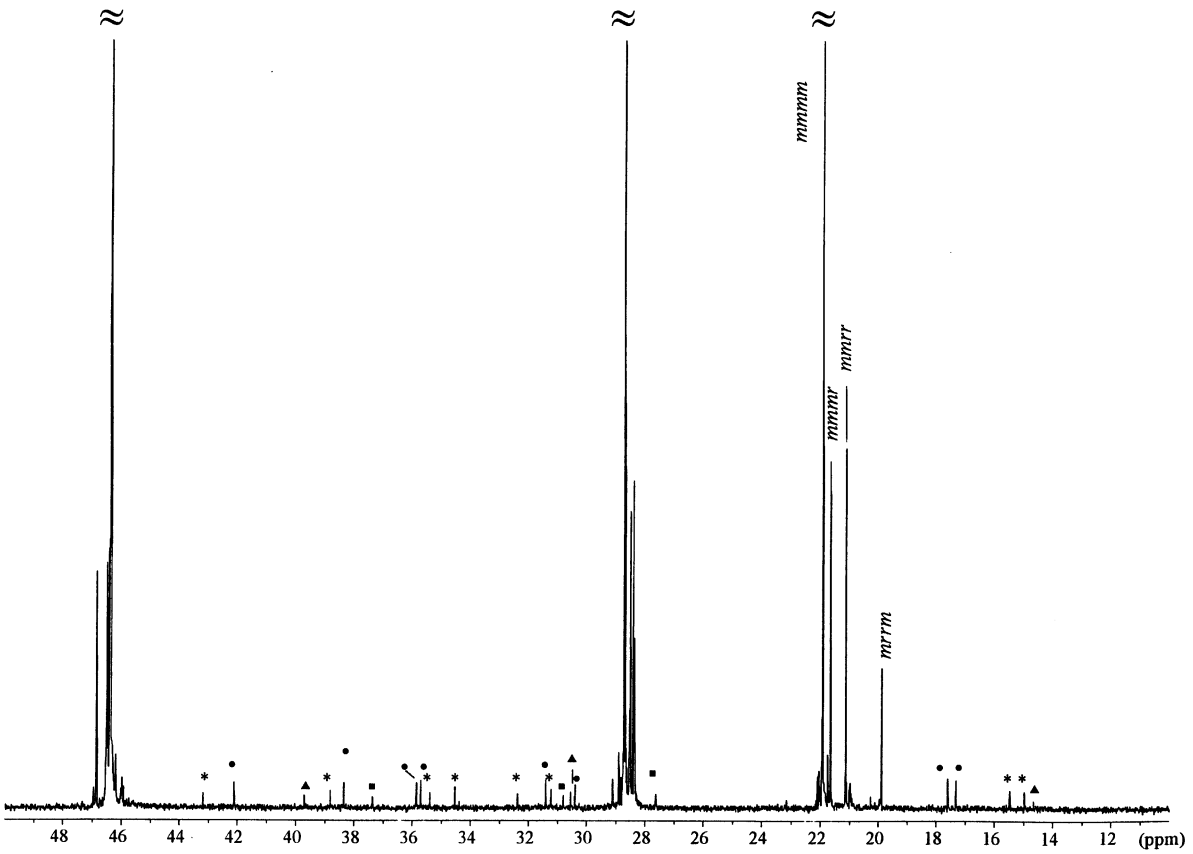

Fig. 14. 100 MHz ^{13}C NMR spectrum (recorded in tetrachloroethane-1,2-d_2 at 90°C; chemical shift scale in ppm downfield of TMS) of an isotactic polypropylene sample prepared with the catalyst system *rac*-$Me_2Si(1\text{-}Ind)_2ZrCl_2$/MAO at $T = 80$°C, $[C_3H_6] = 5.7$ mol/l (in toluene). In the methyl region, the resonances of the four main pentads in regioregular sequences are explicitly assigned. Minor peaks arising from stereoregular (●) and stereoirregular (*) isolated 2,1 units, 3,1 units (■) and propyl end-groups (▲) are also indicated.

the *methyl* group, as a result of an isomerization process. Although the mechanistic aspects are not yet completely clarified, considerable experimental [76–78] and theoretical [79] evidence has been accumulated in favor of the epimerazion pathway shown in Scheme 4.

In Fig. 16, the dependence of the stereoselectivity of *rac*-$Me_2Si(1\text{-}Ind)_2ZrCl_2$/MAO on propene concentration in the whole range from infinite dilution in toluene to liquid monomer at 80°C is compared with that of the substituted homologue *rac*-$Me_2Si(2\text{-}Me\text{-}4\text{-}Ph\text{-}1\text{-}Ind)_2ZrCl_2$/MAO [80]. Although the two curves are qualitatively similar, it can be seen that the competing effect of chain epimerization is much less important for the latter catalyst, which is more efficient with respect to chain propagation.

Not unexpectedly, the temperature has a major effect on the stereoselectivity. Increasing the temperature favors (in relative sense) chain epimerization over monomer insertion [77], and results in a decrease of enantioselectivity of the latter process (particularly for *ansa*-metallocenes of lower stereorigidity, as are those with the conformationally flexible $-CH_2-CH_2-$ bridge) [7,8].

Table 6
Steric pentad distributions evaluated from the two ^{13}C NMR spectra of Figs. 14 and 15, along with best-fit calculated ones in terms of the enantiomorphic-site model (see text)

Pentad	$[C_3H_6] = 5.7$ M		$[C_3H_6] = 0.08$ M	
	Fraction (exp.) (%)	Fraction (calc.)[a] (%)	Fraction (exp.) (%)	Fraction (calc.)[a] (%)
mmmm	86.6	86.5	43.2	43.1
mmmr	5.3	5.1	14.8	15.9
rmmr	[b]	0.1	2.1	1.7
mmrr	5.4	5.1	15.1	15.9
mmrm + rmrr	[b]	0.3	7.6	6.8
rmrm	[b]	0.2	2.8	3.4
rrrr	[b]	0.1	1.7	1.7
rrrm	[b]	0.2	4.1	3.4
mrrm	2.7	2.55	8.6	8.0
		$\sigma = 0.971$		$\sigma = 0.845$

[a] According to the enantiomorphic-site statistical model.
[b] Too weak for accurate integration.

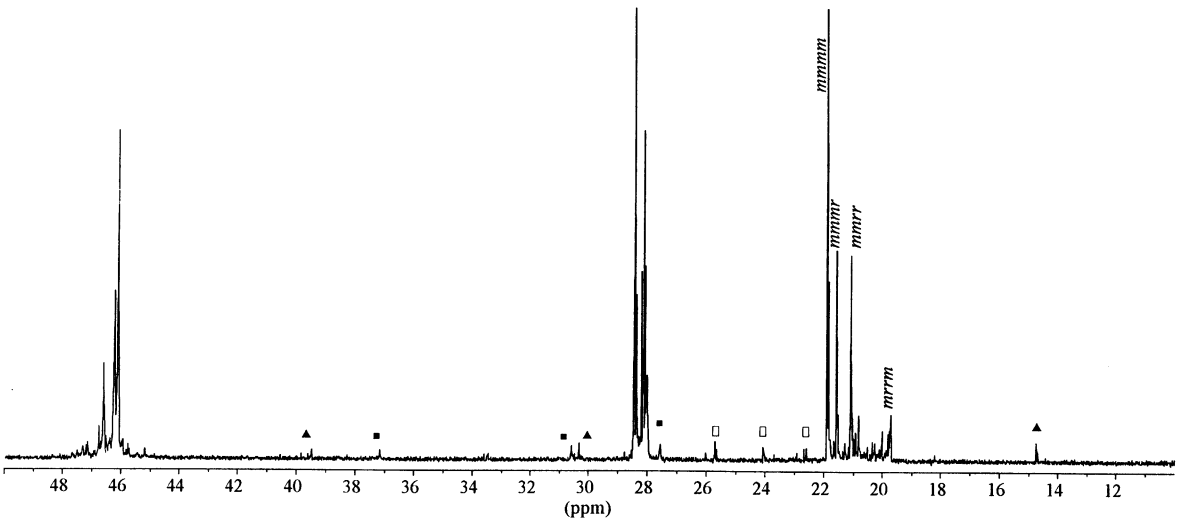

Fig. 15. 150 MHz ^{13}C NMR spectrum (recorded in tetrachloroethane-1,2-d_2 at 70°C; chemical shift scale in ppm downfield of TMS) of a predominantly isotactic polypropylene sample prepared with the catalyst system *rac*-$Me_2Si(1\text{-}Ind)_2ZrCl_2$/MAO at $T = 80$°C, $[C_3H_6] = 0.08$ mol/l (in toluene). In the methyl region, the resonances of the four main pentads in regioregular sequences are explicitly assigned. Minor peaks arising from 3,1 units (■), and from propyl (▲) and *iso*-butyl (□) end-groups, are also indicated.

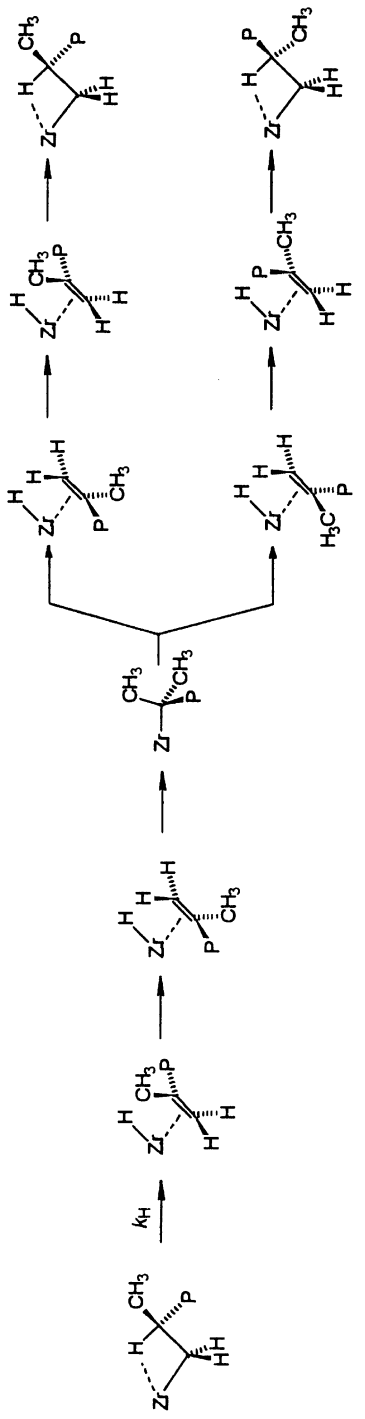

Scheme 4.

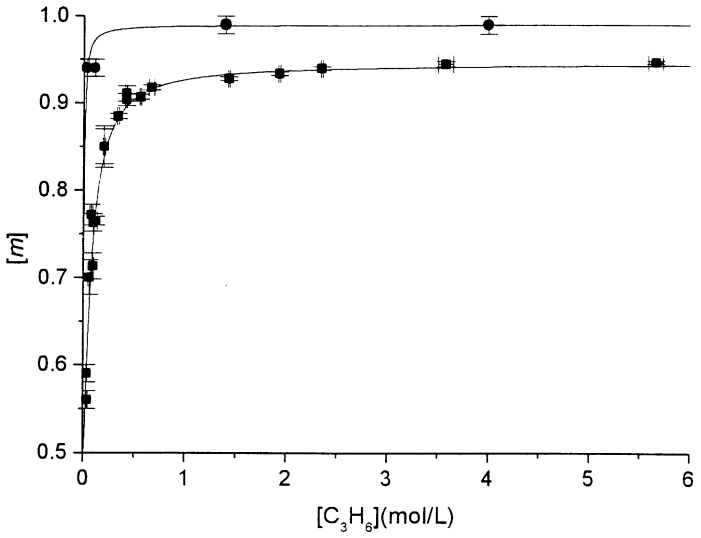

Fig. 16. ^{13}C NMR fraction of *meso* diads, [*m*] for polypropylene samples prepared at 80°C in the presence of the catalyst systems *rac*-$Me_2Si(1\text{-}Ind)_2ZrCl_2$/MAO (■) and *rac*-$Me_2Si(2\text{-}Me\text{-}4\text{-}Ph\text{-}1\text{-}Ind)_2ZrCl_2$/MAO (●), as a function of propene concentration in toluene, $[C_3H_6]$.

In view of all this, reporting a value of stereoselectivity for a given C_2-symmetric metallocene without specifying the polymerization conditions makes little sense. Indeed, in all cases the lower limit at infinite monomer dilution is nil (atactic polymer); the higher limit, on the other hand, which in some cases is not reached even in liquid propene, coincides with the enantioselectivity in monomer insertion.

Importantly, irrespective of the origin (wrong enantioselection or isomerization), the distribution of the stereoerrors in the polymer chains is always Bernoullian and in accordance with the enantiomorphic-site model. This is a classical demonstration that, as noted long ago by Price [81], "Markovian mathematics [...] is only a framework within which it is possible to describe polymer chains having particular sequential characteristics, regardless of how these chains were produced".

A number of C_2-symmetric metallocenes with remarkably high stereo- and enantioselectivities at practical polymerization temperatures ($T \geq 70$°C) have been disclosed in recent years. Polypropylenes with $[mmmm] > 0.95$ (conditional probability $\sigma > 0.99$ in matrix $\mathbf{M}_{ES}$) and melting temperature $T_m > 150$°C can be obtained with catalysts belonging to both structural types (**I**) and (**II**) of Chart 23, e.g.: *rac*-$Me_2Si(2\text{-}Me\text{-}4\text{-}t\text{-}Bu\text{-}Cp)_2ZrCl_2$ [82], *rac*-$Me_2Si(3\text{-}t\text{-}Bu\text{-}Cp)_2ZrCl_2$ [83], *rac*-$Me_2Si(2\text{-}Me\text{-}4\text{-}Ph\text{-}1\text{-}Ind)_2ZrCl_2$ [84], *rac*-$H_2C(3\text{-}t\text{-}Bu\text{-}1\text{-}Ind)_2ZrCl_2$ [85] (Bu = Butyl).

Also interesting for applications are 'softer', lower-melting polypropylenes with [*mmmm*] in the range 0.80–0.90, that can be obtained with high productivity in the presence of specific metallocenes formally deriving from structural type (**II**) of Chart 23, with a further benzene ring fused in position [*e*] of the indenyl moiety (e.g. *rac*-$Me_2Si(2\text{-}Me\text{-}Benz\text{-}[e]\text{-}1\text{-}Ind)_2ZrCl_2$ [86]).

4.2.2.3. Chain constitution. On average, C_2-symmetric metallocenes are not exceedingly regioselective in propene polymerization. Most polypropylene samples prepared with such catalysts have a content of regioirregular enchainments in the range of 0.3–1.0 mol%; however, the regioselectivity is extremely

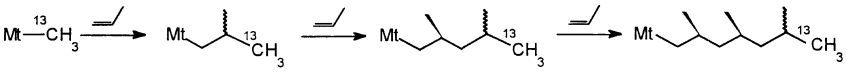

Scheme 5.

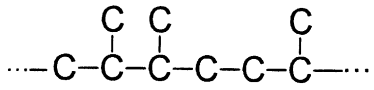

Chart 24.

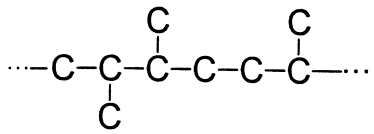

Chart 25.

sensitive to even small changes in the ligand framework [7,8]. Just as an indication of two extremes, polypropylenes with up to 20 mol% of regioerrors can be obtained, e.g. with *rac*-C_2H_4(2,4-Me_2-4,5,6,7-H_4-1-Ind)$_2ZrCl_2$ [87], whereas *rac*-H_2C(3-*t*-Bu-1-Ind)$_2ZrCl_2$ is one of the few catalysts for which the propene/ethene-[1-^{13}C] method (Section 2.3.2) failed to detect regioirregular propene enchainments (which suggests that these are below 0.002 mol%).[3]

^{13}C NMR end-group analysis proved that the predominant monomer insertion mode is 1,2. In particular, the first insertion into a Mt–$^{13}CH_3$ bond gives rise to a –CH_2–CH(CH_3)–$^{13}CH_3$ end-group; it is interesting to note that this insertion is not enantioselective (Scheme 5), which confirms the crucial importance of the first C–C bond of the growing chain for the onset of the stereocontrol (Section 2.3.2 and 4.2.2.1) [48,51–53].

The occasional 2,1 propene misinsertions tend to remain isolated. ^{13}C NMR gave evidence [40,46,47] for the two head-to-head enchainments shown in Charts 24 and 25. This indicates that: (i) 2,1 insertion is highly enantioselective (though the preferred enantioface is opposite to that favored for 1,2 insertion); (ii) the subsequent regioregular insertion occurs with lower enantioselectivity, and in some cases (e.g. metallocenes with a rather open steric environment of the transition metal, such as *rac*-C_2H_4(1-Ind)$_2ZrCl_2$ and *rac*-Me_2Si(1-Ind)$_2ZrCl_2$), appreciable amounts of the stereoirregular structure shown in Chart 25 are also formed.

As already noted in Section 2.3.2, a growing polypropylene chain with a last-inserted 2,1 unit is sterically hindered, and undergoes monomer insertion at a specific rate (k_{sp}) which, for the most crowded C_2-symmetric metallocene catalysts, can be up to 10^3 times lower than the 'normal' specific rate k_{pp} [40,56]. Therefore it can happen that, alternatively to chain propagation, this 'dormant' species isomerizes to a much less congested structure in which the last-inserted unit has a 3,1 enchainment

[3] Unpublished results from the authors' laboratory.

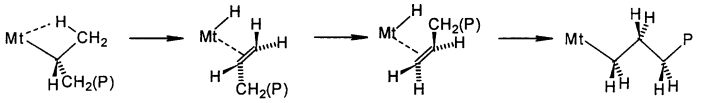

Scheme 6.

(Chart 26) [40,88]. The commonly accepted mechanism for this isomerization, very similar to that proposed for chain epimerization (Scheme 4), is shown in Scheme 6 [88].

In general, the total amount of 2,1 and 3,1 units in polypropylene samples produced with a given C_2-symmetric metallocene at a given temperature is constant, but the relative amount of 3,1 units increases with decreasing monomer concentration, because this obviously favors the intramolecular rearrangement (as already noted for the competition between monomer insertion and chain epimerization) [40]. The trend is apparent on inspection of the two ^{13}C NMR spectra of Figs. 14 and 15.

Increasing the polymerization temperature effects the regioselectivity both in absolute sense (increase of total regioerror content) and in relative sense (increase of 3,1 over 2,1 enchainments) [8,40].

4.2.2.4. Structure of the end-groups. Polypropylene samples produced with typical C_2-symmetric metallocene catalysts have mainly propyl and 2-methyl-prop-1-enyl (vinylidene) chain end-groups. Elegant kinetic studies [86] proved that chain transfer by intramolecular β-H elimination (Scheme 7a) is much slower than that assisted by the monomer (Scheme 7b), and that the latter can be effectively inhibited by ligand substitution at positions 2,2′ (e.g. with methyl groups), which shields the catalytic complex in its equatorial belt. As a matter of fact, this substitution easily results in a 10-fold increase of polymer average molecular mass [7,8].

Additional saturated end-groups that have been observed by ^{13}C NMR [8] are *iso*-butyls, which can be traced to chain tranfer with $AlMe_3$ in equilibrium with MAO (when used; Scheme 7c). ^{1}H NMR (Fig. 17), on the other hand, may reveal low amounts of but-2-enyls (vinylenes), most probably arising from (monomer-assisted) β-H elimination at a last-inserted 2,1 unit (Scheme 7d) and — more surprisingly — prop-1-enyls (vinyls). It is not clear yet whether the latter are formed via β-methyl elimination (Scheme 7e) and/or allylic activation (Scheme 7f).

In the presence of H_2 (which is a well-known molecular weight regulator in coordination polymerization catalysis), the chain ends that are formed can also be apparently non-trivial. Indeed, in addition to propyl and *iso*-butyl groups, expected for a polymerization process with high 1,2 regioselectivity (Scheme 8a and c), butyl [54,56] and — in some cases — 2,3-dimethyl-butyl ends [89,90] are also observed. The former, however, are easily understood if one considers that H_2, similarly to ethene, is much faster to react with a 'dormant' site than propene (Scheme 8b) [54,56]. 2,3-dimethyl-butyl end-groups, in turn, are a clear indication that propene insertion into an initial Mt–H bond is not highly regioselective (Scheme 8d) (in accordance with the outcome of recent mixed quantum-mechanics/molecular mechanics investigations) [90].

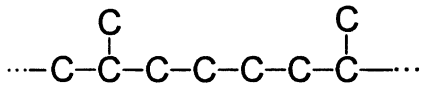

Chart 26.

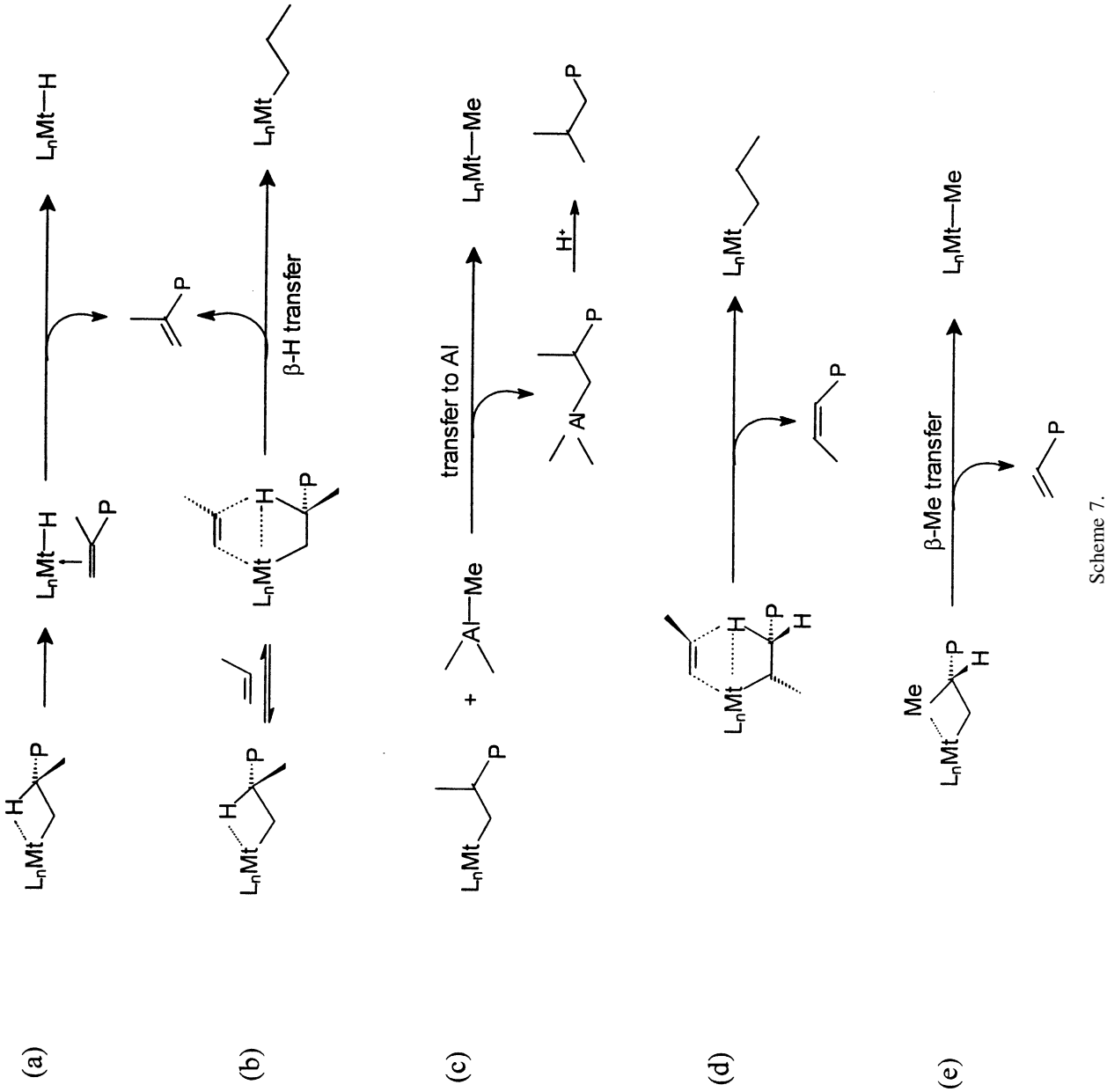

Scheme 7.

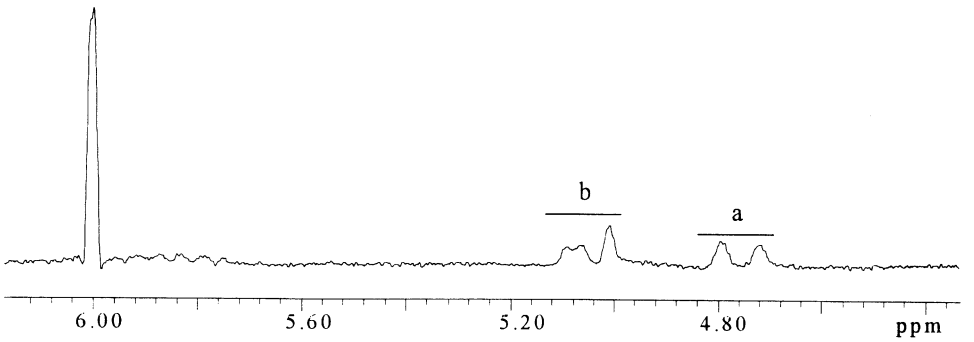

Fig. 17. Olefinic region of the 200 MHz ^{1}H NMR spectrum (recorded in tetrachloroethane-1,2-d_2 at 120°C; chemical shift scale in ppm downfield of TMS) of a polypropylene sample prepared at 80°C in the presence of the catalyst system *rac*-Me_2Si(2-Me-4-Ph-1-Ind)$_2ZrCl_2$/MAO. Resonances arising from vinylidene (a) and vinyl (b) end-groups in comparable amounts are clearly observed.

4.2.3. Bridged metallocenes with meso-C_s-symmetry

One of the draw-backs of *rac*-C_2-symmetric *ansa*-metallocene catalysts is that, either during the synthesis of the precursors or by subsequent epimerization, the *meso* form with C_s-symmetry can also be obtained (Fig. 18; see also Section 4.2.2.1) [91].

The active sites of catalytic species formed from *meso*-C_s-symmetric precursors are obviously non-chirotopic, and therefore cannot exert any stereocontrol on chain propagation [92]; moreover, at variance with C_{2v}-symmetric metallocenes, no case of enantioselective propagation due to chain end control has been reported up to now for this catalyst class. As a result, purely atactic polypropylene is invariably obtained.

In most cases, the polymers are highly regioregular, no head-to-head enchainments being observed by ^{13}C NMR [93].

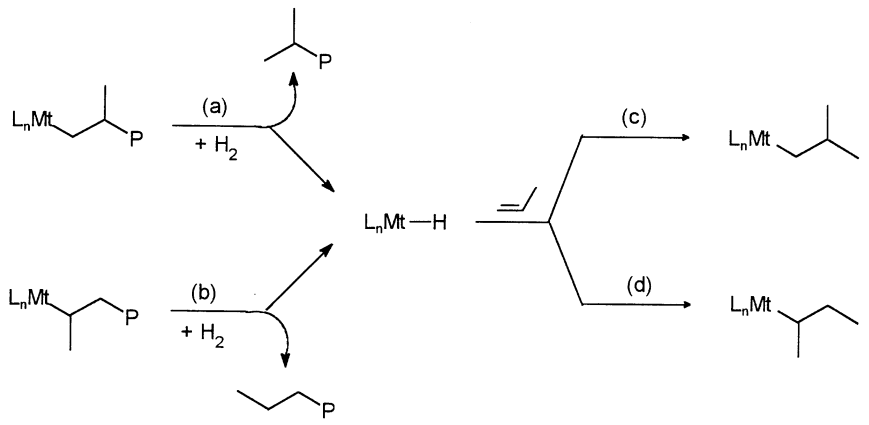

Scheme 8.

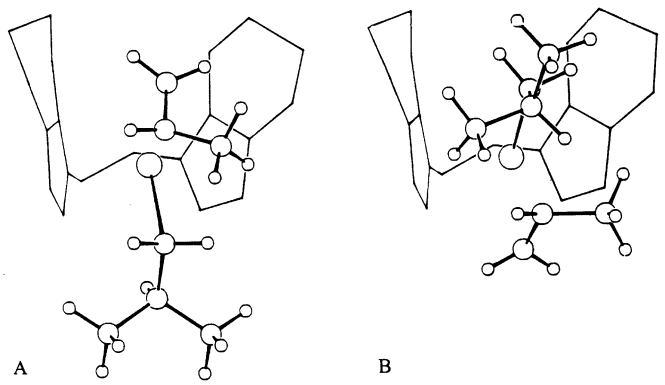

Fig. 18. Models of a *meso*-C_2H_4-(4,5,6,7-H_4-1-Ind)$_2$Mt(*iso*-butyl)]$^+$ cation (Mt = Zr), with a h^2-coordinated propene molecule. The growing polymer chain does not undergo any chiral orientation at the two non-chirotopic coordination sites (A and B); as a result, according to molecular mechanics calculations, propene coordination (and subsequent 1,2 insertion) is not enantioselective. Reprinted with permission from Ziegler Catalysts. ©1995 Springer-Verlag, Berlin [92].

4.2.4. Bridged metallocenes with C_s-symmetry

4.2.4.1. Catalysts and polymerization mechanism. The prototype of this class of *ansa*-metallocenes is $Me_2C(Cp)(9\text{-Flu})ZrCl_2$ [94] (Flu = Fluorenyl; Chart 27). A computer model of the cationic catalytic species, with an *iso*-butyl group simulating the growing polymer chain, is shown in Fig. 19.

Each of the two active sites has a local steric environment closely resembling that of bridged *rac*-bis(1-indenyl) complexes (Fig. 13), which ensures a high enantioselectivity in monomer insertion. On the other hand, the C_s-symmetry implies site *enantiotopicity* (i.e. the preference for opposite propene enantiofaces); therefore, chain propagation is expected to be syndiotactic in case of a chain migratory insertion mechanism (see Section 4.2.2.1) [8,73,95].

As a matter of fact, the first highly syndiotactic polymerization of propene was reported in 1987 in the presence of the catalyst system $Me_2C(Cp)(9\text{-Flu})ZrCl_2$/MAO [94]. However, a strictly alternated monomer insertion can be achieved only at relatively low temperature and high propene concentration. Under different conditions, the growing polymer chain can flip back to the original coordination site in between two consecutive insertions, with the corresponding formation of a stereoirregular unit (an event that has been variously described as *chain back-skip*, *skipped insertion* or *site epimerization*) [8,95].

Changes in the nature of the catalyst precursor may lead to amazing differences in catalytic behavior [8,16]. In particular, it has been reported [96] that when the transition metal in the complex of Chart 27 is Ti instead of Zr, a syndiotactic polymer is never obtained, whatever the temperature and

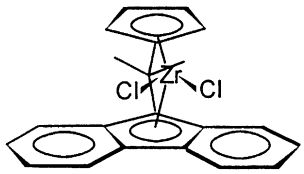

Chart 27.

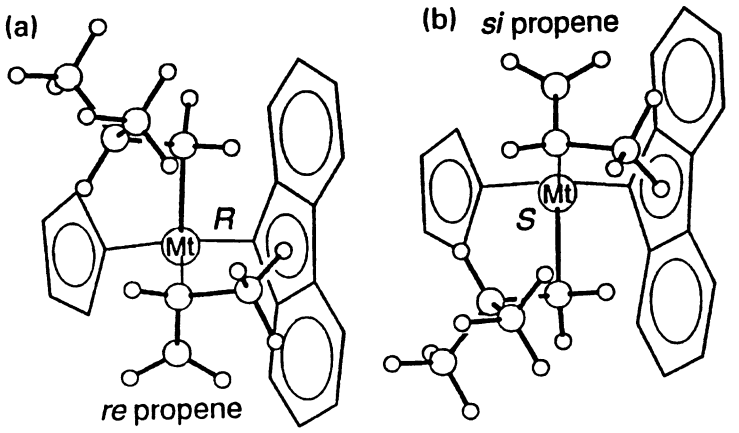

Fig. 19. Models of a $Me_2C(Cp)(9\text{-}Flu)Mt(iso\text{-}butyl)]^+$ cation (Mt = Zr), with a h^2-coordinated propene molecule. The mutual arrangements of the first C–C bond of the *iso*-butyl group (simulating a growing polypropylene chain) and of the monomer are the ones which minimize the non-bonded interactions at the 1,2 insertion step. According to the chain migratory polymerization mechanism, situations (a) and (b) alternate regularly during chain propagation, which explains the observed syndiotactic selectivity (reproduced with permission from Ref. [73]).

the concentration of propene. At the moment, it is not known whether, for the Ti catalyst, monomer insertion is not enantioselective, or (more likely) it is always (much) slower than site epimerization.

Rather than substitutions of the aromatic ligand (preserving the C_s symmetry), a different choice of the interannular bridge may sort interesting effects. In particular, changing the bridge from $-Me_2C-$ to $-Ph_2C-$ results in polymers of much higher average molecular mass [97].

4.2.4.2. Chain configuration. The 150 MHz ^{13}C NMR spectra of two samples of syndiotactic polypropylene prepared with the catalyst system $Ph_2C(Cp)(9\text{-}Flu)ZrCl_2$/MAO at 80°C and two different monomer concentrations are shown in Figs. 20 and 21. The full assignment is given in Tables 7 and 8 [14,15].

In spite of a fairly high stereoregularity ([*rrrr*] = 0.658), the sample prepared at $[C_3H_6] = 1.1$ mol/l contains detectable amounts of *m*-type (Chart 28) and *mm*-type (Chart 29) stereodefects, which can be traced to 'skipped insertions' and to monomer insertions with the 'wrong' enantioface, respectively. In agreement with this interpretation, lowering $[C_3H_6]$ from 1.1 to 0.4 mol/l resulted in a strong increase of stereodefective sequences with isolated *m* diads (compare Figs. 20 and 21).

Chain propagation can be described in terms of the following 4×4 stochastic matrix:

$$\mathbf{M}_{\text{CM-}Cs} = \begin{array}{c|cccc} & R & S & R & S \\ \hline R & \sigma P_{sk} & (1\text{-}\sigma)P_{sk} & (1\text{-}\sigma)(1\text{-}P_{sk}) & \sigma(1\text{-}P_{sk}) \\ S & \sigma P_{sk} & (1\text{-}\sigma)P_{sk} & (1\text{-}\sigma)(1\text{-}P_{sk}) & \sigma(1\text{-}P_{sk}) \\ R & \sigma(1\text{-}P_{sk}) & (1\text{-}\sigma)(1\text{-}P_{sk}) & (1\text{-}\sigma)P_{sk} & \sigma P_{sk} \\ S & \sigma(1\text{-}P_{sk}) & (1\text{-}\sigma)(1\text{-}P_{sk}) & (1\text{-}\sigma)P_{sk} & \sigma P_{sk} \end{array}$$

where σ and $(1\text{-}\sigma)$ are the conditional probabilities of selecting a given monomer enantioface at the two

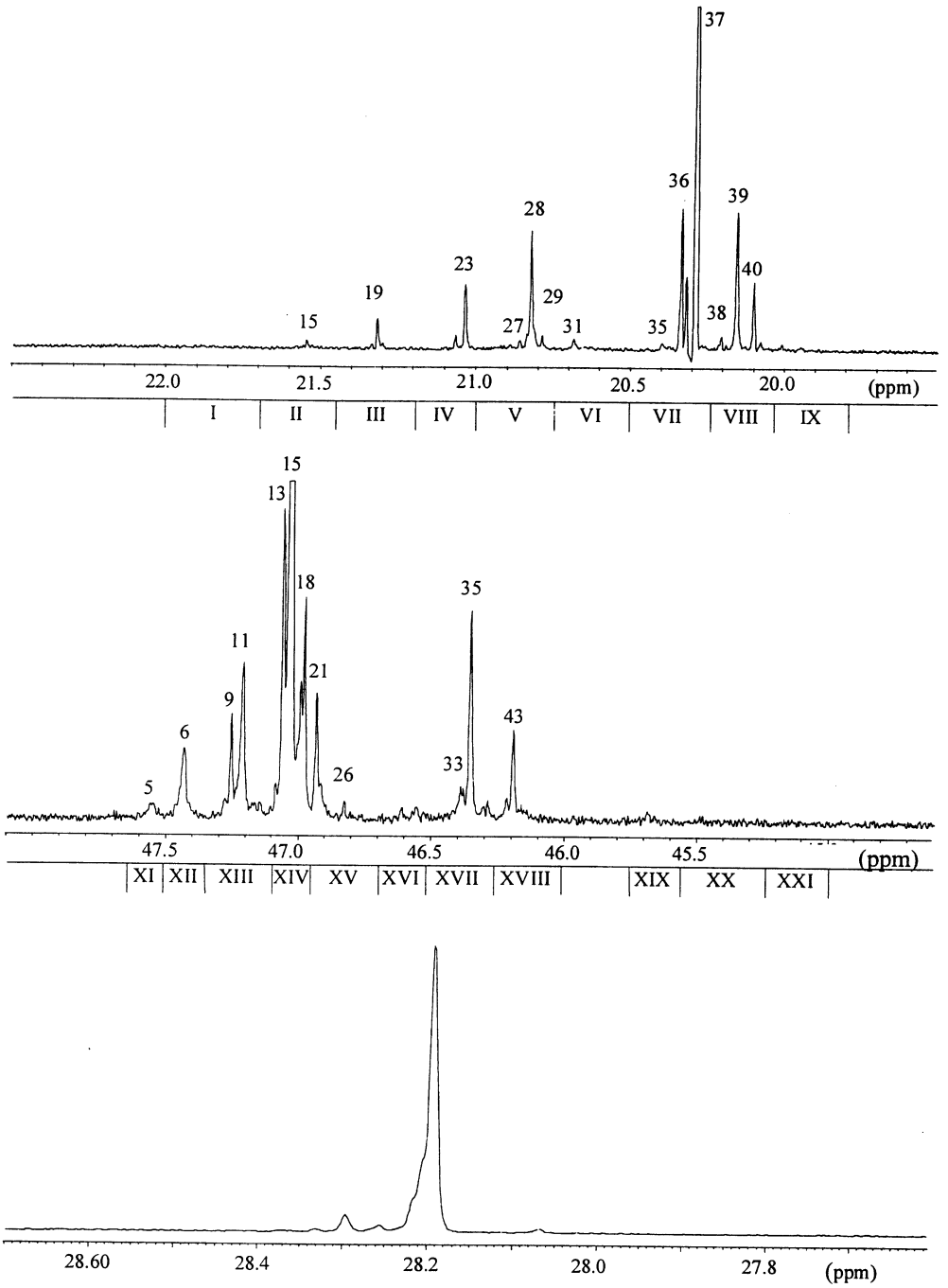

Fig. 20. Methyl (top), methylene (centre) and methine (bottom) regions of the 150 MHz ^{13}C NMR spectrum (recorded in tetrachloroethane-1,2-d_2 at 90°C; chemical shift scale in ppm downfield of TMS) of a predominantly syndiotactic polypropylene sample prepared with the catalyst system $Ph_2C(Cp)(9\text{-Flu})ZrCl_2$/MAO at $T = 80$°C, $[C_3H_6] = 1.1$ mol/l (in toluene). Peak numbering refers to the full assignment reported in Refs. [14,15]; for attributions, see Table 7.

Table 7
Assignment of the 150 MHz ^{13}C NMR spectrum in Fig. 20. In the last two colums, the experimental stereosequence distribution is compared with the best-fit calculated one, according to the appropriate statistical model (see text)

Range/Peak no.	δ (exp.) (ppm)[a]	Assignment	Fraction (exp.) %	Fraction (calc.)[b] (%)
I	22.0–21.7	*mmmm*	n.d.[c]	0.3
II	21.7–21.45	*mmmr*	0.8	0.7
15	21.55	*rmmmrr*		
III	21.45–21.2	*rmmr*	2.4	2.2
19	21.32	*rrmmrr*		1.8
IV	21.2–21.0	*mmrr*	4.7	4.7
23	21.04	*rmmrrr*		3.6
V	21.0–20.75	*mmrm* + *rmrr*	9.8	10.6
27	20.87	*rrrmrrmr*		0.5
28	20.83	*rrmrrr*		8.3
29	20.79	*rmrmrrrr*		0.6
VI	20.75–20.5	*rmrm*	1.7	1.1
31	20.69	*rrmrmr*	1.1	0.7
VII	20.5–20.25	*rrrr*	65.8	66.5
35	20.40	*mrrrrm*	1.0	0.6
36	20.34	*mrrrrr*	9.8	11.1
37	20.30	*rrrrrr*	54.9	54.8
VIII	20.25–20.05	*rrrm*	13.7	13.4
38	20.21	*mrrrmr*	1.0	0.8
39	20.16	*rrrrmr*	8.2	8.3
40	20.11	*mrrrmm* + *rrrrrmmr* + *mrrrrmmr*		
IX	20.05–19.8	*mrrm*	1.2	0.7
X		*mrmrm*	n.d.	0.1
XI	47.65–47.5	*mrmrr*	1.5	1.0
5	47.56	*rmrmrrr*		
XII	47.5–47.35	*rrmrr* + *mrrrm*	4.6	5.2
6	47.44	*rrrmrrr*		3.8
XIII	47.35–47.10	*mrrrr*	11.4	12.2
9	47.26	*mmrrrrr*		3.5
11	47.22	*rmrrrrr*		7.6
XIV	47.10–46.95	*rmmrm* + *rrrrr*	60.1	60.8
13	47.07	*mrrrrrrrr*		8.3
15	47.04	*rrrrrrrrr*		41.1
18	46.99	*rmrrrrrrr* +		6.3
		mmrrrrrrr		2.9
XV	46.95–46.7	*rmmrr* + *mmmrm* + *mmmrr*	5.8	4.7
21		*rrmmmrrr*		3.3
26		*rmmmrrr*		0.4
XVI	46.7–46.5	*rmrrm*	1.7	0.9
XVII	46.5–46.25	*rmmmr* + *mmmmr* + *mmrrm* + *rmrrr* + *mmmmm*	9.3	10.0
33	46.39	*mrmrrrr*		0.8
35	46.36	*rrmrrrr*		7.5
XVIII	46.25–46.0	*mmrrr*	4.5	4.2
43	46.20	*rmmrrrr*		3.3

Table 7 (*continued*)

Range/Peak no.	δ (exp.) (ppm)[a]	Assignment	Fraction (exp.) %	Fraction (calc.)[b] (%)
XIX	45.75–45.55	*rmrmr*	0.7	0.4
XX	45.55–45.25	*mmrmr*	0.4	0.3
XXI		*mmrmm*	n.d.[c]	0.1
				$\sigma = 0.97_3$
				$P_{sk} = 0.067$

[a] Downfield of TMS.
[b] According to the chain migratory C_s-symmetric statistical model (see text).
[c] n.d. = not detected.

enantiotopic active sites, and P_{sk} that of chain 'back-skip' ($P_{sk} = 0$ obviously corresponds to a perfect chain-migratory mechanism). The stereosequence distribution, as usual, can be calculated by means of Eqs. (3.5) and (3.6).

As an alternative to the matricial formalism, an overdetermined set of equations can be derived for the probability of occurrence of each given steric *n*ad. When looking at the cumbersome ones for the ten non-equivalent pentads, developed in Refs. [95,98], it is easy to realize the convenience of the matrix multiplication approach.

The experimental configurations of the two characterized polypropylene samples are compared with the calculated ones in Tables 7 and 8. The agreement is good, and the best-fit values of the conditional probabilities are $\sigma = 0.973$, $P_{sk} = 0.067$ at $[C_3H_6] = 1.1$ mol/l; $\sigma = 0.976$, $P_{sk} = 0.183$ at $[C_3H_6] = 0.4$ mol/l. The fact that the σ parameter is practically independent of monomer concentration implies that the effect of growing chain epimerization [74–76] on the stereoselectivity is negligible.

Syndiotactic polypropylenes of very high stereoregularity ($[rrrr] > 0.95$) can be obtained at low polymerization temperatures in liquid propene. For such samples, melting points close to those of highly isotactic polypropylenes ($T_m > 150°C$) have been reported [99].

4.2.4.3. Chain constitution and structure of the end-groups. C_s-symmetric metallocene catalysts, in general, are highly regioselective, and the ^{13}C NMR spectra of typical syndiotactic polypropylene

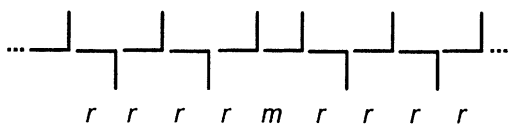

Chart 28.

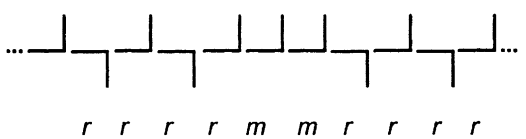

Chart 29.

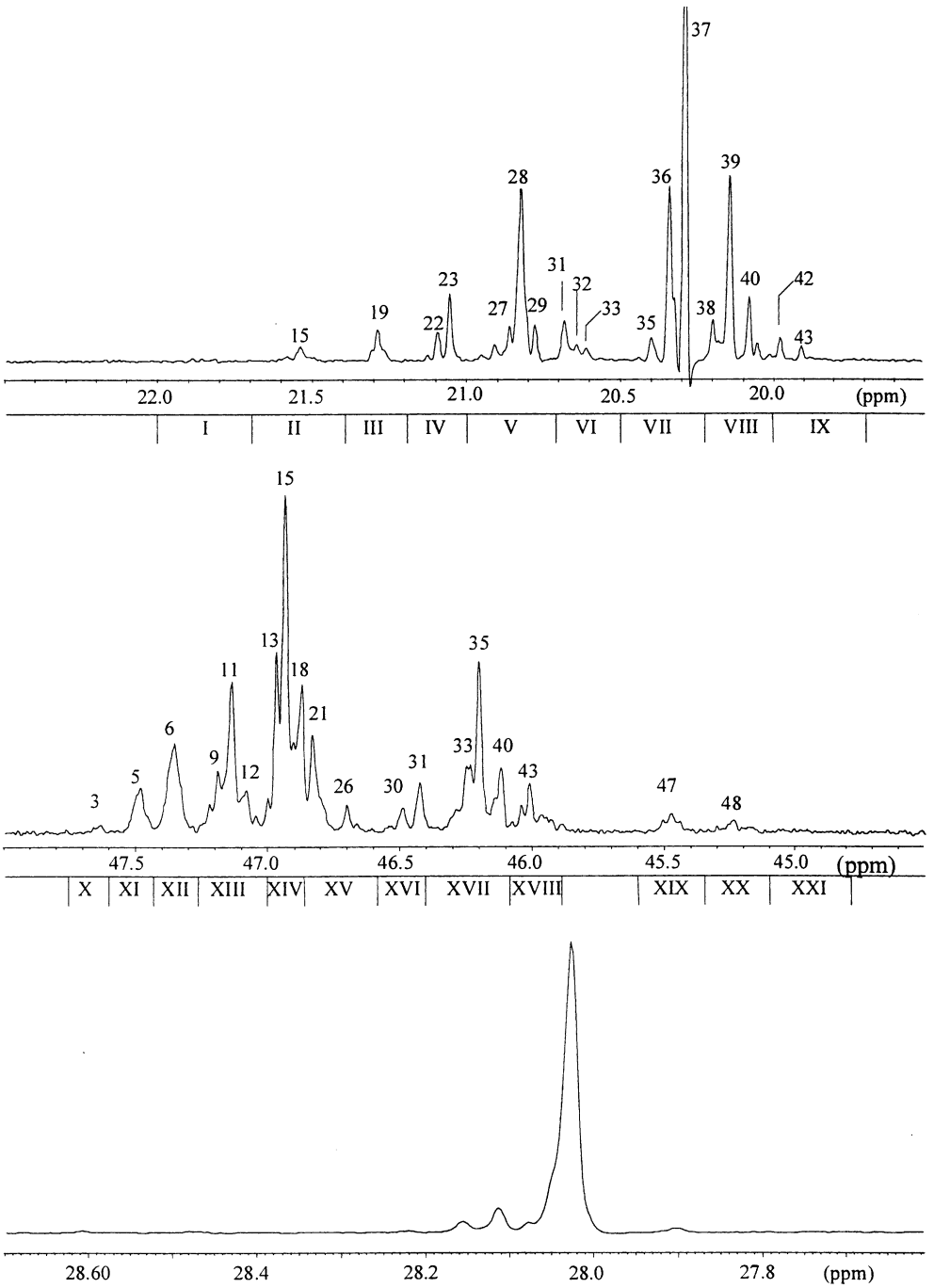

Fig. 21. Methyl (top), methylene (centre) and methine (bottom) regions of the 150 MHz ^{13}C NMR spectrum (recorded in tetrachloroethane-1,2-d_2 at 70°C; chemical shift scale in ppm downfield of TMS) of a predominantly syndiotactic polypropylene sample prepared with the catalyst system $Ph_2C(Cp)(9\text{-Flu})ZrCl_2$/MAO at $T = 80$°C, $[C_3H_6] = 0.4$ mol/l (in toluene). Peak numbering refers to the full assignment reported in Refs. [14,15]; for attributions, see Table 8.

Table 8
Assignment of the 150 MHz ^{13}C NMR spectrum in Fig. 21. In the last two colums, the experimental stereosequence distribution is compared with the best-fit calculated one, according to the appropriate statistical model (see text)

Range/Peak no.	δ (ppm)[a]	Assignment	Fraction (exp.) %	Fraction (calc.)[b] (%)
I	22.0–21.7	*mmmm*	n.d.[c]	0.3
II	21.7–21.4	*mmmr*	1.9	2.0
15	21.54	*rmmmrr*		1.2
III	21.4–21.2	*rmmr*	2.9	3.1
19	21.29	*rrmmrr*		2.0
IV	21.2–21.0	*mmrr*	5.9	6.5
22	21.12	*mmmrrr* +		1.2
		mmmrrm		0.3
23	21.06	*rmmrrr* +	4.1	3.9
		rmmrrm		1.0
V	21.0–20.7	*mmrm* + *rmrr*	20.2	20.5
27	20.86	*rrrmrrmr*	1.9	1.8
28	20.83	*rrmrrr*		12.0
29	20.78	*rmrmrrrr*	2.0	1.8
VI	20.7–20.5	*rmrm*	5.5	4.8
31	20.68	*rrmrmr*	3.3	2.8
32	20.64	*rrmrmm*		1.0
33	20.61	*mrmrmr*		0.7
VII	20.5–20.25	*rrrr*	40.3	40.1
35	20.40	*mrrrrm*	1.4	1.6
36	20.34	*mrrrrr*	12.0	12.9
37	20.29	*rrrrrr*	26.9	25.6
VIII	20.25–20.0	*rrrm*	20.0	20.2
38	20.20	*mrrrmr*	3.0	3.0
39	20.14	*rrrrmr*	12.5	12.0
40	20.08	*mrrrmm* +	4.5	1.1
		rrrrrmmr +		2.5
		mrrrrmmr		0.6
IX	20.0–19.7	*mrrm*	3.2	2.6
42	19.98	*rmrrmr*	2.0	1.4
43	19.91	*mmrrmr*	1.0	1.0
X	47.75–47.60	*mrmrm*	0.6	0.5
3	47.64	*rmrmrmr*		0.3
XI	47.60–47.42	*mrmrr*	4.1	3.8
5	47.49	*rmrmrrr*		2.3
XII	47.42–47.28	*rrmrr* + *mrrrm*	8.5	9.5
6	47.36	*rrrmrrr*		4.8
XIII	47.28–47.02	*mrrrr*	15.6	16.1
9	47.20	*mmrrrrr*		3.3
11	47.14	*rmrrrrr*		9.6
12	47.09	*rmrrrrm*		2.4
XIV	47.02–46.85	*rmmrm* + *rrrrr*	32.2	33.3
13	46.98	*mrrrrrrrr*		6.6
15	46.94	*rrrrrrrr*		13.0
18	46.88	*rmrrrrrrr* +		6.1
		mmrrrrrrr		2.1

Table 8 (*continued*)

Range/Peak no.	δ (ppm)[a]	Assignment	Fraction (exp.) %	Fraction (calc.)[b] (%)
XV	46.85–46.58	*rmmrr + mmmrm + mmmrr*	8.0	6.9
21	46.84	*rrmmrrr*		3.2
26	46.71	*rmmmrrr*		1.0
XVI	46.58–46.40	*rmrrm*	4.7	3.8
30	46.50	*rrmrrmm*		0.8
31	46.43	*rrmrrmr*		2.2
XVII	46.40–46.08	*rmmmr + mmmmr + mmrrm + rmrrr + mmmmm*	18.1	17.6
33	46.25	*mrmrrrr*		2.4
35	46.21	*rrmrrrr*		9.6
40	46.13	*rrmrrrm*		2.4
XVIII	46.08–45.90	*mmrrr*	5.1	5.2
43	46.02	*rmmrrrr*		3.1
XIX	45.60–45.35	*rmrmr*	1.9	1.8
47	45.48	*rrmrmrr*		1.1
XX	45.35–45.10	*mmrmr*	1.2	1.2
48	45.25	*rmmrmrr*		0.7
XXI	45.10–44.80	*mmrmm*	n.d.[c]	0.2
				$\sigma = 0.97_6$
				$P_{sk} = 0.18_3$

[a] Downfield of TMS.
[b] According to the chain migratory C_s-symmetric statistical model (see text).
[c] n.d. = not detected.

samples give no evidence of regioerrors [100]. However, in copolymers of propene with ethene-[1-^{13}C], low amounts of ethene units in between two propene units with opposite enchainments were detected [58,60].

As an example, the mole fraction of such units in a series of copolymers prepared with the catalyst system $Ph_2C(Cp)(9\text{-Flu})ZrCl_2$/MAO at 10°C is plotted against ethene-[1-^{13}C] incorporation in Fig. 22; the 150 MHz ^{13}C NMR spectrum of one such copolymer with an ethene-[1-^{13}C] content of 2.46 mol% is also shown in Fig. 23. As discussed in Section 2.3.2, the plateau value of 0.08 mol% in the plot of Fig. 22 can be taken as the fraction of misinsertions in propene homopolymerization under the same experimental conditions.

The ^{13}C NMR characterization of syndiotactic polypropylene samples obtained with $Me_2C(Cp)(9\text{-Flu})ZrCl_2$/MAO/Al($^{13}CH_3$)$_3$ pointed out the presence of $-CH_2-CH(CH_3)-{}^{13}CH_3$ end-groups, which indicates that the preferred mode of propene insertion is 1,2 [101]. Consistently, the main type of unsaturated chain ends observed by ^{1}H NMR are 2-methyl-prop-1-enyls (vinylidenes). At lower monomer concentration, chain transfer to $AlMe_3$ (in equilibrium with MAO) becomes appreciable, and leads to the formation of detectable amounts of *iso*-butyl end-groups [95].

4.2.5. Bridged metallocenes with C_1-symmetry

4.2.5.1. Catalysts and polymerization mechanism. A wide variety of *ansa*-metallocene complexes with

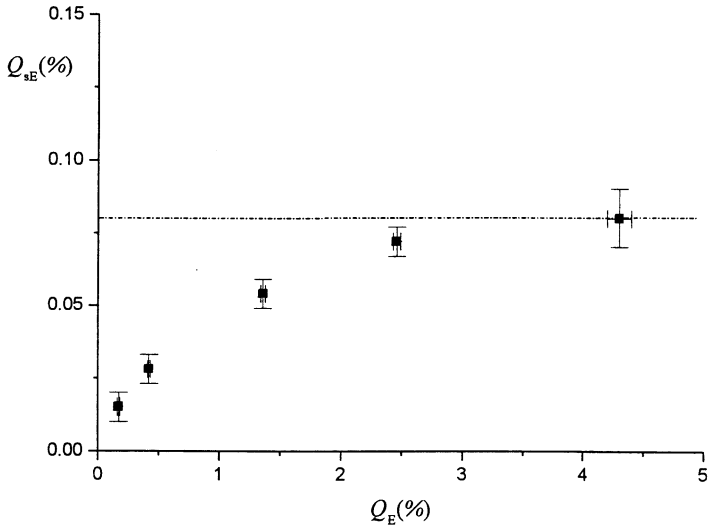

Fig. 22. Fraction of ethene-[1-^{13}C] units adjacent to a regioirregular 2,1 propene unit (Q_{sE}) vs. total ethene-[1-^{13}C] content (Q_E) for a series of propene/ethene-[1-^{13}C] copolymers prepared with the catalyst system $Ph_2C(Cp)(9\text{-Flu})ZrCl_2$/MAO at $T = 10°C$. The plateau value of $Q_{sE} = 0.08\%$ can be assumed as the fraction of 2,1 misinsertions in propene homopolymerization at the same temperature (adapted from Ref. [58]).

C_1-symmetry and *diastereotopic* active sites have been synthesized. Typical structural types are shown in Chart 30 (**I**) and Chart 31 (**II**); the latter formally derives from the C_s-symmetric structure of Chart 27, by substitution of the Cp ring at position 3.

At variance with C_2-symmetric and C_s-symmetric catalysts, the stereoselectivity of C_1-symmetric ones in propene polymerization is not easy to predict a priori, although not beyond rationalization. For the prototype of structure **II**, namely $Me_2C(3\text{-Me-Cp})(9\text{-Flu})ZrCl_2$, a detailed molecular mechanics study has been reported [104]; a computer model of the cationic catalytic species, with the growing polymer chain simulated — as usual — by an *iso*-butyl group, is shown in Fig. 24. Propene insertion at the more crowded coordination site (site S1 in Chart 31) is highly enantioselective, for the reason already discussed for the conceptually related unsubstituted catalytic species with C_s-symmetry (Fig. 19). On the other hand, when it is the growing chain to reside at such site, it undergoes equally unfavorable steric contacts with the Me substituent of the Cp ring and with one of the C_6 rings of the fluorenyl ligand; as a result, the orientation of the first C–C bond is practically random, and — consequently — propene insertion at the other coordination site (site S2 in Chart 31) is not enantioselective.

As a matter of fact, polypropylenes with almost ideal hemiisotactic structure (Chart 9) can be obtained with $Me_2C(3\text{-Me-Cp})(9\text{-Flu})ZrCl_2$/MAO under conditions of chain-migratory propagation (comparatively low temperature, high propene concentration) [105].

The stereoselectivity, however, is critically dependent on the ligand framework. In particular, catalysts of type **I** (Chart 30) [103], as well as those of type **II** (Chart 31) with a bulky R substituent (e.g. R = *t*-butyl or trimethylsilyl) [102], are (predominantly) isotactic-selective, probably due to the preference of the growing chain for the more open coordination site (S2), which forces the monomer to insert more frequently at the more crowded, enantioselective site (S1). This route to isotactic polypropylene has the advantage that the catalyst precursors can exist in only one form (at variance with the case of

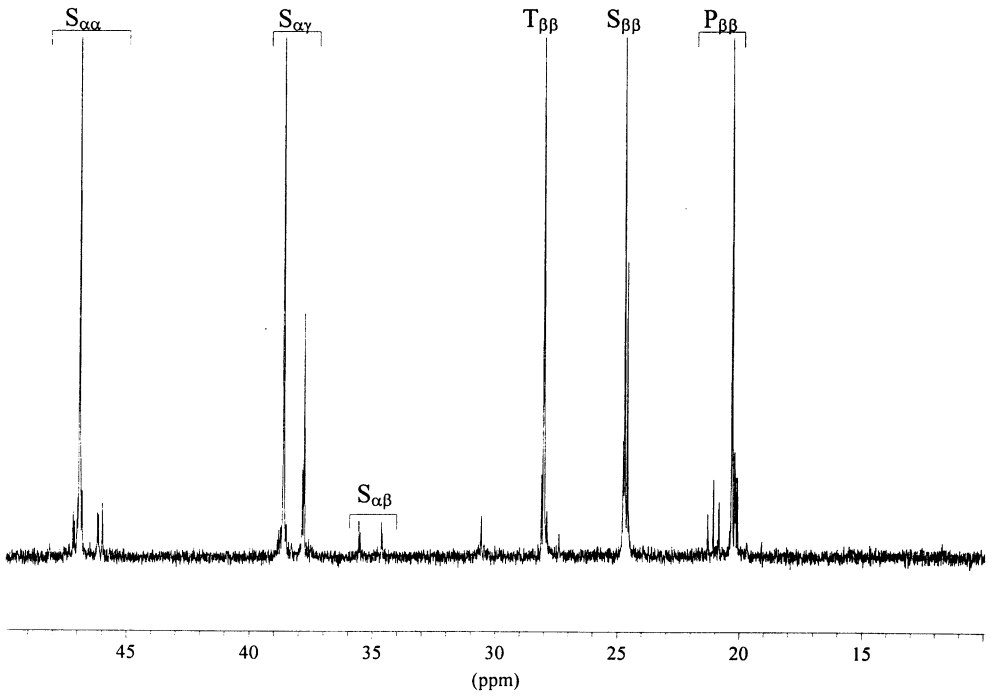

Fig. 23. 150 MHz ^{13}C NMR spectrum (recorded in tetrachloroethane-1,2-d_2 at 70°C; chemical shift scale in ppm downfield of TMS) of a propene/ethene-[1-^{13}C] copolymer (ethene-[1-^{13}C] content, 2.46 mol%) prepared with the catalyst system $Ph_2C(Cp)(9\text{-Flu})ZrCl_2$/MAO at $T = 10$°C. Resonance attributions are explicitly indicated; note, in particular, the clear $S_{\alpha\beta}$ peaks indicative of ethene-[1-^{13}C] units in between two propene units with opposite enchainments (Chart 18) (adapted from Ref. [58]).

rac-C_2-symmetric precursors, which can be contaminated by the non-chiral *meso*-C_s-symmetric form; see Sections 4.2.2 and 4.2.3). A number of C_1-symmetric metallocene catalysts affording polypropylenes with [*mmmm*] > 0.90 have been reported [106,107].

4.2.5.2. Chain configuration. The 150 MHz ^{13}C NMR spectrum of a sample of hemiisotactic polypropylene prepared with the catalyst system $Me_2C(3\text{-Me-Cp})(9\text{-Flu})ZrCl_2$/MAO at −20°C and $[C_3H_6] = 1.8$ mol/l is shown in Fig. 25; peak attributions are given in Table 9 [14,15]. In the same table, the experimental stereosequence distribution is compared with the best-fit one, calculated using

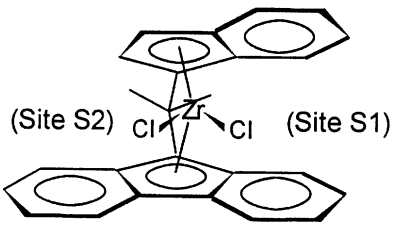

Chart 30.

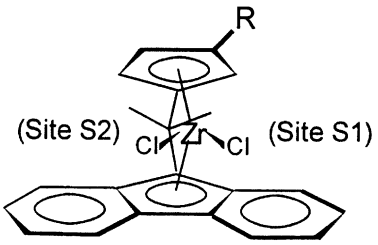

Chart 31.

Eqs. (3.5)–(3.6) and the following 4×4 stochastic matrix [14]:

$\mathbf{M}_{CM\text{-}C1} =$

	R	S	R	S
R	$\sigma_1(1\text{-}P_{12})$	$(1\text{-}\sigma_1)(1\text{-}P_{12})$	$\sigma_2 P_{12}$	$(1\text{-}\sigma_2)P_{12}$
S	$\sigma_1(1\text{-}P_{12})$	$(1\text{-}\sigma_1)(1\text{-}P_{12})$	$\sigma_2 P_{12}$	$(1\text{-}\sigma_2)P_{12}$
R	$\sigma_1 P_{21}$	$(1\text{-}\sigma_1)P_{21}$	$\sigma_2(1\text{-}P_{21})$	$(1\text{-}\sigma_2)(1\text{-}P_{21})$
S	$\sigma_1 P_{21}$	$(1\text{-}\sigma_1)P_{21}$	$\sigma_2(1\text{-}P_{21})$	$(1\text{-}\sigma_2)(1\text{-}P_{21})$

σ_1 and σ_2 are the conditional probabilities that the prochiral monomer inserts with a given enantioface at each of the two diastereotopic sites (S1 and S2, respectively); P_{12} and P_{21}, those of monomer insertion at S2 after a previous insertion at S1 and vice versa. Note that for $\sigma_1 = (1 - \sigma_2)$ and $P_{12} = P_{21}$, matrix $\mathbf{M}_{CM\text{-}C1}$ reduces to $\mathbf{M}_{CM\text{-}Cs}$ (Section 4.2.4.3); for $\sigma_1 = \sigma_2 = \sigma$, to $\mathbf{M}_{ES}$ (Sections 3 and 4.2.2.2).

Ideal hemiisotactic propagation requires a chain-migratory mechanism ($P_{12} = P_{21} = 1$) with $\sigma_1 = 1$ (or $= 0$) and $\sigma_2 = 0.5$. The best-fit values of the four adjustable parameters for the polymer sample of Fig. 25 actually indicate only minor deviations from the ideal case[4] (Table 9) [108].

Fig. 26 shows instead the 150 MHz spectrum of a polypropylene sample obtained with the same catalyst system $Me_2C(3\text{-}Me\text{-}Cp)(9\text{-}Flu)ZrCl_2$/MAO at comparatively high temperature (70°C) and low propene concentration ($[C_3H_6] = 0.3$ mol/l). The sample deviates from hemiisotacticity in isotactic sense; the best-fit of the stereosequence distribution (Table 10) indicates that this is mainly due to a tendency of the growing chain to skip back from S2 to S1 ($1\text{-}P_{12} = 0.28$), whereas, the values of all other conditional probabilities are still similar to those for hemiisotactic propagation. In particular, the fact that $\sigma_1 \approx 1$, $P_{21} \approx 1$ explains the persisting extinction of stereosequences with an odd number of consecutive *r* diads, well-known for ideally hemiisotactic polypropylene [108,109] (and particularly well-evident for the methyl *rmrm* pentad).

A trend of increasing stereoregularity with increasing temperature and decreasing monomer concentration, and the absence of consecutive stereodefects (Chart 32), are common features of predominantly isotactic polypropylenes prepared with C_1-symmetric metallocenes [103]. Catalysts of type **I** (Chart 30), in particular, allow one to modulate the tacticity of the polymer produced over wide ranges, by suitably adjusting $[C_3H_6]$ and reaction temperature. Provided that the average molecular mass is not too low, samples of moderate stereoregularity ([*mmmm*] between 0.4 and 0.7, indicatively), with low values of crystallinity and of melting temperature, behave as thermoplastic elastomers [110].

[4] Hemiisotactic polypropylene was first obtained by hydrogenation of isotactic *trans*-1,4-poly(2-methyl-1,3-pentadiene) [109].

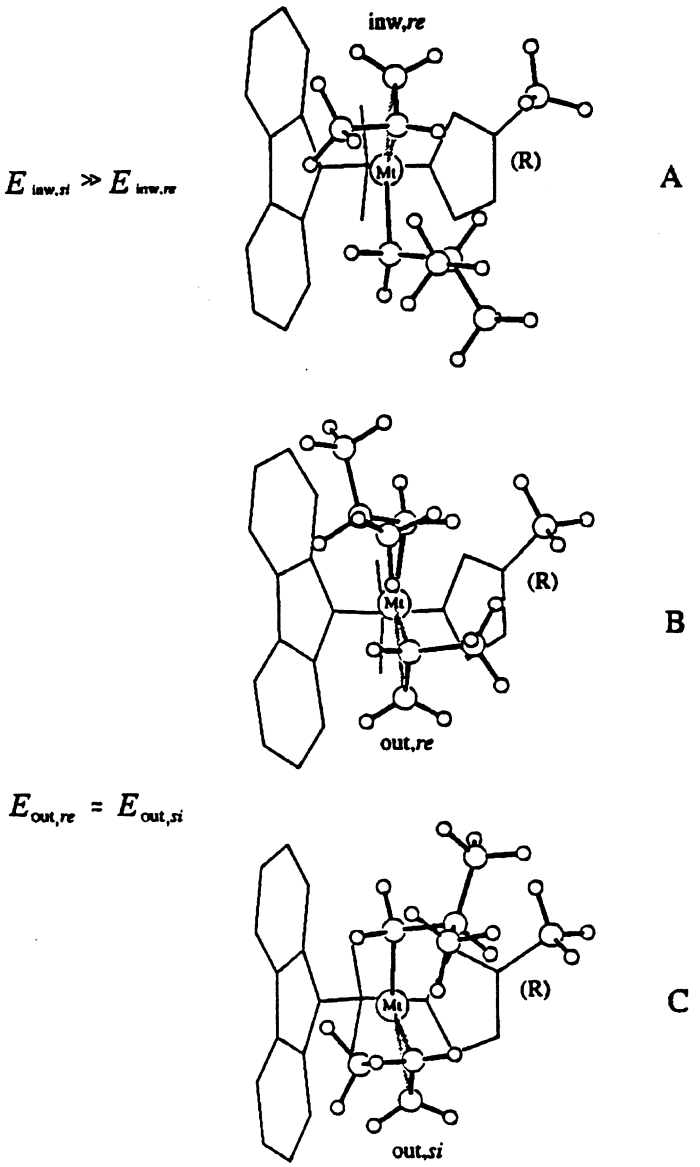

Fig. 24. Models of a $Me_2C(3\text{-Me-Cp})(9\text{-Flu})Mt(\textit{iso}\text{-butyl})]^+$ cation (Mt = Zr), with a h^2-coordinated propene molecule. The mutual arrangements of the first C–C bond of the *iso*-butyl group (simulating a growing polypropylene chain) and of the monomer are the ones which minimize the non-bonded interactions at the 1,2 insertion step. According to the chain migratory polymerization mechanism, the situation labelled as A alternates regularly with either of the two equivalent ones labelled as B and C during chain propagation, which explains the observed hemiisotactic selectivity. Reprinted with permission from Macromolecules 1996; 29:4834. ©1996 American Chemical Society [104].

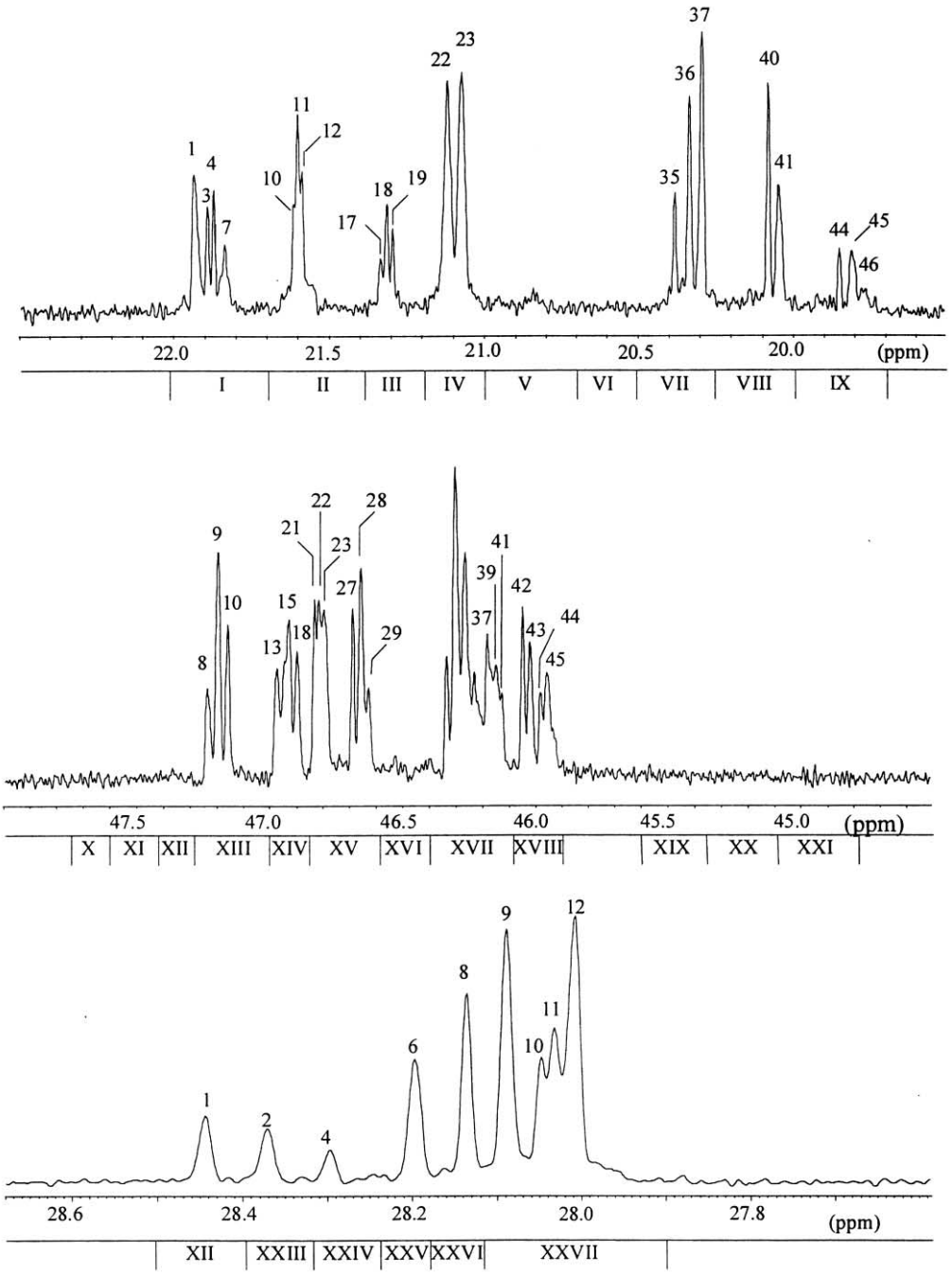

Fig. 25. Methyl (top), methylene (centre) and methine (bottom) regions of the 150 MHz ^{13}C NMR spectrum (recorded in tetrachloroethane-1,2-d_2 at 70°C; chemical shift scale in ppm downfield of TMS) of a hemiisotactic polypropylene sample prepared with the catalyst system Me_2C(3-Me-Cp)(9-Flu)$ZrCl_2$/MAO at $T = -20$°C, $[C_3H_6] = 1.8$ mol/l (in toluene). Peak numbering refers to the full assignment reported in Refs. [14,15]; for attributions, see Table 9.

Table 9
Assignment of the 150 MHz ^{13}C NMR spectrum in Fig. 25. In the last two colums, the experimental stereosequence distribution is compared with the best-fit calculated one, according to the appropriate statistical model (see text)

Range/Peak no.	δ (ppm)[a]	Assignment	Fraction (exp.) %	Fraction (calc.)[b] (%)
I	22.0–21.7	*mmmm*	16.0	16.3
1	21.94	*mmmmmmmm* +	6.8	3.6
		mmmmmmmmrr +		2.6
		rrmmmmmmrr		1.4
3	21.89	*mmmmmmmmrrmm* +	4.9	1.2
		mmmmmmmmrrrr[*]		1.3
4	21.88	*rrmmmmmmrrmm*[*] +		1.3
		rrmmmmmmrrrr		1.4
7	21.84	*rrmmmmrr*	4.3	3.0
II	21.7–21.4	*mmmr*	12.5	11.9
10	21.61	*mmmmmmrrmm*		2.6
11	21.60	*mmmmmmrrrr* +		2.8
		rrmmmmrrmm		2.8
12	21.59	*rrmmmmrrrr*		3.1
III	21.4–21.2	*rmmr*	6.4	6.5
17	21.34	*mmrrmmrrmm*		1.4
18	21.31	*mmrrmmrrrr*		3.1
19	21.30	*rrrrmmrrrr*		1.7
IV	21.2–21.0	*mmrr*	25.6	24.5
22	21.12	*mmmmrrmm* +	12.3	5.4
		mmmmrrrr[*]		5.9
23	21.07	*rrmmrrmm*[*] +	13.3	5.9
		rrmmrrrr		6.5
V	21.0–20.7	*mmrm* + *rmrr*	1.2	0.9
VI	20.7–20.5	*rmrm*	0.6	0.5
VII	20.5–20.25	*rrrr*	19.7	20.3
35	21.38	*mmrrrrmm*	3.8	3.0
36	20.33	*mmrrrrrr*	6.5	6.5
37	20.29	*rrrrrr*	9.4	10.5
VII	20.25–20.0	*rrrm*	11.3	13.1
40	20.08	*rrrrrrmmrr* +	5.8	3.4
		mmrrrrmmrr[*]		3.1
41	20.04	*rrrrrrmmmm*[*] +	5.5	3.1
		mmrrrrmmmm		2.8
IX	20.0–19.7	*mrrm*	6.7	5.9
44	19.85	*rrmmrrmmrr*	2.0	1.5
45	19.81	*mmmmrrmmrr*	4.7	2.8
46	19.76–19.75	*mmmmrrmmmm*		1.3
X	47.75–47.60	*mrmrm*	n.d.[c]	0.1
XI	47.60–47.42	*mrmrr*	n.d.[c]	0.2
XII	47.42–47.28	*rrmrr* + *mrrrm*	n.d.[c]	0.2
XIII	47.28–47.02	*mrrrr*	14.2	12.8
8	47.24	*mmmrrrrrr*	3.0	3.1
9	47.20	*rmmrrrrrr* +	6.8	3.4
		mmmrrrrrmm		2.8
10	47.16	*rmmrrrrmm*	4.4	3.1

Table 9 (*continued*)

Range/Peak no.	δ (ppm)[a]	Assignment	Fraction (exp.) %	Fraction (calc.)[b] (%)
XIV	47.02–46.85	*rmmrm* + *rrrrr*	13.9	14.2
13	46.98	*mrrrrrrrr*	3.1	3.4
15	46.93	*rrrrrrrrr* +	6.9	3.7
		mmrrrrrrm		3.1
18	46.90	*mmrrrrrrr*	3.9	3.4
XV	46.85–46.58	*rmmrr* +	25.6	24.7
		mmmrm + *mmmrr*		
21	46.84	*rrrmmrrrr*		3.4
22	46.82	*mrrmmrrrr*		3.1
23	46.79	*rrrmmrrmm* +		3.1
		mrrmmrrmm		2.8
27	46.69	*rmmmmrrrr*	3.7	3.1
28	46.66	*mmmmmrrrr* +	9.5	2.8
		rmmmmrrmm		2.8
29	46.63	*mmmmmrrmm*		2.6
XVI	46.58–46.40	*rmrrm*	n.d.[c]	0.2
XVII	46.40–46.08	*rmmmr* + *mmmmr* +	33.1	34.2
		mmrrm + *rmrrr* +		
		mmmmm		
37	46.18	*rrmmmmmmr*		2.8
39	46.15	*mmmmmmmrr* +		2.6
		mmmmmmmmr		2.6
41	46.12	*mmmmmmmmm*		2.3
XVIII	46.08–45.90	*mmrrr*	13.2	12.8
42	46.05	*rrmmrrrrm*	3.4	3.1
43	46.02	*rrmmrrrrr*	3.7	3.4
44	45.98	*mmmmrrrrm*	6.1	2.8
45	45.96	*mmmmrrrrr*		3.1
XIX	45.60–45.35	*rmrmr*	n.d.[c]	0.1
XX	45.35–45.10	*mmrmr*	n.d.[c]	0.2
XXI	45.10–44.80	*mmrmm*	n.d.[c]	0.1
XXII	28.5–28.4	*mmmmmm*	6.5	7.7
1	28.45	*mmmmmmmm*		
XXIII	28.4–28.32	*mmmmmr*	5.7	5.4
2	28.37	*mmmmmmrr*		
XXIV	28.32–28.24	*rmmmmr*	3.4	3.0
4	28.30	*rrmmmmrr*		
XXV	28.24–28.19	*mmmmrr*	10.6	11.5
6	28.20	*mmmmrr*		
XXVI	28.18–28.12	*mmmmrm* + *rmmmrr*	13.0	12.2
		mmmrrm + *mmmrrr*		
		mmmrmr		
8	28.14	*mmmrrm* + *mmmrrr*	≈ 13.0	11.6
XXVII	28.13–27.90	*rmmmrm* + *rmmrrm*	60.8	60.0
		rmmrrr + *mmmrmm*		
		rmmrmr + *rmmrmm*		
		rmmr + *rrmr*		
		rmrm + *rr*		

Table 9 (*continued*)

Range/Peak no.	δ (ppm)[a]	Assignment	Fraction (exp.) %	Fraction (calc.)[b] (%)
9	28.09	*rmmrrm*	18.8	6.0
		rmmrrr		6.8
		mmrrmm		5.7
10	28.05	*rrmmrr*	42.0	6.5
11	28.03	*rrrrmm*		13.1
12	28.01	*rrrr*		20.3
				$\sigma_1 = 0.99$
				$\sigma_2 = 0.47_7$
				$P_{12} = 1.00$
				$P_{21} = 1.00$

[a] Downfield of TMS.
[b] According to the chain migratory C_1-symmetric statistical model (see text).
[c] n.d. = not detected.
* Correct assignment of the two peaks possibly reversed.

4.2.5.3. Chain constitution. The regioregularity of polypropylene samples prepared with most C_1-symmetric metallocene catalysts is fairly high. The predominant monomer insertion mode is 1,2; isolated 2,1 and/or 3,1 units (Charts 24–26) can be observed by ^{13}C NMR, but their cumulative fraction is usually below 0.5 mol% [102].

4.2.6. Metallocenes with 'oscillating' structure

In unbridged metallocenes like Cp_2MtX_2 or Ind_2MtX_2, the h^5-coordinated aromatic rings rotate freely even at very low temperatures; however, the rotation may become hindered in the presence of bulky substituents. Of special interest are (2-Ar-Ind)$_2$MtX$_2$ complexes (with Mt=Zr or Hf, and Ar=Phenyl or a more complicated aromatic moiety), which give rise to an equilibrium between two rotational isomers: one with *quasi*-C_2-symmetry (*rac*-like form, Chart 33a), and the other with *quasi*-C_s-symmetry (*meso*-like form, Chart 33b). This behavior has been referred to as 'oscillating' [7,8,111].

Polypropylenes containing both isotactic and atactic sequences have been obtained with (2-Ar-Ind)$_2$MtX$_2$/MAO catalyst systems [8,111,115]. It has been proposed that this is due to the fact that the frequency of interconversion between the two rotamers is (much) lower than that of monomer insertion, and that the stereoselectivities of the *rac*-like and *meso*-like catalytic species are similar to those of bridged bis-indenyl ones with corresponding symmetry; results of molecular mechanics calculations agree with this hypothesis [116].

These polymers perform as thermoplastic elastomers, with the atactic sequences imparting a moderately elastic response and the isotactic sequences acting as physical crosslinks [114]. However, studies

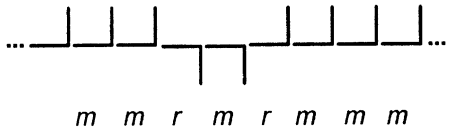

Chart 32.

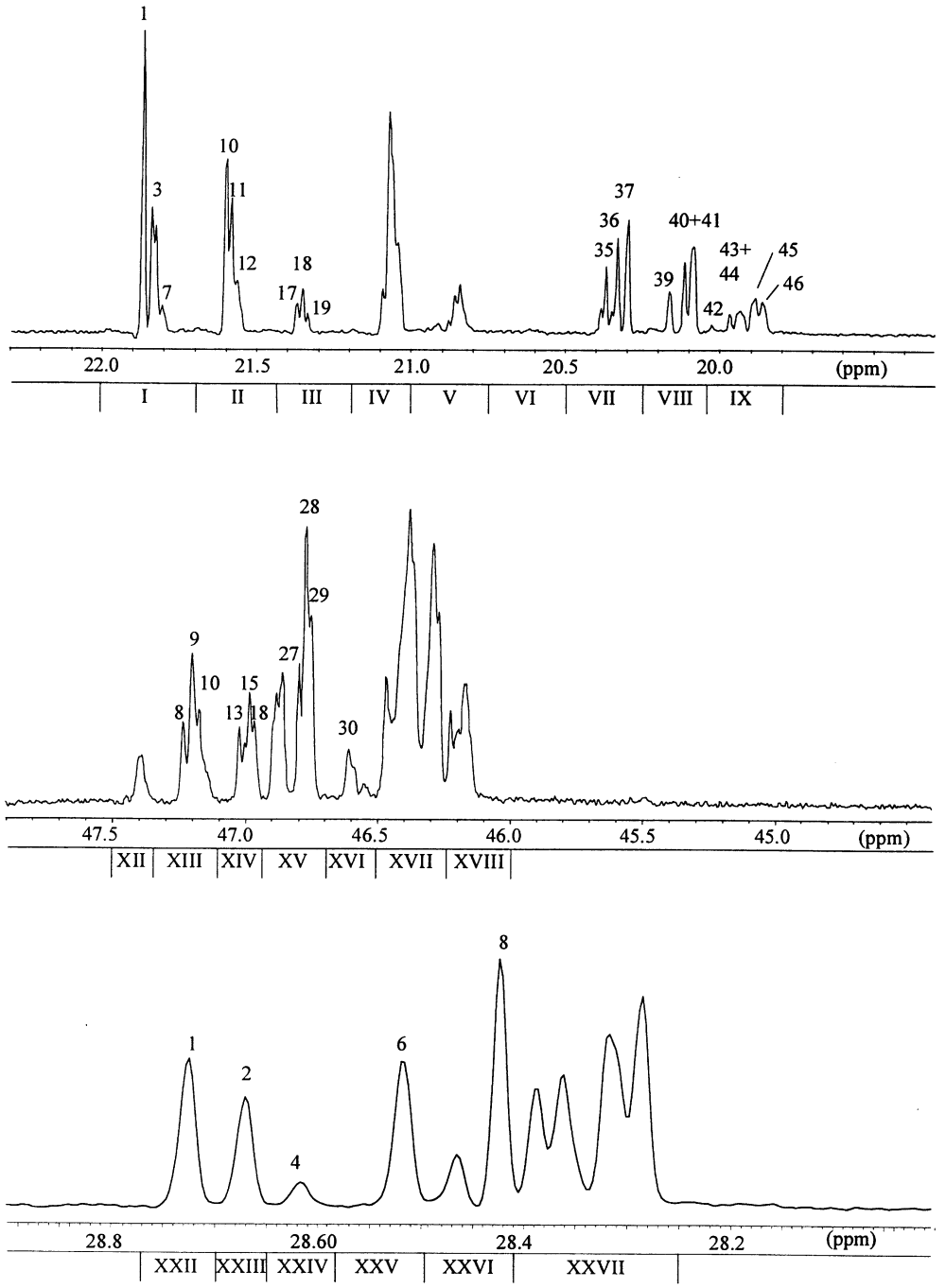

Fig. 26. Methyl (top), methylene (centre) and methine (bottom) regions of the 150 MHz ^{13}C NMR spectrum (recorded in tetrachloroethane-1,2-d_2 at 70°C; chemical shift scale in ppm downfield of TMS) of a polypropylene sample prepared with the catalyst system Me_2C(3-Me-Cp)(9-Flu)$ZrCl_2$/MAO at $T = 70$°C, $[C_3H_6] = 0.3$ mol/l (in toluene). Peak numbering refers to the full assignment reported in Refs. [14,15]; for attributions, see Table 10.

Table 10
Assignment of the 150 MHz ^{13}C NMR spectrum in Fig. 26. In the last two colums, the experimental stereosequence distribution is compared with the best-fit calculated one, according to the appropriate statistical model (see text)

Range/Peak no.	δ (ppm)[a]	Assignment	Fraction (exp.) %	Fraction (calc.)[b] (%)
I	22.0–21.7	*mmmm*	20.0	20.1
1	21.87	*mmmmmm*	10.6	10.6
3	21.85	*mmmmmr*		8.1
7	21.81	*rmmmmr*		1.7
II	21.7–21.45	*mmmr*	15.6	15.2
10	21.61	*mmmmmrrm*		4.8
11	21.59	*mmmmmrrr* +		3.1
		rmmmmrrm		2.0
12	21.57	*rmmmmrrr*		1.3
III	21.45–21.2	*rmmr*	3.4	3.8
17	21.38	*mrrmmrrm*	1.2	1.3
18	21.36	*mrrmmrrr*	1.7	1.7
19	21.34	*rrrmmrrr*		0.6
IV	21.2–21.0	*mmrr*	22.4	22.3
V	21.0–20.75	*mmrm* + *rmrr*	6.1	6.0
VI	20.75–20.5	*rmrm*	0.7	0.5
VII	20.5–20.25	*rrrr*	12.6	12.6
35	20.38	*mrrrrm*	3.1	3.2
36	20.34	*mrrrrr*	4.3	4.4
37	20.30	*rrrr*	5.2	5.0
VIII	20.25–20.05	*rrrm*	11.3	11.2
39	20.17	*rrrrmr*	2.3	2.1
40	20.12	*rrrrrmmr* +	9.0	1.2
		mrrrrmmr[*]		1.7
41	20.09	*rrrrmmm*[*] +		2.3
		mrrrrmmm		3.5
IX	20.05–19.8	*mrrm*	7.9	8.3
42	20.03	*rmrrmr*		0.3
43 +		*mmrrmr*	2.7	2.6
44		*rmmrrmmr*		0.6
45	19.89	*mmmrrmmr*	4.9	2.4
46	19.87	*mmmrrmmm*		2.5
X		*mrmrm*	n.d.[c]	0.1
XI		*mrmrr*	n.d.[c]	0.2
XII	47.5–47.35	*rrmrr* + *mrrrm*	2.7	2.6
XIII	47.35–47.10	*mrrrr*	10.5	10.9
8	47.24	*mmmrrrrrr*		2.3
9	47.20	*rmmrrrrrr* +		1.1
		mmmrrrrmm		2.9
10	47.16	*rmmrrrrmm*		1.4
XIV	47.10–46.95	*rmmrm* + *rrrrr*	7.5	7.4
13	46.98	*mrrrrrrrr*		1.7
15	46.93	*rrrrrrrr* +		1.1
		mmrrrrrrm		2.1
18	46.90	*mmrrrrrrr*		1.4
XV	46.95–46.70	*rmmrr* + *mmmrm* + *mmmrr*	22.0	22.5

Table 10 (*continued*)

Range/Peak no.	δ (ppm)[a]	Assignment	Fraction (exp.) %	Fraction (calc.)[b] (%)
27	46.69	*rmmmmrrrr*	14.5	1.3
28	46.66	*mmmmmrrrr* +		3.1
		rmmmmrrmm		1.6
29	46.63	*mmmmmrrmm*		3.9
XVI	46.70–46.50	*rmrrm*	3.5	3.2
30		*rrmrrmm*		2.5
XVII	46.50–46.25	*rmmmr* + *mmmmr* +	44.6	43.6
		mmrrm + *rmrrr* + *mmmmm*		
XVIII	46.25–46.00	*mmrrr*	9.3	8.9
XIX		*rmrmr*	n.d.[c]	0.2
XX		*mmrmr*	n.d.[c]	0.3
XXI		*mmrmm*	n.d.[c]	0.2
XXII	28.77–28.70	*mmmmmm*	10.9	10.6
1	28.73	*mmmmmmmm*		5.5
XXIII	28.70–28.65	*mmmmmr*	8.0	8.1
2	28.67	*mmmmmmrr*		5.8
XXIV	28.65–28.58	*rmmmmr*	2.1	1.7
4	28.62	*rrmmmmrr*		1.7
XXV	28.58–28.49	*mmmmrr*	11.7	11.3
6	28.52	*mmmmmrrm*		4.8
XXVI	28.49–28.41	*mmmmrm* + *rmmmrrr*		
		mmmrrm + *mmmrrr*	19.3	19.1
		mmmrmr		
8	28.047	*mmmrrm* + *mmmrrr*	15.1	15.0
XXVII	28.41–28.25	*rmmmrm* + *rmmrrm*		
		rmmrrr + *mmmrmm*		
		rmmrmr + *rmmrmm*	47.9	49.3
		rmmr + *rrmr*		
		rmrm + *rr*		
				$\sigma_1 = 0.99$
				$\sigma_2 = 0.45$
				$P_{12} = 0.72$
				$P_{21} = 1.00$

[a] Downfield of TMS.
[b] According to the chain migratory C_1-symmetric statistical model (see text).
[c] n.d. = not detected.
* Correct assignment of the two peaks is possibly reversed.

of solvent fractionation [8,114] proved that their nature is complicated: most samples, indeed, can be separated into an amorphous, atactic fraction and a semicrystalline, predominantly isotactic fraction, along with intermediate fractions that might contain isotactic/atactic stereoblock chains. This would indicate that the frequency of rotamer interconversion is comparable (or somewhat lower) than that of chain transfer.

By changing polymerization conditions (in particular, temperature and monomer concentration), it should be possible to control — to some extent — the relative amount and average length of the isotactic

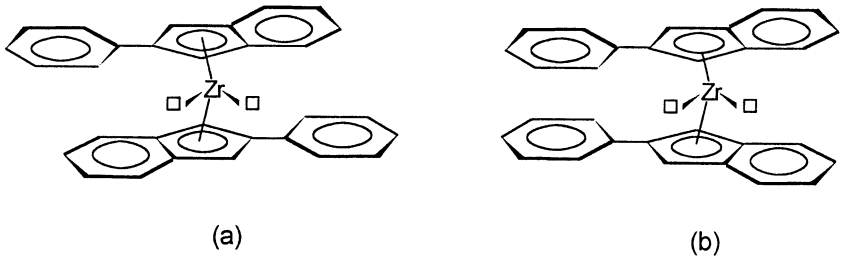

Chart 33.

and atactic sequences, as well as the degree of stereoregularity of the former. However, no high-field ^{13}C NMR data have been published up to now, whereas it has been demonstrated [113,117] that a configurational analysis at pentad level does not represent an adequate description of such materials. Therefore, caution in the interpretation of the microstructural results is mandatory.

The ^{13}C NMR pentad distributions for two representative polypropylene samples prepared with (2-Ph-Ind)$_2$ZrCl$_2$/MAO at 23°C at different monomer concentrations are given in Table 11 [113]. The methyl region of a typical ^{13}C NMR spectrum is shown in Fig. 27 [113].

According to the commonly accepted polymerization mechanism [111,113], matrix $\mathbf{M}_{ES/CE}$ of Section 3 should be used to reproduce such data, but their quality is not good enough for a statistically significant fit. Indeed, the $\Sigma(y_i - y_i^\circ)^2$ function has infinite nearly equivalent local minima, corresponding to largely different values of the switching probabilities $P_{ES/CE}$ and $P_{CE/ES}$ (in the range {0,0.1}, provided that the ratio $[P_{CE/ES}/(P_{ES/CE} + P_{CE/ES})]$, i.e. the weight fraction of isotactic sequences, is kept constant). Just as an example, two such solutions for each polymer sample are given in Table 11. On the other hand, an identical fit is obtained also in terms of a more simple two-site model [63,113], assuming the samples to be physical blends of (predominantly) isotactic and (nearly) atactic polypropylenes (see again Table 11).

An interesting study on the regioregularity of these polypropylenes has been recently published [118]. The predominant propene insertion mode is 1,2; low amounts (0.2–0.3 mol%) of 2,1 units were detected by ^{13}C NMR in propene/ethene-[1-^{13}C] copolymers, but only in predominantly isotactic environment. This was taken as an indication that not only the stereoselectivity, but also the regioselectivity of the *rac*-like and *meso*-like forms of the 'oscillating' catalysts resembles that of the corresponding bridged bis-Indenyl complexes (Sections 4.2.2 and 4.2.3).

Evidence of a fluxional behavior with consequences on the stereoselectivity has been reported also for some *ansa*-metallocene catalysts. In particular, the presence of low amounts of syndiotactic sequences (stereoblocks) in isotactic polypropylene samples prepared with Me$_2$C(3-R-Cp)(9-Flu)MtCl$_2$/MAO systems (Mt = Zr, Hf; R = *t*-butyl or trimethylsilyl) has been explained in terms of a reversible hapticity change of the substituted Cp ring (from h^5 down to h^1), possibly triggered by the steric repulsion between the aromatic ligand and the growing polymer chain [119].

4.2.7. Bridged half-metallocenes

Many half-metallocenes of the fourth column — both bridged and unbridged — have interesting catalytic behaviors. CpTiCl$_3$, for instance, in combination with MAO, is a highly active catalyst for the syndiotactic polymerization of styrene [120,121].

Very few of such complexes, however, perform well with propene. Among them are the so-called

Table 11
^{13}C NMR steric pentad distributions for two polypropylene samples prepared with the 'oscillating' catalyst system (2-Ph-Ind)$_2$ZrCl$_2$/MAO at 23°C and two different propene concentrations in toluene (data from Ref. [113]). Best-fit calculated distributions according to two possible statistical models (see text) are also given

Pentad	Sample PP1 (liquid monomer)				Sample PP3 ($p(C_3H_6) = 50$ psig)			
	% (Exp.)	% (Calc., ES/CE)		% (Calc., ES + CE)	% (Exp.)	% (Calc., ES/CE)		% (Calc., ES + CE)
mmmm	32.4	32.46	32.45	32.46	16.8	16.81	16.81	16.81
mmmr	14.7	14.71	14.56	14.55	16.4	16.27	16.20	16.20
rmmr	4.3	4.00	4.15	4.17	6.0	5.35	5.41	5.42
mmrr	9.8	9.94	10.03	10.04	11.8	11.57	11.61	11.61
mmrm + rmrr	18.0	18.27	18.27	18.26	22.7	23.05	23.03	23.03
rmrm	8.5	8.16	8.32	8.33	11.1	10.74	10.82	10.83
rrrr	2.3	1.90	1.78	1.77	2.8	2.73	2.69	2.69
rrrm	5.2	5.67	5.44	5.42	7.6	7.72	7.63	7.61
mrrm	4.9	4.89	5.01	5.02	5.0	5.75	5.80	5.81
		$\sigma = 0.971$	$\sigma = 0.963$	$\sigma = 0.962$		$\sigma = 0.944$	$\sigma = 0.933$	$\sigma = 0.933$
		$P_m = 0.59$	$P_m = 0.61$	$P_m = 0.61$		$P_m = 0.58$	$P_m = 0.59$	$P_m = 0.59$
		$P_{ES/CE} = 0.053$	$P_{ES/CE} = 0.0052$	$w_{ES} = 0.27$		$P_{ES/CE} = 0.074$	$P_{ES/CE} = 0.0089$	$w_{ES} = 0.08$
		$P_{CE/ES} = 0.024$	$P_{CE/ES} = 0.0020$			$P_{CE/ES} = 0.0082$	$P_{CE/ES} = 0.0008$	
		$\Sigma(y_i - y_i^o)^2 = 5.4 \times 10^{-5}$	$\Sigma(y_i - y_i^o)^2 = 6.8 \times 10^{-5}$	$\Sigma(y_i - y_i^o)^2 = 5.4 \times 10^{-5}$		$\Sigma(y_i - y_i^o)^2 = 1.3 \times 10^{-4}$	$\Sigma(y_i - y_i^o)^2 = 1.3 \times 10^{-4}$	$\Sigma(y_i - y_i^o)^2 = 1.3 \times 10^{-4}$

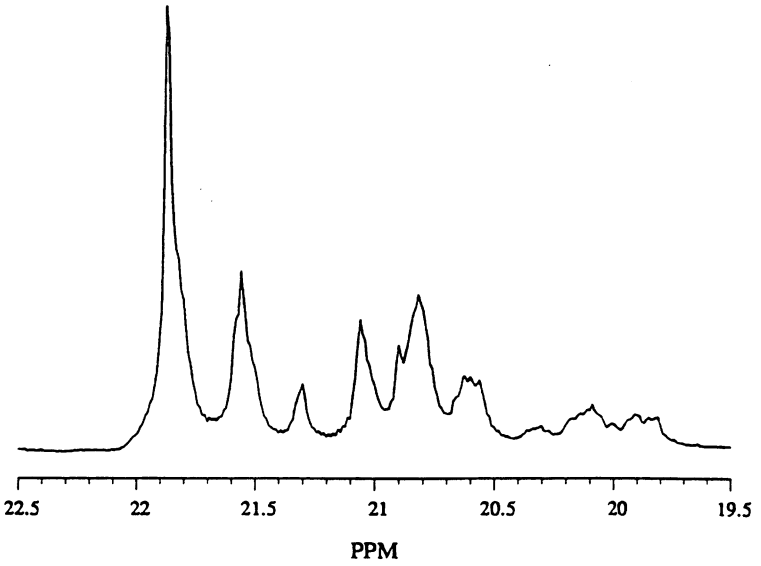

Fig. 27. Methyl region of the 100 MHz ^{13}C NMR spectrum of a typical polypropylene sample obtained with the 'oscillating' catalyst system (2-Ph-Ind)$_2$ZrCl$_2$/MAO. Reprinted with permission from Macromolecules 1998; 31:2707. ©1998 American Chemical Society [113].

constrained geometry catalysts of general formula $Me_2Si(Me_4Cp)(NR)MtX_2$ (Chart 34), with Mt = Ti or Zr, R = alkyl, X = halogen or alkyl [122–124]. The absence of a second Cp ring and the short bridge result in a very open environment of the transition metal, allowing a much easier insertion of bulky monomers compared with bis-Cp systems. This feature is of special importance in the copolymerizations of ethene with higher 1-alkenes and — even — with styrene.

A number of 'constrained geometry' catalysts (as well as related ones with a hydrocarbon bridge) homopolymerize propene with decent activity. The polymers are poorly regioregular (with up to 5 mol% of 2,1 misinsertions) and practically atactic. In the presence of bulky amide groups, a weak chain end control, usually in syndiotactic sense, can be observed at low temperature [125].

On the other hand, related complexes in which the Cp ring is replaced by a 9-fluorenyl moiety (Chart 35) promote the syndiotactic polymerization of propene under site control. Syndiotactic polypropylene with [*rrrr*] as high as 0.77 was obtained with Me_2Si(9-Flu)(N-*t*-Bu)ZrCl$_2$/MAO [126,127]; there is little doubt that the stereoselectivity must be traced to the (pseudo-) C_s-symmetry of the catalytic complex, and that the mechanism of stereocontrol is strictly analogous to that for the C_s-symmetric *ansa*-metallocenes (Section 4.2.4).

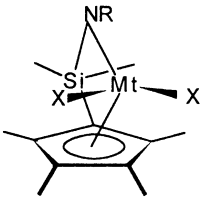

Chart 34.

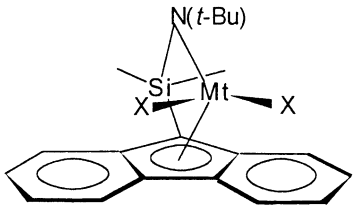

Chart 35.

Quite surprisingly, predominantly syndiotactic polymerization under *chain end* control was claimed instead for the homologous Ti complex [128]. The pentad distribution of a typical polymer obtained at 40°C, $[C_3H_6] \approx 2$ mol/l is given in Table 12. The sample, with $[rrrr] = 0.38$, contains mainly …*rrrrmrrrr*… stereodefects, which can be diagnostic for 1,3-*unlike* asymmetric induction (see Sections 2 and 3); as a matter of fact, a calculated distribution in terms of matrix $\mathbf{M}_{CE}$ of Section 3 agrees well with the experimental one (columns 2 and 3 of Table 12). However, an even better fit is obtained under the hypothesis of *site*-controlled, chain migratory propagation, using matrix $\mathbf{M}_{CM\text{-}Cs}$ of Section 4.2.4.2 (columns 2 and 4 of Table 12); according to the latter interpretation, the catalyst is highly enantioselective ($\sigma = 0.97$), and the observed *m*-type stereoerrors must be traced to frequent 'skipped insertions' ($P_{sk} = 0.19$).

The above can be taken as an exemplification of the ambiguity possibly associated with the use of microstructural data, in the absence of other elements, for mechanistic purposes. In the considered case, an easy way to remove such ambiguity would have been to investigate the effect of monomer concentration on polymer stereoregularity; indeed, no effect should be observed for chain-end-controlled

Table 12
^{13}C NMR steric pentad distribution for a predominantly syndiotactic polypropylene sample prepared with the catalyst system Me_2Si(9-Flu)(N-*t*-Bu)$TiCl_2$/MAO (data from Ref. [128]). Best-fit calculated distributions according to two alternative statistical models (see text) are also given

Pentad	Fraction (exp.)	Fraction (calc.)	
		CE[a]	CM-C_s[b]
mmmm	0.00	0.0021	0.004
mmmr	0.02	0.015	0.023
rmmr	0.03	0.028	0.034
mmrr	0.07	0.057	0.071
mmrm + *rmrr*	0.20	0.223	0.206
rmrm	0.05	0.057	0.051
rrrr	0.38	0.381	0.381
rrrm	0.21	0.208	0.204
mrrm	0.04	0.028	0.027
		$\Sigma(y_i - y_i^o)^2 \times 10^4 = 9.4$	$\Sigma(y_i - y_i^o)^2 \times 10^4 = 2.8$
		$P_r = 0.786$	$\sigma = 0.97$
			$P_{sk} = 0.187$

[a] According to the chain end model.
[b] According to the chain migratory, C_s-symmetric model.

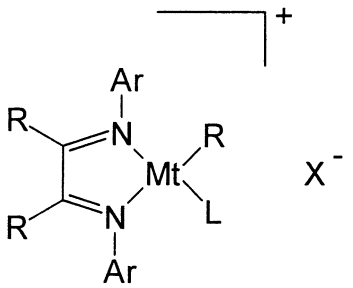

Chart 36.

propagation, whereas a trend of decreasing stereoregularity with decreasing propene feeding pressure is expected for site-controlled, chain migratory propagation. Unfortunately, up to now this aspect has not been clarified for the quoted catalyst.

4.3. Polypropylene from homogeneous late transition metal catalysts

Late transition metals have long been considered unable to catalyze the homopolymerization of 1-alkenes, due to their high tendency to promote β-H elimination. However, it is now well proved that this tendency can be contrasted with a proper choice of the ancillary ligands, that must hinder the regions of space around the active metal needed for the agostic back-biting of the growing chain and for monomer-assisted chain transfer.

Brookhart and coworkers, in particular, developed several classes of Ni(II), Pd(II), and — more recently — Fe(II) catalysts with chelating N ligands, mainly for ethene polymerization [18].

Square-planar diimine complexes of the type shown in Chart 36 (Mt = Ni(II), Pd(II)), in combination with MAO, at room temperature afford atactic polypropylene of comparatively low average molecular mass. At lower temperatures, however, for some of them (with Mt = Ni(II)), chain propagation becomes predominantly *syndiotactic* ([*rr*] up to 0.8), due to the onset of chain-end control (1,3-*unlike* asymmetric induction) [129]. The analysis of the chain ends proved [130] that the predominant propene insertion mode is 1,2; however, the regioselectivity is not high, and the polymers contain up to 10 mol% of 2,1 and/or 3,1 units, which prevents reliable measurements of ^{13}C NMR methyl pentad distributions. That notwithstanding, there is little doubt that the stereodefects are mainly of …*rrrrmrrrr*… type, as expected for chain end control.

On the other hand, predominantly *isotactic*, chain-end-controlled polypropylene, with [*mmmm*] values up to 0.67 and …*mmmrmmm*… type stereodefects, has been obtained at low temperatures with pentacoordinated Fe(II) catalysts bearing tridentate pyridine-bis(imine) ligands (again, in combination with MAO) [131]. Such polymer is highly regioregular, and — quite surprisingly — the predominant monomer insertion mode is 2,1, which makes it a unique microstructural type.

4.4. Polypropylene from Ziegler–Natta catalysts

4.4.1. $TiCl_3$ and $MgCl_2$/$TiCl_4$-based systems

4.4.1.1. Catalysts and polymerization mechanism. The 25 Mt of isotactic polypropylene consumed in

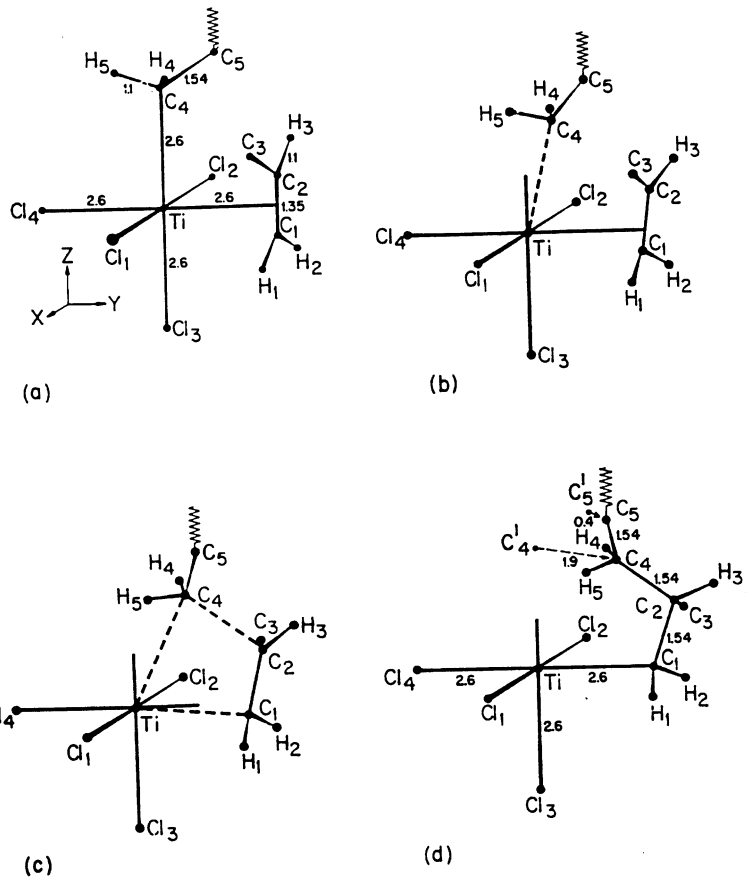

Fig. 28. Possible propene insertion path for Ti-based Ziegler–Natta catalysts, according to Cossee (reproduced with permission from Ref. [134]).

the world in 1999 were practically all produced with technologies relying on heterogeneous catalysts that are a direct derivation of those discovered in the laboratories of Karl Ziegler and Giulio Natta in 1953–54 [1].

The first generations of these catalysts were based on $TiCl_3$ in one of its 'violet' modifications with layered structure (α, γ, δ), in combination with an alkyl-Al-halide (e.g. $AlEt_2Cl$) [3]. Cossee was the first to suggest that the active sites are located on the thin, coordinatively unsaturated side faces of the platelet-like $TiCl_3$ crystals, and to relate the chirality of the surface Ti atoms with the stereoselectivity [134]. With some adaptations, his mechanism of isotactic chain propagation (Fig. 28) is still considered a sound basis for the description of the polymerization process; its key points can be summarized as follows [20,134].

(i) The Ti atoms in the bulk of 'violet' $TiCl_3$ crystals are chiral; indeed, each of them is bonded to three neighboring ones by double Cl bridges, which results in an octahedral tris-chelate coordination with Δ or Λ configuration (Fig. 29-top).

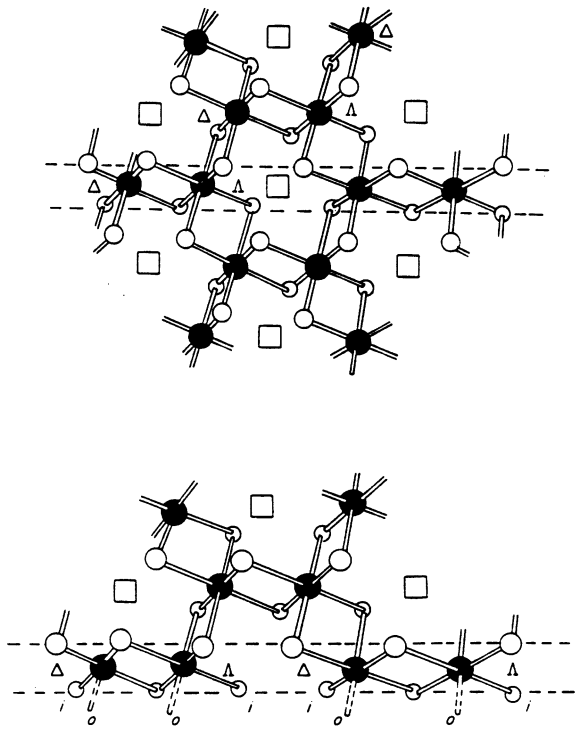

Fig. 29. Schematic drawing of a structural layer of 'violet' $TiCl_3$, before (top) and after (bottom) a cut along the (110) crystallographic direction. The chirality of the Ti atoms, and the inward (i) or outward (o) orientation of the two coordination sites not involved in Cl bridging to the crystal interior at the coordinatively unsaturated Ti atoms on the cut are explicitly indicated. Reprinted with permission from Comprehensive Polymer Science. © 1988 Elsevier Science Ltd [20].

(ii) Plausible lateral terminations of the structural layers are obtained by breaking one out of three double bridges around the Ti atoms on the cut (e.g. parallel to the (110) or (100) crystallographic directions; Fig. 29-bottom). This generates linear racemic arrays of enantiomorphous Ti centres with two *cis* double Cl bridges directed towards the crystal interior, and one unbridged Cl ligand (as a remnant of the third broken bridge) to ensure the electroneutrality.
(iii) The catalytic species are formed by ligand exchange with the alkyl-Al cocatalyst, which replaces the unbridged Cl with an R group. The monomer can coordinate to the remaining empty site of the octahedron, and insert into the Ti–R bond.
(iv) Monomer insertion is enantioselective due to site control, and opposite monomer enantiofaces are preferred at Ti centres of opposite chirality.

At the time of the original formulation, point (iv) was rather weak, because the steric contacts involved in the chiral recognition were not clearly identified. However, the first ^{13}C NMR characterizations of the polymers (Section 2) confirmed the site-controlled origin of the isotacticity, and ultimately molecular mechanics studies on models of catalytic species pointed out the key role of the growing chain in the asymmetric induction [20,51,135].

Two such models, which refer to (100) and (110) cuts of a structural layer of 'violet' $TiCl_3$, are shown

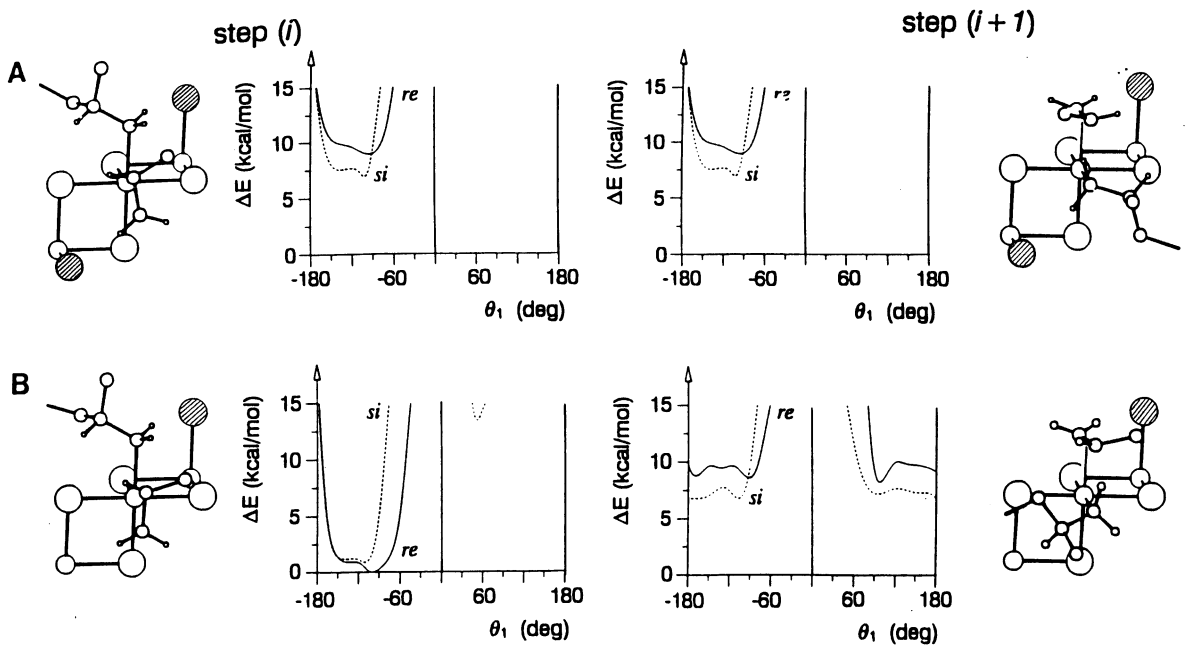

Fig. 30. Possible models of catalytic species on a (110) (A) or (100) (B) cut of a structural layer of 'violet' $TiCl_3$. The situations labelled as step (*i*) and (i + 1) correspond to consecutive 1,2 propene pre-insertion intermediates, in the hypothesis of a chain migratory propagation mechanism. In both cases, the configuration of the active Ti centre is Δ; however, the local symmetry is C_2 for species A, C_1 for species B. According to molecular mechanics calculations (see internal energy maps shown), at the two homotopic active sites of species A propene coordination (and subsequent 1,2 insertion) is enantioselective, due to non-bonded contacts between one of the two dashed Cl ligands and the growing polymer chain, which must bend to one side. This favors, in turn, propene coordination with the *si* enantioface (shown), which orients the methyl group *anti* to the first chain C–C bond; as a result, chain propagation is predicted to be *isotactic*. On the other hand, the absence of one of the said crucial Cl ligands in the case of species B results in a loss of enantioselectivity at step (i + 1); this would lead to *hemiisotactic* propagation in case of a regular chain migratory mechanism (adapted from Ref. [135]).

in Fig. 30. In the former case (Fig. 30a), a local C_2 axis relates the two coordination sites available at each surface Ti atom, which implies their equivalence. In each of them, a growing polymer chain experiences repulsive non-bonded contacts with one of the Cl atoms of the surface (dashed in the figure); as a result, the first C–C bond is conformationally constrained and chirally oriented. In turn, this favors the 1,2 insertion of a propene molecule π-coordinated to the other site with the enantioface that brings the methyl substituent *anti* to the said C–C bond.

This mechanism of stereocontrol is strikingly analogous to that discussed in Section 4.2.2.1 for the C_2-symmetric *ansa*-metallocene catalysts (for which, of course, the role of the surface is played by the aromatic ligand framework). In both cases, a growing chain with at least one C–C bond is needed in order to pass the chiral information from the active metal to the incoming monomer, and propene insertion into a Mt–methyl bond is not enantioselective.

An analogy with C_1-symmetric metallocene catalysts (Section 4.2.5.1) can be invoked instead for the model of catalytic species on a (110) cut of $TiCl_3$ (Fig. 30b). Indeed, according to molecular mechanics calculations [135], the absence of one of the two surface Cl atoms required for the orientation of the

growing chain makes propene insertion at 'step (i + 1)' non-enantioselective. Therefore, chain propagation is expected to be hemiisotactic if the mechanism is of chain migratory type, whereas a predominantly isotactic control can be obtained if monomer insertion occurs in preference as shown at 'step (i)'; recent experimental data (discussed in Section 4.4.1.2) indicate that the latter is actually the case.

In the late 1960s, 'activated' $TiCl_3$ catalysts (in some cases, containing minor amounts of $AlCl_3$ in solid solution) with specific surface areas of the order of 150 m^2/g became available [1,3,4]. These second-generation systems, that found large-scale industrial application in the 1970s and are still used today by a number of minor polypropylene manufacturers, have productivities of the order of 5 kg of polymer per g of $TiCl_3$ when used in combination with $AlEt_2Cl$; the polymers have [*mmmm*] values >0.90, DSC melting points $T_m > 165$°C and are almost completely insoluble in high-boiling solvents such as heptane, though minor amounts (<5% by weight) of by-products of lower stereoregularity are also formed. Higher productivities, but also (much) lower stereoselectivities, are observed when the co-catalyst is an Al-trialkyl such as, e.g. $AlEt_3$.

The main problem of the polypropylene produced with $TiCl_3/AlEt_2Cl$ systems is that it contains non-negligible residual amounts of hydrolizable Cl, which requires expensive procedures of catalyst de-ashing. In order to increase the productivity (referred to Ti), attempts were made to support active Ti compounds (usually, $TiCl_4$) on inert matrices. Good results were obtained only with matrices structurally similar to 'violet' $TiCl_3$, such as — in particular — $MgCl_2$ [1,132,133]. The first simple $MgCl_2/TiCl_4$-AlR_3 systems had a productivity in excess of 10 kg of polypropylene per g of catalyst (roughly corresponding to 500 kg per g of Ti), but the 'poorly tactic' fraction exceeded 50% by weight of the raw polymer. However, spectacular increases of stereoselectivity were obtained by the addition of suitable Lewis bases to the co-catalyst (*external* donors) and/or to the solid catalyst (*internal* donors).

$TiCl_4$ chemisorption takes place at coordinatively unsaturated side faces of the platelet-like $MgCl_2$ crystals. Corradini and coworkers [20,136] and, more recently, Barino and Scordamaglia [137] showed how epitactic coordination of $TiCl_4$ units to (100) and (110) cuts of $MgCl_2$ structural layers can give rise to a variety of catalytic species, some of which are practically identical to those previously proposed for 'violet' $TiCl_3$ (Fig. 31). It seems likely that the Lewis bases used as catalyst modifiers are able to 'poison' the most 'open' of these Ti species, that would be unable to exert a strong stereocontrol on the polymerization, and/or to change them into stereoselective species by providing the necessary steric hindrance; possible mechanisms for this action are discussed in Section 4.4.1.2.

The last generations of $MgCl_2$-supported *high-yield* catalysts, modified with aromatic diesters or 1,3-diethers as internal donors and alcoxysilanes as external donors, afford polypropylenes with [*mmmm*] values well above 0.90 and negligible contents of 'poorly tactic' by-products, with a mileage in excess of 100 kg of polymer per g of catalyst [1,132,133].

4.4.1.2. Chain configuration. The multi-site nature of Ziegler–Natta systems (either $TiCl_3$-based or $MgCl_2$-supported) results in the fact that the polypropylenes produced are complicated mixtures of macromolecules with different tacticity (from highly isotactic to poorly isotactic (*isotactoid*) and — even — predominantly syndiotactic) [20].

A rough but practical method for evaluating the stereoregularity of a given polymer sample is to measure the weight fraction that is insoluble in a certain solvent under certain conditions, and as such is conventionally referred to as 'isotactic'. Although it is well known that polymer solubility depends on the molecular mass as well, it is commonly assumed that in the range of average molecular masses of

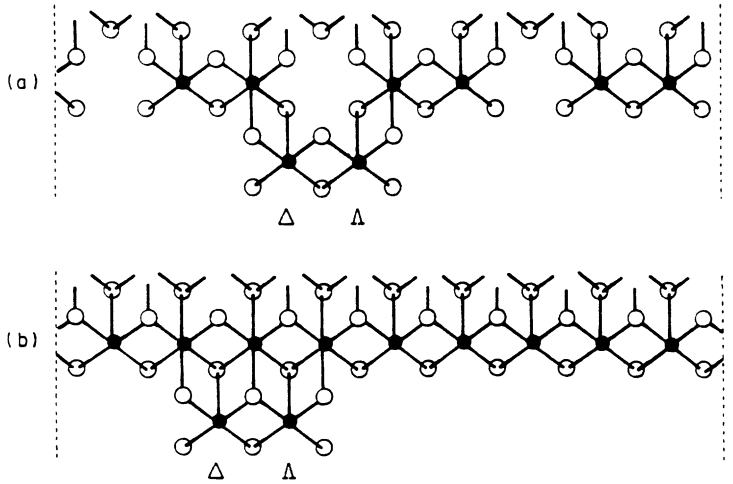

Fig. 31. Model of a Ti_2Cl_6 relief on a (110) cut of a structural layer of 'violet' $TiCl_3$ (a), and of a Ti_2Cl_6 species chemisorbed epitactically on the (100) cut of a structural layer of $MgCl_2$ (b). Molecular mechanics studies [20,135,136] pointed out that the two species (whose close similarity is immediately apparent) can give rise to isotactic-selective catalytic species. Reprinted with permission from Comprehensive Polymer Science. ©1988 Elsevier Science Ltd [20].

commercial grade polypropylenes this dependence is only marginal, and that the fractionation is mainly governed by tacticity [1,3,4].

Two popular (and substantially equivalent) procedures are extraction with boiling heptane and fractional crystallization after complete dissolution in hot (>130°C) xylene. The so-called *index of isotacticity* (*II*) is the weight fraction of polymer insoluble in boiling heptane; the weight fraction of polymer which crystallizes from xylene solution at room temperature, instead, is called *xylene index* (*XI*) [1,3,4].

Polypropylene samples made with industrial catalysts are characterized by *II* and/or *XI* values higher than 95% [1,3,4]. ^{13}C NMR confirms the effectiveness of the fractionation, in the sense that typical 'isotactic' fractions (i.e. heptane- or xylene-insoluble) have values of [*mmmm*] in excess of 0.90; however, in most cases the spectra also reveal low amounts of syndiotactic blocks, owing their insolubility to the fact they are chemically bound to the isotactic part [138,139].

The polymer fraction soluble in boiling heptane or in xylene at room temperature, in turn, is often referred to as 'atactic', although it has long been recognized that this notation is not appropriate. Indeed, no truly atactic chains are found in such fraction, which contains instead poorly isotactic (isotactoid) and syndiotactic sequences [20,63,140]. 'Atactic' fractions made with $MgCl_2$-supported systems have a certain stereochemical variability; in particular, the use of an 'external' donor tends to increase the relative amount of syndiotactic sequences, which in a few special cases can even become predominant [141,142]. Quite surprisingly, recent high-field ^{13}C NMR investigations proved the presence also of isotactic sequences, occurring in the form of short stereoblocks (which largely prevents their crystallization) [39].

The above indicates that the difference between 'isotactic' and 'atactic' fractions is less clearcut than has long been assumed, and that the mechanisms of stereocontrol leading to their formation are intimately related.

A high-field ^{13}C NMR study of a polypropylene sample obtained with the catalyst system $MgCl_2$/$TiCl_4$ — 2,6-dimethylpyridine/$AlEt_3$ has been recently reported [39]. This system is peculiar in that it

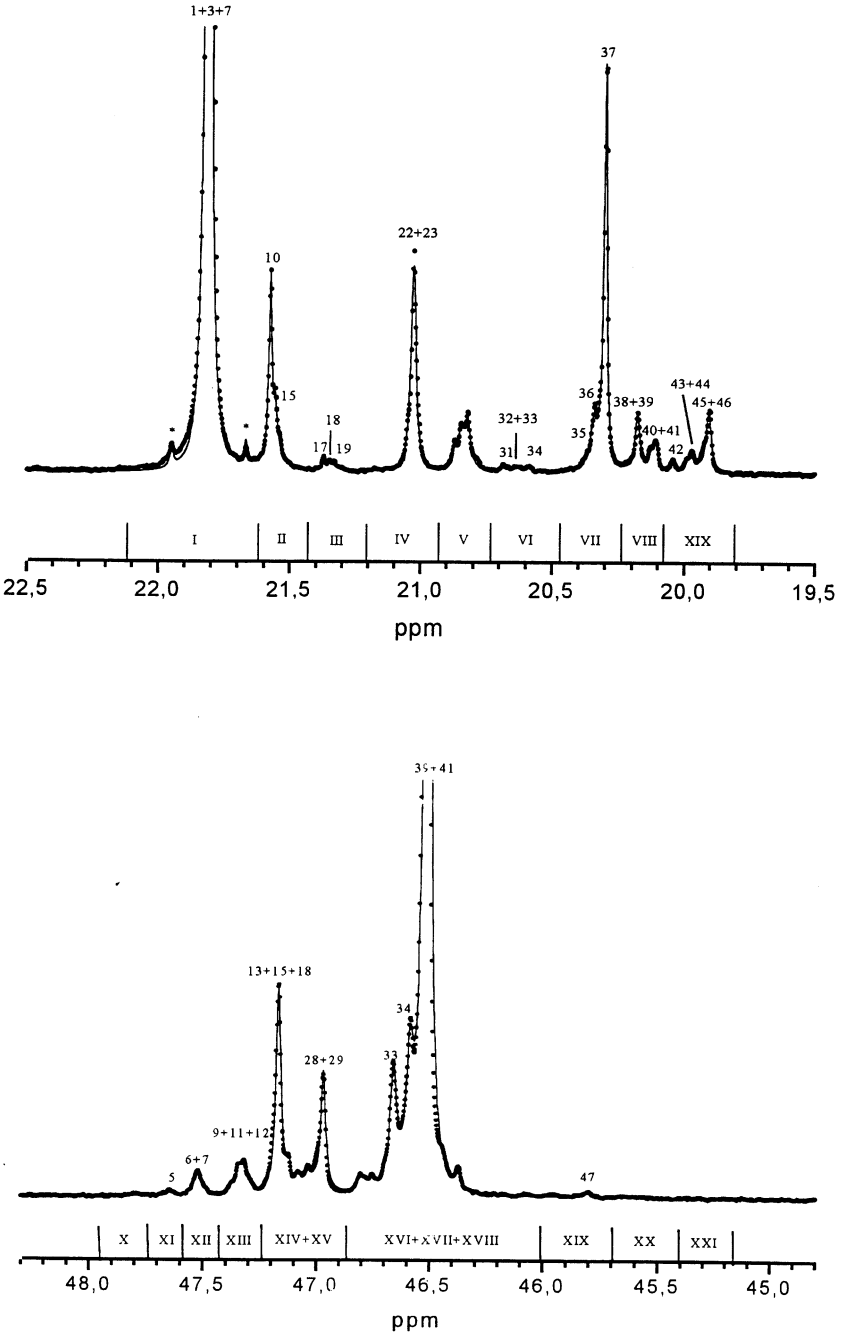

Fig. 32. Methyl (top) and methylene (bottom) regions of the 125 MHz ^{13}C NMR spectrum (recorded in tetrachloroethane-1,2-d_2 at 130°C; chemical shift scale in ppm downfield of TMS) of the xylene-insoluble fraction of a polypropylene sample prepared with the catalyst system $MgCl_2/TiCl_4$-2,6-dimethylpyridine/$AlEt_3$. Peak numbering refers to the full assignment reported in Refs. [14,15]; for attributions, see Table 13 (adapted from Ref. [39]).

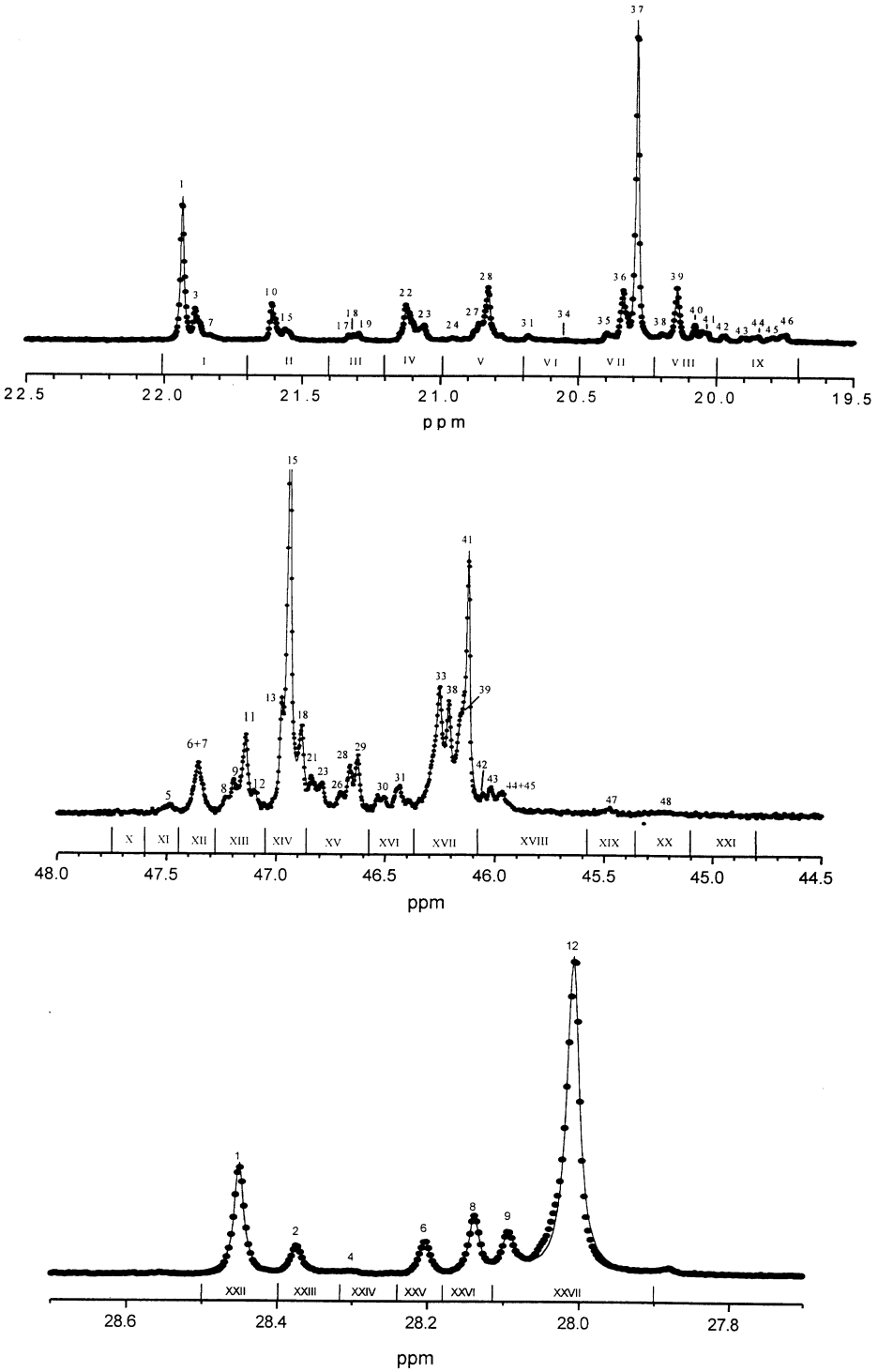

Fig. 33. Methyl (top), methylene (centre) and methine (bottom) regions of the 150 MHz ^{13}C NMR spectrum (recorded in tetrachloroethane-1,2-d_2 at 70°C; chemical shift scale in ppm downfield of TMS) of the diethyl-ether-insoluble/pentane-soluble fraction of a polypropylene sample prepared with the catalyst system $MgCl_2/TiCl_4$ - 2,6-dimethylpyridine/$AlEt_3$. Peak numbering refers to the full assignment reported in Refs. [14,15]; for attributions, see Table 14 (adapted from Ref. [39]).

Table 13
Assignment of the 125 MHz ^{13}C NMR spectrum in Fig. 32. In the last two colums, the experimental stereosequence distribution, evaluated by full spectral simulation, is compared with the best-fit calculated one, according to the appropriate three-site statistical model (see text)

Range/Peak No.	Assignment	Normalized fraction		
		(Exp.)	(Calc.)	
I	*mmmm*	0.6515(18)	0.6524	
II	*mmmr*	0.0621(12)	0.0591	
III	*rmmr*	0.0065(5)	0.0065	
III/17	*mrrmmrrm*	0.0025(7)	0.0034	
III/18	*mrrmmrrr*	0.0019(9)	0.0015	
IV	*mmrr*	0.0670(8)	0.0685	
V	*mmrm* +	0.0378(13)	0.0358	0.0037
	rmrr			0.0321
VI	*rmrm*	0.0060(5)	0.0063	
VI/31	*rrmrmr*	0.0020(10)	0.0022	
VI/34	*mrmrmm*	0.0020(10)	0.0026	
VII	*rrrr*	0.1045(7)	0.1046	
VIII/38 + 39	*mrrrmr* +	0.0180(14)	0.0202	0.0179
	rrrrmr			0.0023
VIII/40 + 41	*rrrrmm* +	0.0130(20)	0.0129	0.0122
	mrrrmm			0.0007
IX	*mrrm*	0.0341(8)	0.0337	
IX/43 + 44	*mmrrmr*	0.0129(33)	0.0087	
IX/45 + 46	*mmrrmm*	0.0192(17)	0.0234	
X	*mrmrm*	0.0013(8)	0.0016	
XI	*mrmrr*	0.0028(13)	0.0030	
XII	*rrmrr* +	0.0149(15)	0.0161	0.0146
	mrrrm			0.0015
XIII	*mrrrr*	0.0274(36)	0.0301	
XIV +	*rmmrm* +	0.1571(103)	0.1617	0.0008
XV	*rrrrr* +			0.0896
	rmmrr +			0.0122
	mmmrm +			0.0028
	mmmrr			0.0563
XIX	*rmrmr*	0.0042(17)	0.0015	
XX	*mmrmr*	0.0010(10)	0.0033	
			$\Sigma(y_{i,c} - y_{i,o})^2 \times 10^4 = 1.01$	
			$\chi^2_r = 2.2$	
			$\sigma = \sigma_1 = 0.99_8$	
			$\sigma_2 = 0.39$	
			$P_{12} = 0.28$	
			$P_{21} = 0.92$	
			$P_r = 0.91$	
			$w_{ES} = 0.51$	
			$w_{CE} = 0.14$	
			$(w_{CM-Cl} = 0.35)$	

Table 14
Assignment of the 150 MHz ^{13}C NMR spectrum in Fig. 33. In the last two colums, the experimental stereosequence distribution, evaluated by full spectral simulation, is compared with the best-fit calculated one, according to the appropriate three-site statistical model (see text)

Range/Peak No.	Assignment	Normalized fraction		
		(Exp.)	(Calc.)	
I	*mmmm*	0.1937(50)	0.1971	
XXII	*mmmmmm*	0.1514(38)	0.1514	
XXIII	*mmmmmr*	0.0389(35)	0.0390	
II	*mmmr*	0.0708(29)	0.0711	
XXVI/6	*mmmmrr*	0.0426(33)	0.0508	
III	*rmmr*	0.0141(31)	0.0161	
III/17	*mrrmmrrm*	0.0042(15)	0.0056	
III/18	*mrrmmrrr*	0.0044(22)	0.0055	
IV	*mmrr*	0.0999(32)	0.0995	
IV/22	*mmmrrm* +	0.0709(22)	0.0688	0.0474
	mmmrrr			0.0214
V	*mmrm* +	0.1048(79)	0.1026	0.0040
	rmrr			0.0986
V/24	*mmmrmr*	0.0030(15)	0.0022	
VI	*rmrm*	0.0110(16)	0.0121	
VI/31	*rrmrmr*	0.0090(10)	0.0071	
VI/34	*mrmrmm*	0.0010(10)	0.0021	
VII	*rrrr*	0.3423(47)	0.3494	
VII/37	*rrrrrr*	0.2736(36)	0.2674	
VIII/38	*mrrrmr*	0.0086(13)	0.0073	
VIII/39	*rrrrmr*	0.0665(15)	0.0642	
VIII/40 + 41	*rrrrmm* +	0.0364(30)	0.0348	0.0332
	mrrrmm			0.0016
IX/42	*rmrrmr*	0.0090(15)	0.0055	
IX/43 + 44	*mmrrmr*	0.0189(36)	0.0161	
IX/45 + 46	*mmrrmm*	0.0248(36)	0.0243	
X	*mrmrm*	0.0006(15)	0.0017	
XI	*mrmrr*	0.0077(15)	0.0086	
XII	*rrmrr* +	0.0486(7)	0.0494	0.0450
	mrrrm			0.0044
XIII +	*mrrrr* +	0.4946(52)	0.5015	0.0975
XIV +	*rmmrm* +			0.0016
XV	*rrrrr* +			0.3006
	rmmrr +			0.0307
	mmmrm +			0.0023
	mmmrr			0.0688
XIII/9	*mmrrrrm*	0.0200(12)	0.0194	
XIII/11	*rmrrrrr*	0.0525(11)	0.0528	
XIX	*rmrmr*	0.0046(15)	0.0042	
XX	*mmrmr*	0.0052(15)	0.0037	
			$\Sigma(y_{i,c} - y_{i,o})^2 \times 10^3 = .28$	
			$\chi^2_r = 1.46$	
			$\sigma = 0.99_5$	

Table 14 (*continued*)

Range/Peak No.	Assignment	Normalized fraction	
		(Exp.)	(Calc.)
			$\sigma_1 = 1.00$ $\sigma_2 = 0.35$ $P_{12} = 0.49$ $P_{21} = 0.95$ $P_r = 0.90$ $w_{ES} = 0.10$ $w_{CE} = 0.47$ ($w_{CM-Cl} = 0.43$)

affords polypropylenes with relatively high amounts of crystallizable syndiotactic sequences both in the 'atactic' and in the 'isotactic' fraction; therefore, in the statistical analysis of chain configuration, it can be assumed that the average length of such sequences is high enough to neglect the presence of block junctions with the isotactic part that would represent a major source of complication.

Figs. 32 and 33 show the ^{13}C NMR spectra of the 'isotactic' (xylene-insoluble) fraction and of an 'atactic' (diethyl-ether-insoluble/pentane-soluble) sub-fraction, respectively. Resonance attributions are given in Tables 13 and 14, along with the normalized stereosequence distributions obtained by full spectral simulation. The latter could be reproduced satisfactorily only in terms of a linear combination of *three* statistical models: enantiomorphic-site, chain end, and chain migratory with diastereotopic sites. This required eight adjustable parameters: conditional probabilities σ of matrix $\mathbf{M}_{ES}$ and P_r of matrix $\mathbf{M}_{CE}$ (Section 3); σ_1, σ_2, P_{12}, P_{21} of matrix $\mathbf{M}_{CM\text{-}C1}$ (Section 4.2.5.2); mixing coefficients (weight fractions) w_{ES} and w_{CE} (of course, $w_{CM-C1} = 1 - w_{ES} - w_{CE}$). The calculated distributions, along with the best-fit values of all adjustable parameters, are also reported in Tables 13 and 14.

According to this interpretation, the two fractions comprise the same three configurational 'building blocks' (Chart 37): highly isotactic (enantiomorphic-site-controlled — *A*); syndiotactic (chain-end-controlled — *C*); isotactoid (*B*). The latter have a configurational statistics very similar to that observed for predominantly isotactic samples obtained in the presence of C_1-symmetric *ansa*-metallocenes, and discussed in detail in Section 4.2.5.2; particularly revealing is the substantial absence of consecutive stereoerrors (…*mrmr*… sequences, Chart 32), in spite of a rather poor average stereoregularity, and the trend of increasing isotacticity with decreasing monomer concentration [143].

The main difference between the two fractions is the relative amount of the three constituting stereosequences: the xylene-soluble fraction contains predominantly isotactoid ($w_{CM-C1} = 0.43$) and syndiotactic ($w_{CE} = 0.47$) blocks, whereas the xylene-insoluble one is made in prevalence of highly isotactic blocks ($w_{ES} = 0.51$).

Qualitatively, the above picture seems to have a general validity for $TiCl_3$ and $MgCl_2/TiCl_4$ catalysts [144], although the specific nature of the catalyst system has profound effects on the quantitative aspects of polymer configuration. For $MgCl_2$-supported catalysts, in particular, the modification with different Lewis bases may result in largely different polymerization products.

As an example, Tables 15 and 16 document the case of a polypropylene sample prepared with the catalyst system $MgCl_2$/di-(*iso*-butyl)phthalate/$TiCl_4$ - $AlEt_3$/phenyl-triethoxysilane [144]. Also in this case, the configuration of the xylene-insoluble and xylene-soluble fractions can be described in terms of

Table 15
150 MHz ^{13}C NMR stereosequence distribution for the xylene-insoluble fraction of a polypropylene sample prepared with the catalyst system $MgCl_2$/di-(*iso*-butyl)phthalate/$TiCl_4$-Phenyl-triethoxysilane/$AlEt_3$, along with best-fit calculated one, according to the appropriate three-site statistical model (see text)

Stereosequence	Normalized fraction		
	(Exp.)	(Calc.)	
mmmm	0.8880(110)	0.8891	
mmmr	0.0303(10)	0.0302	
rmmr	0.0028(10)	0.0018	
mmrr	0.0322(5)	0.0321	
mmrm +	0.0096(6)	0.0090	0.0017
rmrr			0.0073
rmrm	0.0022(4)	0.0025	
mrrrrm +	0.0043(3)	0.0047	
rrrrrm			
rrrrrr	0.0071(3)	0.0071	
mrrrmr +	0.0043(3)	0.0040	0.0008
rrrrmr			0.0032
rrrrmm +	0.0032(1)	0.0033	0.0030
mrrrmm			0.0003
rmrrmr	0.0008(2)	0.0004	
mmrrmr	0.0026(1)	0.0025	
mmrrmm	0.0131(3)	0.0132	
mrmrr	0.0006(6)	0.0010	
rrmrr +	0.0045(5)	0.0036	0.0031
mrrrm			0.0005
mrrrr	0.0063(8)	0.0063	
rmrmr	0.0005(5)	0.0005	
		$\chi^2_r = 1.9$	
		$\sigma = \sigma_1 = 0.99_9$	
		$\sigma_2 = 0$	
		$P_{12} = 0.08$	
		$P_{21} = 0.96$	
		$P_r = 0.82$	
		$w_{ES} = 0.72$	
		$w_{CE} = 0.02$	
		($w_{CM-Cl} = 0.26$)	

the previously discussed three-site model; however, relative to that of the $MgCl_2/TiCl_4$ — 2,6-dimethylpyridine/$AlEt_3$ system, the use of an internal donor coupled with a more effective external donor resulted in a drastic decrease in the proportion of syndiotactic and isotactoid sequences, and also in an increased stereoregularity of the latter (compare the best-fit values of corresponding adjustable parameters in Tables 13–16).

This configurational description of Ziegler–Natta polypropylenes fits nicely with their physical properties [39]. In particular, it provides a simple explanation for the fact that such polymers melt invariably at higher temperatures than those prepared with metallocene catalysts and containing the same *average* fraction of stereoirregularities (see also following Section 5); indeed, it is easy to understand that a

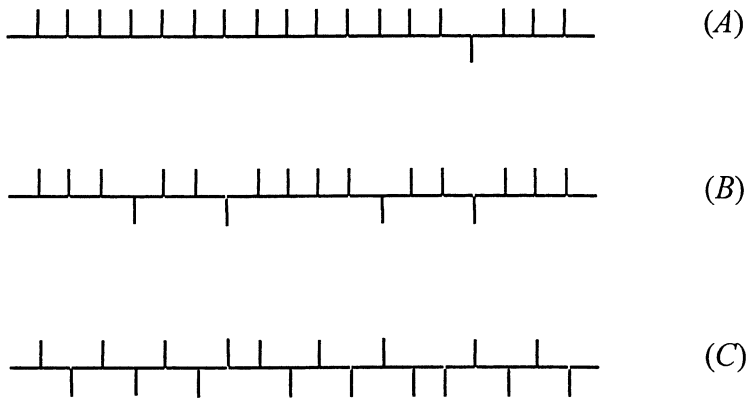

Chart 37.

random distribution of stereodefects corresponds to a lower *average* length of perfectly isotactic sequences, compared to the case in which such stereodefects are segregated in isotactoid blocks. On the other hand, it also accounts for the (otherwise surprising) observation, in the X-ray diffraction spectra of heptane-soluble ('atactic') fractions, of weak isotactic crystallinity [39], which can be traced to the low amounts of highly isotactic blocks.

A model of catalytic species consistent with the said configurational statistics has been recently proposed (Fig. 34) [39]. The basic structure of the catalytic complex is the chiral octahedral one proposed by Cossee and discussed in Section 4.4.1.1; however, differences in the substitution of the two coordination positions labelled in the figure as L1 and L2, known to be crucial for the onset of site control in terms of the 'growing-chain orientation' mechanism (see also Fig. 30), are invoked to explain the three observed types of chain propagation. In particular, this would be highly isotactic whenever (bulky) ligands (e.g. Cl atoms, Al-alkyl or Lewis base molecules) are present at both positions (with a resulting C_2 or *pseudo*-C_2 symmetry and homotopic active sites); isotactoid, when one of the two positions is vacant (C_1 symmetry and diastereotopic sites); syndiotactic, when both positions are vacant, so that site control is lost and chain-end control can become influent. A variety of surface Ti complexes corresponding to one of these three basic structural types can be envisaged, in particular for $MgCl_2$-supported catalysts [137].

Ligand exchanges at the two coordination positions can result in reversible switches between the different types of stereocontrol, with the formation of stereoblock chains. 'Second-order' effects (such as the conditional probability of monomer insertion at the weakly enantioselective active site of the C_1-symmetric species, and therefore the average content of stereoirregularities in the isotactoid sequences) can be related to the specific nature of the ligand(s) involved in such equilibria, and in particular of the Lewis bases used as catalyst modifiers.

More detailed studies of polymer fractionation are unquestionably needed in order to complete the picture. Up to now, high-field ^{13}C NMR characterizations of polypropylene samples subjected to temperature rising elution fractionation (TREF) have not been reported, and only pentad data are available [145–147] (which is not enough for a realistic configurational analysis). Both for 'violet' $TiCl_3$ and for $MgCl_2/TiCl_4$ catalysts, fractions of exceedingly high regioregularity ($[mmmm] > 0.98$) were isolated; it seems important to verify whether the distributions of stereodefects is not random even in such fractions.

Table 16
150 MHz ^{13}C NMR stereosequence distribution for the xylene-soluble fraction of a polypropylene sample prepared with the catalyst system $MgCl_2$/di-(*iso*-butyl)phthalate/$TiCl_4$-Phenyl-triethoxysilane/$AlEt_3$, along with best-fit calculated one, according to the appropriate three-site statistical model (see text)

Stereosequence	Normalized fraction		
	(Exp.)	(Calc.)	
mmmm	0.1585(35)	0.1667	
mmmmmm	0.1011(37)	0.1032	
mmmmmr	0.0479(28)	0.0523	
mmmr	0.1048(15)	0.1090	
rmmr	0.0310(12)	0.0310	
mrrmmrrm	0.0100(8)	0.0088	
mrrmmrrr	0.0081(3)	0.0087	
mmrr	0.1472(14)	0.1479	
mmmrrm +	0.0987(15)	0.0962	0.0663
mmmrrr			0.0299
mmrm +	0.1569(53)	0.1453	0.0231
rmrr			0.1222
mmmrmr	0.0116(19)	0.0111	
rmrm	0.0370(26)	0.0427	
rrmrmr	0.0129(27)	0.0167	
mrmrmm	0.0043(24)	0.0111	
rrrr	0.1524(35)	0.1613	
rrrrrr	0.0869(16)	0.0853	
mrrrmr + *rrrrmr*	0.0712(38)	0.0706	0.0167
			0.0539
rrrrmm +	0.0474(20)	0.0517	0.0443
mrrrmm			0.0074
rmrrmr	0.0221(16)	0.0109	
mmrrmr	0.0396(15)	0.0299	
mmrrmm	0.0320(15)	0.0331	
mrmrm	0.0036(26)	0.0093	
mrmrr	0.0124(39)	0.0241	
rrmrr +	0.1512(25)	0.1592	0.0490
mrrrm +			0.0121
mrrrr			0.0981
rmmrm +	0.2730(39)	0.2832	0.0103
rrrrr +			0.1122
rmmrr +			0.0517
mmmrm +			0.0128
mmmrr			0.0962
mmrrrrm	0.0248(11)	0.0263	
rmrrrr	0.0376(12)	0.0359	
rmrmr	0.0177(74)	0.0121	
mmrmr	0.0195(40)	0.0185	
		$\chi^2_r = 8.6$	
		$\sigma = \sigma_1 = 0.99_9$	
		$\sigma_2 = 0$	
		$P_{12} = 0.29$	
		$P_{21} = 0.89$	
		$P_r = 0.80$	
		$w_{ES} = 0.04$	
		$w_{CE} = 0.29$	
		$(w_{CM-Cl} = 0.67)$	

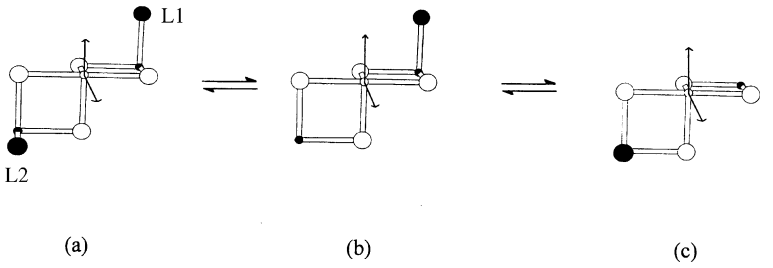

Fig. 34. Schematic models of active species for highly isotactic (a), isotactoid (b), and syndiotactic (c) propagation in heterogeneous Ziegler–Natta catalysts (see text). (○) = Ti; (●) = Ti or Mg; (○) = Cl; (●) = Cl or donor (adapted from Ref. [39]).

4.4.1.3. Chain constitution and structure of the end-groups. Most heterogeneous Ziegler–Natta catalysts are highly regioselective in propene insertion. The ^{13}C NMR spectra of raw polymers usually give no evidence of regioerrors, which means that their concentration is below 0.1 mol% (indicatively). Occasionally, traces of head-to-head enchainments were detected in the spectra of xylene-soluble or heptane-soluble ('atactic') fractions [148].

The ^{13}C NMR analysis of the end-groups formed in the presence of ^{13}C-enriched Al-alkyls proved that the predominant propene insertion mode is 1,2 [48–50]. This is also consistent with the ^{1}H NMR observation of 2-methyl-but-2-enyl (vinylidene) structures deriving from (monomer assisted) β-H elimination.

When H_2 is used as a chain transfer agent, mostly propyl, *iso*-butyl and butyl end-groups are detected by ^{13}C NMR [45,55,149–151] (Scheme 8). The amount of butyl structures often exceeds that of *iso*-butyl ones, which has been taken as an indication of a significant 'dormancy' of the growing chains due to occasional 2,1 propene misinsertions. From the fraction of butyl end-groups in H_2-terminated polymers, it is possible to estimate a lower limit for catalyst regioselectivity; values comprised between 99.8 and 99.99% can be desumed for typical $MgCl_2$-supported systems [149,151]. Recently, the presence of 2,3-dimethyl-butyl end-groups, particularly in polypropylene fractions of low stereoregularity, has also been documented [89,151]; this indicates that propene insertion into an initial Ti–H bond is not fully regioselective (as already found for a number of *ansa*-metallocene catalysts [89,90]).

4.4.2. In situ $TiCl_4/AlR_3$ mixtures and other Ti-based systems

The original Ziegler's *Metallorganische Mischkatalysator* was an in situ mixture of $TiCl_4$ and $AlEt_3$ in aliphatic hydrocarbons. It is well known [3] that the two components react with separation of a β-$TiCl_3$ crystalline phase (the only polymorphic modification of $TiCl_3$ with a non-layered structure). However, at typical polymerization temperatures (50–80°C) the reaction is slow, and intermediate alkylation products of $TiCl_4$ (e.g. $TiCl_3Et$) are also present in solution and may contribute appreciably to the catalytic activity [152].

As a matter of fact, polypropylene samples obtained with $TiCl_4/AlR_3$ systems are even more complex than those produced with pre-formed $TiCl_3$ catalysts. Indeed, in addition to semicrystalline polymer fractions that closely resemble, both from the regiochemical and the stereochemical viewpoint, those described in the previous Section 4.4.1, an amorphous fraction can also be isolated which contains macromolecules of unusually poor regioregularity (up to 5 mol% of head-to-head enchainments)

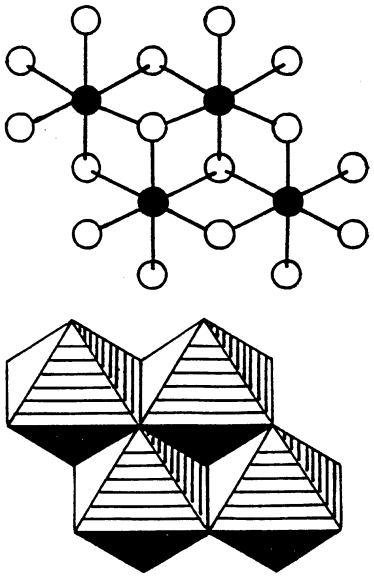

Fig. 35. Structure of the tetrameric species $[Ti(OEt)_4]_4$ (reproduced with permission from Ref. [156]).

[152,153]. The molecular mass distribution of the polymers is extremely broad, which is consistent with the presence of several types of catalytic species, but the detailed nature of such species is still largely unknown.

Similarly complicated polypropylenes are formed in the presence of homogeneous $Ti(OR)_4$/MAO or $Ti(Bz)_4$/MAO systems (with R = alkyl, Bz = benzyl) [154]. Ti-alcoxides are known to aggregate in solution, with a highly fluxional behavior [155,156]. One of the possible structures for $Ti(OEt)_4$ is tetrameric (Fig. 35), with two out of four Ti atoms having an asymmetric coordination environment. The alkylation of such Ti atoms by the cocatalyst may result in chiral active species closely resembling those present on the surface of 'violet' $TiCl_3$ crystals (Fig. 30); this would explain the observed formation of a predominantly isotactic polypropylene fraction with a configurational statistics (*rr*-type stereodefects) consistent with an enantiomorphic-site origin of the stereocontrol, along with a fraction of poor regio- and stereoregularity [154]. An enantiomorphic-site-type isotactic polypropylene fraction obtained with $Ti(Bz)_4$-based catalysts [154], on the other hand, might be traced to the back-biting of at least part of the benzyl ligands, resulting in a chiral and sterically crowded environment of the transition metal [157].

4.4.3. V-based systems

In the early '60s, it was found that predominantly syndiotactic polypropylene can be obtained in the presence of homogeneous catalyst systems comprising a V compound, such as VCl_4 or $V(acac)_3$ (acac = acetylacetonate), an alkyl-Al-halide (typically, $AlEt_2Cl$), and a Lewis base (e.g. anisole), provided that the polymerization temperature is very low [159,160]. Polymers made at −78°C may have [*r*] values up to 0.9 [161], but the syndiotacticity fades out rapidly with increasing temperature, and practically atactic polypropylene is produced above 0°C. An interesting feature of these catalysts is that below −50°C, they

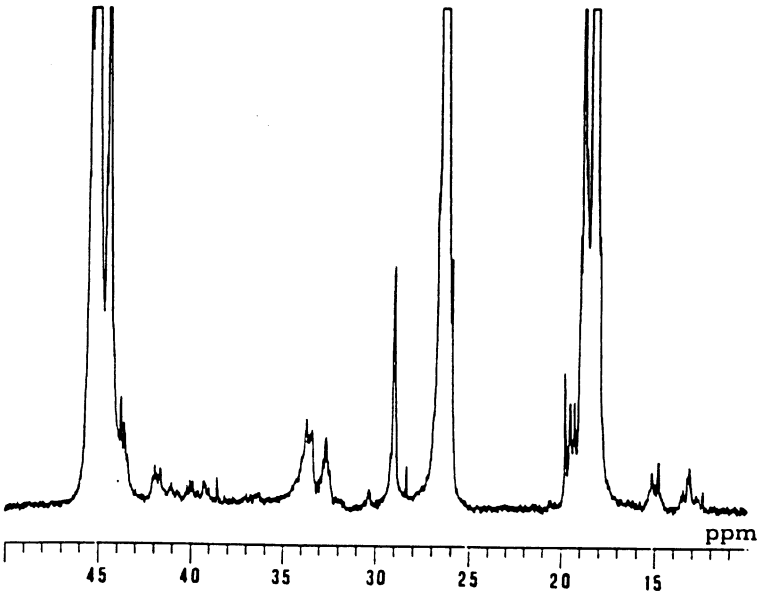

Fig. 36. ^{13}C NMR spectrum of a predominantly syndiotactic ([*rr*] ≈ 0.7) polypropylene sample prepared with the catalyst system $VCl_4/AlEt_2Cl$ at −78°C. The chemical shift scale is in ppm downfield of hexamethyl-disiloxane (HDMS). The weaker resonances in the regions 12–16 ppm and 27–43 ppm are due to regioirregular sequences (reproduced with permission from Gazz Chim Ital 1988;118:539, Ref. [164]).

have a quasi-living character, and consequently afford almost monodisperse polymers ($M_w/M_n < 1.1$) [162,163].

^{13}C NMR microstructural characterizations dating back to the 1970s shed complete light on the mechanism of stereocontrol, which is rather unique [158,164]. From the analysis of the saturated chain ends generated by initiation at V-(^{13}C-enriched-alkyl) species, it came out that propene insertion into a $V–CH_2R$ bond is prevailingly 1,2 and is not enantioselective. However, the regioselectivity is not high (Fig. 36), and once a $V–CH(CH_3)–CH_2R$ bond is occasionally formed, the 2,1 insertion mode tends to be maintained and chain propagation becomes predominantly syndiotactic. The *m*-type stereodefects are clearly indicative of a chain end origin of the stereocontrol.

All this results in the peculiar block structure sketched in Chart 38. The chains comprise syndiotactic stereoblocks spanned by shorter atactic ones, with systematic reversals of monomer enchainment at the block junctions. The polymers are only weakly crystalline, with melting points never exceeding 120–130°C (hence, much lower than those of highly syndiotactic polypropylenes made with C_s-symmetric *ansa*-metallocene catalysts; see Section 4.2.4).

5. Microstructure and physical properties of polypropylene

The physical behavior of all synthetic polymers is the combined result of chain microstructure, average molecular mass and molecular mass distribution; however, at least for some properties (such

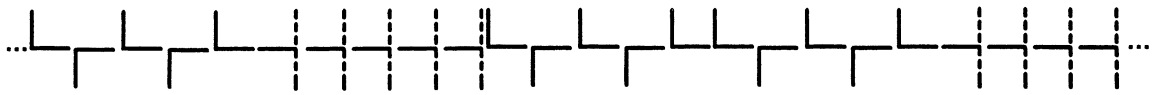

Chart 38.

as, e.g. the melting and crystallization parameters), when the average molecular mass exceeds a certain value (that differs from polymer to polymer), the microstructure becomes the dominant controlling factor. For chains with polar functional groups, this threshold is comparatively low, and number average polymerization degrees (P_n) in the range of 10 to 100 may suffice. In the case of polypropylene, instead, P_n must be of the order of 10^3 (a value that many catalysts cannot afford). This sets an important limitation to structure/properties investigations for this polymer; indeed, for $P_n < 10^3$ the effects of chain microstructure may be masked or — even — overwhelmed by those related to the molecular mass.

Another major problem comes from the fact that it is not simple to determine polypropylene microstructure with an adequate accuracy. In the previous sections, we have seen that the sensitivity of natural abundance ^{13}C NMR is often too low for the precise evaluation of chain *constitution*, and that in many cases (e.g. samples of low stereoregularity, with a stereoblock nature or deriving from multi-site catalysts) the steric pentad distribution typically afforded by 'routine' spectrometers is not enough for an unambiguous description of chain *configuration*.

Therefore, it is by no means surprising that structure/properties studies on polypropylene are still at a rather primitive stage, and that many fundamental and supposedly elementary aspects found a convincing rationalization only in very recent times.

The correlation between microtacticity and melting temperature (T_m) of site-controlled isotactic polypropylene is a good exemplification of the previous assertion. A plot of T_m vs. [*mmmm*] is shown in Fig. 37; the experimental data clearly belong to two sets, with different interpolating lines, which correspond to polymers produced with heterogeneous Ziegler–Natta[5] and homogeneous *ansa*-metallocene catalysts [8, Fig. 52], respectively. For a given value of [*mmmm*], samples obtained with the former catalysts melt at a higher temperature than those prepared with the latter, and the two sets tend to converge only in the limit of [*mmmm*] → 1 (perfect isotacticity). For many years, this observation did not find a satisfactory quantitative explanation, although the lower *regio*regularity of metallocene-made polypropylene was perceived as an important factor, and the presence of *regio*defects suspected to be particularly detrimental to chain crystallizability. It is now clear, instead that both regio- and stereoirregular units are largely incompatible with the crystal lattice [165,166], and that the key difference lies in the *distribution* of the *stereo*defects (cf. Sections 4.2.2 and 4.4.2): 'blocky' for Ziegler–Natta polypropylenes, random for metallocene ones (the latter corresponding to the minimum average length of the crystallizable sequences).

Unfortunately, it is not trivial to discriminate between the two cases by means of ^{13}C NMR at pentad level. Indeed, predominantly isotactic materials with uniformly distributed …*mmmrrmmm*… stereoerrors and isotactic/isotactoid stereoblock ones *with the same average content of stereoirregular units* may have deceptively similar pentad distributions, with virtually identical values of [*mmmm*] and

[5] Data from the authors' laboratory.

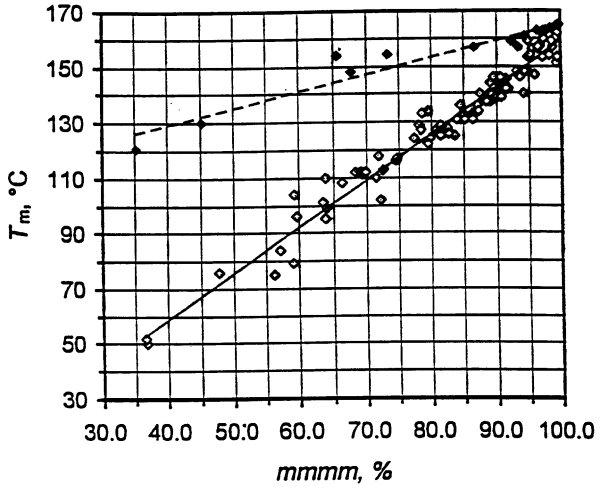

Fig. 37. Correlation between degree of isotacticity (expressed as % of *mmmm* pentad) and DSC melting temperature (T_m; 2nd heating scan) for (predominantly) isotactic polypropylenes. (◇) = samples made with metallocene catalysts [8, Fig. 52]; (◆) fractions obtained by temperature rising elution fractionation of samples made with heterogeneous Ziegler–Natta catalysts (data from the authors' laboratory). The interpolating lines are only orientative.

[*mrrm*]. On the other hand, the difference becomes immediately apparent as soon as the heptad level is reached (Table 17).

The correlation diagram of Fig. 37 strongly suggests that the 'classical' Ziegler–Natta systems still provide the most convenient route to high-melting isotactic polypropylene. On the other hand, C_2-symmetric and C_1-symmetric *ansa*-metallocenes are elective catalysts for the production of lower-melting isotactic polypropylene; indeed, by tailoring the aromatic ligand framework and reaction conditions, it is possible to tune the stereoselectivity, so as to produce homopolymer chains with the desired average length of crystallizable sequences [110]. When propene is polymerized with $TiCl_3$ or $MgCl_2/TiCl_4$ catalysts, a similar result can be achieved by introducing controlled amounts of a co-monomer (e.g. ethene or 1-butene), but this approach is more complicated, and suffers from the broad distribution of copolymer composition consequent to the presence of several catalytic species [1].

The fact that Ziegler–Natta isotactic polypropylenes largely crystallize in the α polymorphic modification [1], whereas metallocene-made ones easily give rise to γ-form crystallinity [1,165,166], can also be traced to the different distribution of stereodefects. It is often claimed that the γ modification is favored by a low average polymer molecular mass [1,167,168]; the reality is instead that it develops preferentially when the average length of the crystallizable sequences is (indicatively) in the range of 10–30 monomeric units [165,166], a condition frequently matched by polypropylene samples produced with metallocene catalysts (which often happen to be of rather low molecular mass). On the other hand, Ziegler–Natta polypropylenes normally contain — as was discussed before — long, almost ideally isotactic sequences (forming predominantly α-type crystals), along with isotactoid sequences which are practically unable to crystallize. It may be of interest to add that appreciable amounts of γ-form crystallinity are observed in copolymers of propene with low amounts of a co-monomer (e.g. ethene) made with either metallocene or Ziegler–Natta catalysts, because — as already noted above — for such materials it

Table 17
Calculated normalized fractions of *mmmm* and *mrrm* pentads, and of *mrrm*-centred heptads, for two predominantly isotactic polypropylene samples with the same average fraction but different distributions of *rr*-type stereodefects. The expected DSC melting temperatures (T_m) are also given

Sample	*mmmm* (%)	*mrrm*(%)	*mmrrmm*(%)	*mmrrmr*(%)	*rmrrmr*(%)	T_m (°C)
A[a]	90.4	1.84	1.77	0.07	0.00	140
B[b]	88.9	1.70	1.37	0.28	0.04	150

[a] Site-controlled isotactic (2.0% stereoirregular units).
[b] Blend: 90 wt% site-controlled isotactic (1.0% stereoirregular units) + 10 wt% site-controlled isotactoid (20% stereoirregular units).

is easy to achieve the required (low) length of crystallizable sequences due to the controlled incorporation of co-monomeric units acting as chain defects [165,169].

Concerning the effects of chain microstructure on mechanical properties, in general it can be stated that the presence of very long highly isotactic sequences tends to result in high values of modulus, tensile strength and hardness, whereas a lower stereoregularity improves the impact strength. However, a wide variety of factors play a role in this context, including the molecular mass distribution and the morphology of the crystalline regions [1].

For syndiotactic polypropylene, structure-property studies are at an even earlier stage, due to the fact that this polymer was obtained with high steric purity only in the late 1980s. It appears that the limiting thermodynamic melting temperature for $[rrrr] \rightarrow 1$ is similar to that of isotactic polypropylene (≈ 180°C); however, samples produced with C_s-symmetric *ansa*-metallocene catalysts (Section 4.2.4) under practical reaction conditions have [*rrrr*] values of the order of 0.8, and melt at around 130–140°C [99]. In such samples, the average length of the crystallizable sequences is rather low (≈20 monomeric units); this results in a small size of the crystallites, which probably explains the remarkably high optical clarity of syndiotactic polypropylene films [1,170]. Another interesting feature of the polymer is its low brittleness compared with isotactic polypropylene [1,170], possibly due to the higher conformational flexibility of the chain segments in the amorphous regions, resulting from a reduced mutual steric interference of the *anti* methyl substituents.

Weakly tactic polypropylenes [110,171] also represent a fascinating field, with a number of interesting patent applications recently filed [172]. As discussed in Section 4, many homogeneous (mostly metallocene) catalysts afford polymers with a slight prevalence of *meso* or of *racemo* diads, and as such able to develop traces of isotactic or syndiotactic crystallinity (respectively). These materials may perform as thermoplastic elastomers (provided that the average polymer molecular mass is high enough), because the short chain segments trapped in micro- or (even) 'nano'-crystals act as physical crosslinks between the large amorphous regions.

Elastoplastic polypropylenes may also have a stereoblock structure, and many papers and patents claimed the synthesis of isotactic-*block*-atactic or isotactic-*block*-syndiotactic chains (Section 4.2.6) [111–115,117,173–175]. Upto now, however, conclusive ^{13}C NMR microstructural evidence is still pending, and it is likely that most of such materials are actually reactor blends of polypropylenes of different tacticities, possibly including minor amounts of a true stereoblock fraction, acting as a compatibilizer.

The near future is likely to bring new polypropylene-based materials. The incredible variety of

innovative catalysts with unprecedented selectivities developed in the last 15 years [1,7,8,16–18] has shown how dull was the concept (widely diffuse within the chemical community in the late 1970s) of polypropylene as a mature commodity polymer with no scientific perspectives.

The ever growing interest of the organometallic chemists in catalytic olefin polymerization is a strong premise for further discoveries. High-field ^{13}C NMR, in turn, has proved to be an adequate tool for the thorough microstructural characterization of the new materials, and a rational explanation of their properties. Today like in the 1950s, it is still the right time to work with polypropylene.

Acknowledgements

The authors wish to heartily thank Prof. Anna Laura Segre and Prof. Michele Vacatello, without whom this work would have been impossible. Valuable discussions with Dr John C. Chadwick, Prof. Paolo Corradini, Dr Abbas Razavi, Dr Luigi Resconi, and Prof. Adolfo Zambelli are gratefully acknowledged. The project on high-field ^{13}C NMR microstructural analysis of polypropylene has been co-funded by the Italian Ministry for University and Scientific Research (Progetto di Rilevante Interesse Nazionale su Polimerizzazione Stereoselettiva: Nuovi Catalizzatori e Nuovi Materiali Polimerici).

References

[1] Moore EP. Polypropylene handbook. Munich: Hanser, 1996.
[2] Pavan A, Provasoli A, Moraglio G, Zambelli A. Makromol Chem 1977;178:1099.
[3] Boor J. Ziegler–Natta catalysts and polymerizations. New York: Academic Press, 1979.
[4] Kissin YV. Isospecific polymerization of olefins. New York: Springer, 1985.
[5] Ewen JA. J Am Chem Soc 1984;106:6355.
[6] Kaminsky W, Külper K, Brintzinger HH, Wild FRWP. Angew Chem, Int Ed Engl 1985;24:507.
[7] Brintzinger HH, Fischer D, Mülhaupt R, Rieger B, Waymouth RM. Angew Chem, Int Ed Engl 1995;34:1143–70 (review).
[8] Resconi L, Cavallo L, Fait A, Piemontesi F. Chem Rev 2000;100:1253–346 (review).
[9] Farina M. Topics Stereochem 1987;17:1–111.
[10] Bovey FA. Chain structure and conformation of macromolecules. New York: Academic Press, 1982.
[11] Tonelli AE. NMR spectroscopy and polymer microstructure: the conformational connection. Deers Field, FL: VCH, 1989.
[12] Randall JC. Polymer sequence determination — carbon-13 NMR method. New York: Academic Press, 1977.
[13] Busico V, Cipullo R, Corradini P, Landriani L, Vacatello M, Segre AL. Macromolecules 1995;28:1887.
[14] Busico V, Cipullo R, Monaco G, Vacatello M, Segre AL. Macromolecules 1997;30:6251.
[15] Busico V, Cipullo R, Monaco G, Vacatello M, Bella J, Segre AL. Macromolecules 1998;31:8713.
[16] Alt HG, Koppl A. Chem Rev 2000;100:1205–21 (review).
[17] Britovsek GJP, Gibson VC, Wass DF. Angew Chem, Int Ed Engl 1999;38:429 (review).
[18] Ittel SD, Johnson LK, Brookhart M. Chem Rev 2000;100:1169–203 (review).
[19] Jenkins AD. Pure Appl Chem 1981;53:733–52 (review).
[20] Corradini P, Busico V, Guerra G. Comprehensive polymer science, vol. 4. Oxford: Pergamon Press, 1988 (p. 29–50).
[21] Natta G, Pino P, Corradini P, Danusso P, Mantica E, Mazzanti G, Moraglio G. J Am Chem Soc 1955;77:1708.
[22] Bunn CW. Proc R Soc (London) 1942;A180:67.
[23] Natta G, Corradini P. J Polym Sci 1959;39:29 (and refs. therein).
[24] Natta G, Corradini P. Nuovo Cimento 1960; XV(Ser. X, Suppl.):40.
[25] Burfield DR, Loi PST. J Appl Polym Sci 1988;36:279.
[26] Zambelli A, Segre AL, Farina M, Natta G. Makromol Chem 1967;110:1.

[27] Zambelli A, Segre AL. J Polym Sci, Polym Lett 1968;6:473.
[28] Heatley F, Zambelli A. Macromolecules 1969;2:618.
[29] Inoue Y, Nishioka A, Chujo R. Makromol Chem 1973;168:163.
[30] Grant DM, Paul EG. J Am Chem Soc 1964;86:2984.
[31] Lindeman LP, Adams JQ. Anal Chem 1971;43:1245.
[32] Inoue Y, Nishioka A, Chujo R. Makromol Chem 1972;152:15.
[33] Zambelli A, Locatelli P, Bajo G, Bovey FA. Macromolecules 1975;8:687.
[34] Provasoli A, Ferro DR. Macromolecules 1977;10:874.
[35] Boyd RH, Breitling SM. Macromolecules 1972;5:279.
[36] Tonelli AE. Macromolecules 1978;11:565.
[37] Suter UW, Flory PJ. Macromolecules 1975;8:765.
[38] Schilling FC, Tonelli AE. Macromolecules 1980;13:270.
[39] Busico V, Cipullo R, Monaco G, Talarico G, Vacatello M, Chadwick JC, Segre AL, Sudmeijer O. Macromolecules 1999;32:4173.
[40] Busico V, Cipullo R, Chadwick JC, Modder JF, Sudmeijer O. Macromolecules 1994;27:7538.
[41] Zambelli A, Locatelli P, Bajo G. Macromolecules 1979;12:154.
[42] Zambelli A, Locatelli P, Rigamonti E. Macromolecules 1979;12:156.
[43] Cheng HN, Smith DD. Macromolecules 1986;19:2065.
[44] Asakura T, Nishiyama Y, Doi Y. Macromolecules 1987;20:616.
[45] Hayashi T, Inoue Y, Chujo R, Asakura T. Macromolecules 1988;21:2675.
[46] Tsutsui T, Ishimara N, Mizuno A, Toyota A, Kashiwa N. Polymer 1989;30:1350.
[47] Cheng HN, Ewen JA. Makromol Chem 1989;190:1931.
[48] Zambelli A, Ammendola P. Prog Polym Sci 1991;16:203–18 (review).
[49] Zambelli A, Sacchi MC, Locatelli P, Zannoni G. Macromolecules 1982;15:211.
[50] Zambelli A, Locatelli P, Sacchi MC, Tritto I. Macromolecules 1982;15:831.
[51] Corradini P, Guerra G. Prog Polym Sci 1991;16:239–57 (review).
[52] Longo P, Grassi A, Pellecchia C, Zambelli A. Macromolecules 1987;20:1015.
[53] Dahlmann M, Erker G, Nissinen M, Frilich R. J Am Chem Soc 1999;121:2820.
[54] Tsutsui T, Kashiwa N, Mizuno A. Makromol Chem, Rapid Commun 1990;11:565.
[55] Busico V, Cipullo R, Corradini P. Makromol Chem 1993;194:1079.
[56] Busico V, Cipullo R, Corradini P. Makromol Chem, Rapid Commun 1993;14:97.
[57] Bovey FA, Sacchi MC, Zambelli A. Macromolecules 1974;7:752.
[58] Busico V, Cipullo R, Talarico G, Caporaso L. Macromolecules 1998;31:2387.
[59] Zambelli A, Bajo G, Rigamonti E. Makromol Chem 1978;179:1249.
[60] Busico V, Cipullo R, Talarico G, Segre AL, Caporaso L. Macromolecules 1998;31:8720.
[61] Shelden RA, Fueno T, Tsunetsugu T, Furukawa J. J Polym Sci: Part B 1965;3:23.
[62] Bovey FA, Tiers GVD. J Polym Sci 1960;44:173.
[63] Doi Y. Makromol Chem, Rapid Commun 1982;3:635.
[64] Schevis J, Kaminsky W, editors. Metallocene-based polyolefins, vol. 1. Chichester: Wiley, 2000.
[65] Natta G, Pino P, Mazzanti G, Giannini U. J Inorg Nucl Chem 1958;8:612.
[66] Breslow DS, Newburg NR. J Am Chem Soc 1957;79:5073.
[67] Andresen A, Cordes HG, Herwig J, Kaminsky W, Merck A, Mottweiler R, Pein J, Sinn H, Vollmer HJ. Angew Chem, Int Ed Engl 1976;15:630.
[68] Külper K, Niedoba S. Makromol Chem, Macromol Symp 1986;3:377.
[69] Resconi L, Jones RL, Rheingold AL, Yap GPA. Organometallics 1996;15:998.
[70] Tsutsui T, Mizuno A, Kashiwa N. Polymer 1989;30:428.
[71] Borrelli M, Busico V, Cipullo R, Ronca S, Budzelaar P. To be published.
[72] Resconi L, Piemontesi F, Franciscono G, Abis L, Fiorani T. J Am Chem Soc 1992;114:1025.
[73] Corradini P, Cavallo L, Guerra G. In: Schevis J, Kaminsky W, editors. Metallocene-based polyolefins, vol. 2. Chichester: Wiley, 2000. p. 3–36.
[74] Busico V, Cipullo R. J Am Chem Soc 1994;116:9329.
[75] Leclerc M, Brintzinger HH. J Am Chem Soc 1995;117:1651.

[76] Busico V, Caporaso L, Cipullo R, Landriani L, Angelini G, Margonelli A, Segre AL. J Am Chem Soc 1996;118:2105.
[77] Busico V, Brita D, Caporaso L, Cipullo R, Vacatello M. Macromolecules 1997;30:3971.
[78] Busico V, Cipullo R, Caporaso L, Angelini G, Segre AL. J Mol Catal, Part A (Chem) 1998;128:53.
[79] Prosenc MH, Brintzinger HH. Organometallics 1997;16:3889.
[80] Busico V, Cipullo R, Cutillo F. To be published.
[81] Price FP. In: Lowry GG, editor. Markov chains and MonteCarlo calculations in polymer chains. New York: Marcel Dekker, 1970 (chap. 7).
[82] Rieger B, Reinmuth A, Röll W, Brintzinger HH. J Mol Catal 1993;82:67.
[83] Resconi L, Piemontesi F, Nifant'ev I, Ivchenko P. (Montell Polyolefins), PTC Int Appl WO 96/22995, 1996.
[84] Spaleck W, Küber F, Winter A, Rohrmann J, Bachmann B, Antberg M, Dolle V, Paulus EF. Organometallics 1994;13:954.
[85] Resconi L, Balboni D, Baruzzi G, Fiori C, Guidotti S, Mercandelli P, Sironi A. Organometallics 2000;19:420.
[86] Stehling U, Diebold J, Kirsten R, Röll W, Brintzinger HH, Jüngling S, Mülhaupt R, Langhauser F. Organometallics 1994;13:964.
[87] Spaleck W, Antberg M, Aulbach M, Bachmann B, Dolle V, Haftka S, Küber F, Rohrmann J, Winter A. In: Fink G, Mülhaupt R, Brintzinger HH, editors. Ziegler catalysts. Berlin: Springer, 1995. p. 83–97.
[88] Rieger B, Mu X, Mallin DT, Rausch M, Chien JCW. Macromolecules 1990;23:3559.
[89] Randall JC, Ruff CJ, Vizzini JC, Spesa AN, Burkhardt TJ. In: Kaminsky W, editor. Metalorganic catalysts for synthesis and polymerisation. Berlin: Springer, 1999. p. 601–15.
[90] Moscardi G, Piemontesi F, Resconi L. Organometallics 1999;18:5264.
[91] Kaminsky W. Macromol Chem Phys 1996;197:3907.
[92] Corradini P, Guerra G, Cavallo L, Moscardi G, Vacatello M. In: Fink G, Mülhaupt R, Brintzinger HH, editors. Ziegler catalysts. Berlin: Springer, 1995. p. 237–49.
[93] Collins S, Gauthier WJ, Holden DA, Kuntz BA, Taylor NJ, Ward DG. Organometallics 1991;10:2061.
[94] Ewen JA, Jones RL, Razavi A, Ferrara JD. J Am Chem Soc 1988;110:6255.
[95] Ewen JA, Elder MJ, Jones RL, Curtis S, Cheng HN. In: Keii T, Soga K, editors. Catalytic olefin polymerization. Tokyo: Kodansha, 1990. p. 439–82.
[96] Grisi F, Longo P, Zambelli A, Ewen JA. J Mol Catal 1999;140:225.
[97] Razavi A, Peters L, Nafpliotis L, Atwood JL. In: Soga K, Terano M, editors. Catalyst design for tailor-made polyolefins. Tokyo: Kodansha, 1994 (supplement).
[98] Farina M, Di Silvestro G, Terragni A. Macromol Chem Phys 1995;196:353.
[99] De Rosa C, Auriemma F, Vinti V, Galimberti M. Macromolecules 1998;31:6206.
[100] Guerra G, Longo P, Cavallo L, Corradini P, Resconi L. J Am Chem Soc 1997;119:4394.
[101] Longo P, Proto A, Grassi A, Ammendola P. Macromolecules 1991;24:4624.
[102] Razavi A, Peters L, Nafpliotis L, Vereecke D, Den Dauw K, Atwood JL, Thewald U. Makromol Chem, Macromol Symp 1995;89:345–67 (review).
[103] Rieger B, Jany G, Fawzi R, Steimann M. Organometallics 1994;13:647.
[104] Guerra G, Cavallo L, Moscardi G, Vacatello M, Corradini P. Macromolecules 1996;29:4834.
[105] Ewen JA, Elder MJ, Jones RL, Haspeslagh L, Atwood JL, Bott SG, Robinson K. Macromol Symp 1991;48:253.
[106] Deng H, Winkelback H, Taeji K, Kaminsky W, Soga K. Macromolecules 1996;29:6371.
[107] Spaleck W, Kuber F, Bachmann B, Fritze C, Winter A. J Mol Catal A: Chem 1998;128:279.
[108] Farina M, Di Silvestro G, Sozzani P. Macromolecules 1993;26:946.
[109] Farina M, Di Silvestro G, Sozzani P. Macromolecules 1982;15:1451.
[110] Dietrich U, Hackmann M, Rieger B, Klinga M, Leskela M. J Am Chem Soc 1999;121:4348.
[111] Coates GW, Waymouth RM. Science 1995;267:217.
[112] Hauptmann E, Waymouth RM, Ziller JW. J Am Chem Soc 1995;117:11586.
[113] Bruce MD, Waymouth RM. Macromolecules 1998;31:2707.
[114] Hu Y, Krejchi MT, Shah CD, Myers CL, Waymouth RM. Macromolecules 1998;31:6908.
[115] Witte P, Lal JK, Waymouth RM. Organometallics 1999;18:4147.
[116] Cavallo L, Guerra G, Corradini P. Gazz Chim Ital 1996;126:463.
[117] Gauthier WJ, Collins S. Macromolecules 1995;28:3779.
[118] Lin S, Waymouth RM. Macromolecules 1999;32:8283.

[119] Razavi A, Bellia V, De Brauwer Y, Hortmann K, Lambrecht M, Miserque O, Peters L, Van Belle S. In: Kaminsky W, editor. Metalorganic catalysts for synthesis and polymerization. Berlin: Springer, 1999. p. 236–47.
[120] Yokota K, Inoue T, Naganuma S, Shozaki H, Tomotsu N, Kuramoto M, Ishihara N. Metalorganic catalysts for synthesis and polymerization. Berlin: Springer, 1999 (p. 435–45; review).
[121] Zambelli A, Pellecchia C, Proto A. Macromol Symp 1995;89:373 (review).
[122] Okuda J. In: Kaminsky W, editor. Metalorganic catalysts for synthesis and polimerisation. Berlin: Springer, 1999 (p. 200–11; review).
[123] Stevens JC, Timmers FJ, Rosen GW, Knight GW, Lai SY. (Dow Chemical Co.), Eur Patent Appl EP 0416815 A2, 1991.
[124] Canich JA. (Exxon Chemical Co.), Eur Patent Appl EP 0420436 A1, 1991.
[125] McKnight AL, Masood MdA, Waymouth RM, Straus DA. Organometallics 1997;16:2879.
[126] Shiomura T, Asakura T, Inoue N. Macromol Rapid Commun 1996;17:9.
[127] Shiomura T, Asakura T, Sunaga T. Macromol Rapid Commun 1997;18:169.
[128] Hagihara H, Shiono T, Ikeda T. Macromolecules 1997;30:4783.
[129] Pellecchia C, Zambelli A. Macromol Rapid Commun 1996;29:6990.
[130] Pellecchia C, Zambelli A, Oliva L, Pappalardo D. Macromolecules 1996;29:6990.
[131] Small BL, Brookhart M. Macromolecules 1999;32:2120.
[132] Barbè PC, Cecchin G, Noristi L. Adv Polym Sci 1987;81:1–81 (review).
[133] Albizzati E, Giannini U, Morini G, Galimberti M, Barino L, Scordamaglia R. Macromol Symp 1995;89:73–89 (review).
[134] Cossee P. The mechanism of Ziegler–Natta polymerization. II. Quantum chemical and crystal-chemical aspects. In: Ketley AD, editor. The stereochemistry of macromolecules, vol.1. New York: Marcel Dekker, 1967. p. 145–75 (chap. 3; review).
[135] Corradini P, Busico V, Cavallo P, Guerra G, Vacatello M, Venditto V. J Mol Catal 1992;74:433 (and refs. therein).
[136] Corradini P, Barone V, Fusco R, Guerra G. Gazz Chim Ital 1983;113:601.
[137] Barino L, Scordamaglia R. Macromol Theory Simul 1998;7:407.
[138] Martuscelli E, Avella M, Segre AL, Rossi E, Di Drusco G, Galli P, Simonazzi T. Polymer 1985;26:259.
[139] Busico V, Cipullo R, Corradini P, De Biasio R. Macromol Chem Phys 1995;196:491 (and refs. therein).
[140] Busico V, Corradini P, De Martino L, Graziano F, Iadicicco A. Makromol Chem 1991;192:49.
[141] Pino P, Mülhaupt R. Angew Chem, Int Ed Engl 1980;19:857–75.
[142] Busico V, Cipullo R, Corradini P, Landriani L, Vacatello M, Segre AL. Macromolecules 1995;28:1887.
[143] Busico V, Cipullo R, Talarico G, Segre AL, Chadwick JC. Macromolecules 1997;30:4787.
[144] Busico V, Cipullo R, Talarico G. Proceedings of the International Symposium on Microkinetics and Dynamics of Individual Active Sites in Catalytic Reactions, Kanazawa (Japan), March 6–8, 2001.
[145] Kakugo M, Miyatake T, Naito Y, Mizunuma K. Macromolecules 1988;21:314.
[146] Kioka M, Makio H, Mizuno A, Kashiwa N. Polymer 1994;35:580.
[147] Morini G, Albizzati E, Balbontin G, Mingozzi I, Sacchi MC, Forlini F, Tritto I. Macromolecules 1994;35:580.
[148] Hayashi T, Inoue Y, Chujo R, Doi Y. Polymer 1989;30:1714.
[149] Chadwick JC, Miedema A, Sudmeijer O. Macromol Chem Phys 1994;195:167.
[150] Chadwick JC, Morini G, Albizzati E, Balbontin G, Mingozzi I, Cristofori A. Macromol Chem Phys 1996;197:2501.
[151] Chadwick JC, Morini G, Balbontin G, Busico V, Talarico G, Sudmeijer O. ACS Symp Ser 2000;749:50.
[152] Busico V, Corradini P, De Martino L, Trifuoggi M. Eur Polym J 1992;28:519.
[153] Doi Y. Makromol Chem 1979;180:2447.
[154] Oliva L, Longo P, Pellecchia C. Makromol Chem, Rapid Commun 1988;9:51.
[155] Holloway CE. J Chem Soc, Dalton Trans 1976:1050.
[156] Ibers JA. Nature 1963;197:686.
[157] Pellecchia C, Grassi A, Zambelli A. Organometallics 1994;13:298.
[158] Zambelli A, Tosi C. Adv Polym Sci 1974;15:31–60 (review).
[159] Natta G, Pasquon I, Zambelli A. J Am Chem Soc 1962;84:1488.
[160] Zambelli A, Natta G, Pasquon I. J Polym Sci, Part C 1963;4:411.
[161] Doi Y, Jakada M, Keii T. Makromol Chem 1979;180:57.
[162] Doi Y, Ueki S, Keii T. Macromolecules 1979;12:814.
[163] Doi Y, Ueki S, Keii T. Makromol Chem 1979;180:1359.
[164] Ammendola P, Shijing X, Grassi A, Zambelli A. Gazz Chim Ital 1988;118:769.

[165] Fischer D, Mülhaupt R. Makromol Chem Phys 1994;195:1143.
[166] Alamo RG, Kim MH, Galante MJ, Isasi JR, Mandelkern L. Macromolecules 1999;32:4050.
[167] Brückner S, Meille SV. Nature 1989;340:455.
[168] Brückner S, Meille SV, Petraccone V, Pirozzi B. Prog Polym Sci 1991;16:361.
[169] Busico V, Corradini P, De Rosa C, Di Benedetto E. Eur Polym J 1985;21:239.
[170] Shamshoum ES, Sun L, Reddy BR, Turner D. Properties and Applications of Low Density Syndiotactic Polypropylene. Proc MetCon '94, Houston (TX), 1994.
[171] Bravakis AM, Bailey LE, Pigeon M, Collins S. Macromolecules 1998;31:1000.
[172] Siedle AR, Misemer DK, Kolpe VV, Duerr BF. (Minnesota Mining & Manufacturing Co.) PTC Int Appl WO 99/20664, 1999 (and refs. therein).
[173] Mallin DT, Rausch MD, Lin Y-G, Dong S, Chien JCW. J Am Chem Soc 1990;112:2030.
[174] Chien JCW, Iwamoto Y, Rausch MD, Wedler W, Winter HH. Macromolecules 1997;30:3447.
[175] Chien JCW, Iwamoto Y, Rausch MD. J Polym Sci, Part A 1999;37:2439.